GREGG

www.greggdrilling.com

www.greggdrilling.ca

GUIDE TO CONE PENETRATION TESTING

6th Edition 2015

Engineering Units

Multiples

Micro (μ)	$= 10^{-6}$
Milli (m)	$= 10^{-3}$
Kilo (k)	$= 10^{+3}$
Mega (M)	$= 10^{+6}$

Imperial Units			**SI Units**	
Length	feet	(ft)	meter	(m)
Area	square feet	(ft^2)	square meter	(m^2)
Force	pounds	(p)	Newton	(N)
Pressure/Stress	pounds/$foot^2$	(psf)	Pascal	(Pa) = (N/m^2)

Multiple Units				
Length	inches	(in)	millimeter	(mm)
Area	square feet	(ft^2)	square millimeter	(mm^2)
Force	ton	(t)	kilonewton	(kN)
Pressure/Stress	pounds/$inch^2$	(psi)	kilonewton/$meter^2$	kPa)
	tons/$foot^2$	(tsf)	meganewton/$meter^2$	(MPa)

Conversion Factors

Force:	1 ton	= 9.8 kN	
	1 kg	= 9.8 N	
Pressure/Stress	1kg/cm^2	= 100 kPa	= 100 kN/m^2 = 1 bar
	1 tsf	= 96 kPa	(~100 kPa = 0.1 MPa)
	1 t/m^2	~ 10 kPa	
	14.5 psi	= 100 kPa	
2.31 foot of water		= 1 psi	1 meter of water = 10 kPa

Derived Values from CPT

Friction ratio:	$R_f = (f_s/q_t) \times 100\%$
Corrected cone resistance:	$q_t = q_c + u_2(1\text{-}a)$
Net cone resistance:	$q_n = q_t - \sigma_{vo}$
Excess pore pressure:	$\Delta u = u_2 - u_0$
Pore pressure ratio:	$Bq = \Delta u / q_n$
Normalized excess pore pressure:	$U = (u_t - u_0) / (u_i - u_0)$

where: u_t is the pore pressure at time *t* in a dissipation test, and
u_i is the initial pore pressure at the start of the dissipation test

Guide to Cone Penetration Testing for Geotechnical Engineering

By

P. K. Robertson
and
K.L. Cabal

Gregg Drilling & Testing, Inc.

6th Edition
2015

Gregg Drilling & Testing, Inc.
Corporate Headquarters
2726 Walnut Avenue
Signal Hill, California 90755

Telephone: (562) 427-6899
Fax: (562) 427-3314
E-mail: info@greggdrilling.com
Website: www.greggdrilling.com

TABLE OF CONTENTS

Glossary

This glossary contains the most commonly used terms related to CPT and are presented in alphabetical order.

CPT
: Cone penetration test.

CPTu
: Cone penetration test with pore pressure measurement – *piezocone* test.

Cone
: The part of the cone penetrometer on which the cone resistance is measured.

Cone penetrometer
: The assembly containing the cone, friction sleeve, and any other sensors, as well as the connections to the push rods.

Cone resistance, q_c
: The force acting on the cone, Q_c, divided by the projected area of the cone, A_c.

$$q_c = Q_c / A_c$$

Corrected cone resistance, q_t
: The cone resistance q_c corrected for pore water effects.

$$q_t = q_c + u_2(1- a)$$

Data acquisition system
: The system used to record the measurements made by the cone.

Dissipation test
: A test when the decay of the pore pressure is monitored during a pause in penetration.

Filter element
: The porous element inserted into the cone penetrometer to allow transmission of pore water pressure to the pore pressure sensor, while maintaining the correct dimensions of the cone penetrometer.

Friction ratio, R_f
: The ratio, expressed as a percentage, of the sleeve friction resistance, f_s, to the cone resistance, q_t, both measured at the same depth.

$$R_f = (f_s/q_t) \times 100\%$$

Friction reducer

A local enlargement on the push rods placed a short distance above the cone penetrometer, to reduce the friction on the push rods.

Friction sleeve

The section of the cone penetrometer upon which the friction resistance is measured.

Normalized cone resistance, Q_t

The cone resistance expressed in a non-dimensional form and taking account of the in-situ vertical stresses.

$$Q_t = (q_t - \sigma_{vo}) / \sigma'_{vo}$$

Normalized cone resistance, Q_{tn}

The cone resistance expressed in a non-dimensional form taking account of the in-situ vertical stresses and where the stress exponent (n) varies with soil type and stress level. When n = 1, $Q_{tn} = Q_t$.

$$Q_{tn} = \left(\frac{q_t - \sigma_{vo}}{P_{a2}} \right) \left(\frac{P_a}{\sigma'_{vo}} \right)^n$$

Net cone resistance, q_n

The corrected cone resistance minus the vertical total stress.

$$q_n = q_t - \sigma_{vo}$$

Excess pore pressure (or net pore pressure), Δu

The measured pore pressure less the in-situ equilibrium pore pressure.

$$\Delta u = u_2 - u_0$$

Pore pressure

The pore pressure generated during cone penetration and measured by a pore pressure sensor:

u_1 when measured on the cone face

u_2 when measured just behind the cone.

Pore pressure ratio, B_q

The net pore pressure normalized with respect to the net cone resistance.

$$B_q = \Delta u / q_n$$

Push rods

Thick-walled tubes used to advance the cone penetrometer

Sleeve friction resistance, f_s

The frictional force acting on the friction sleeve, F_s, divided by its surface area, A_s.

$$f_s = F_s / A_s$$

Introduction

The purpose of this guide is to provide a concise resource for the application of the CPT to geotechnical engineering practice. This guide is a supplement and update to the book 'CPT in Geotechnical Practice' by Lunne, Robertson and Powell (1997). This guide is applicable primarily to data obtained using a standard electronic cone with a 60-degree apex angle and either a diameter of 35.7 mm or 43.7 mm (10 or 15 cm^2 cross-sectional area).

Recommendations are provided on applications of CPT data for soil profiling, material identification and evaluation of geotechnical parameters and design. The companion book (Lunne et al., 1997) provides more details on the history of the CPT, equipment, specification and performance. A companion Guide to CPT for Geo-environmental Applications is also available. The companion book also provides extensive background on interpretation techniques. This guide provides only the basic recommendations for the application of the CPT for geotechnical design

A list of the main references is included at the end of this guide. A more comprehensive reference list can be found in the companion CPT book and the recently listed technical papers. Some recent technical papers can be downloaded from either www.greggdrilling.com, www.cpt-robertson.com or www.cpt10.com and www.cpt14.com.

Additional details on CPT interpretation are provided in a series of free webinars that can be viewed at http://www.greggdrilling.com/webinars. A copy of the webinar slides can also be downloaded from the same web site.

Risk Based Site Characterization

Risk and uncertainty are characteristics of the ground and are never fully eliminated. The appropriate level of sophistication for site characterization and analyses should be based on the following criteria:

- Precedent and local experience
- Design objectives
- Level of geotechnical risk
- Potential cost savings

The evaluation of geotechnical risk is dependent on hazards, probability of occurrence and the consequences. Projects can be classified as either: low, moderate or high risk, depending on the above criteria. Table 1 shows a generalized flow chart to illustrate the likely geotechnical ground investigation approach associated with risk. The level of sophistication in a site investigation is also a function of the project design objectives and the potential for cost savings.

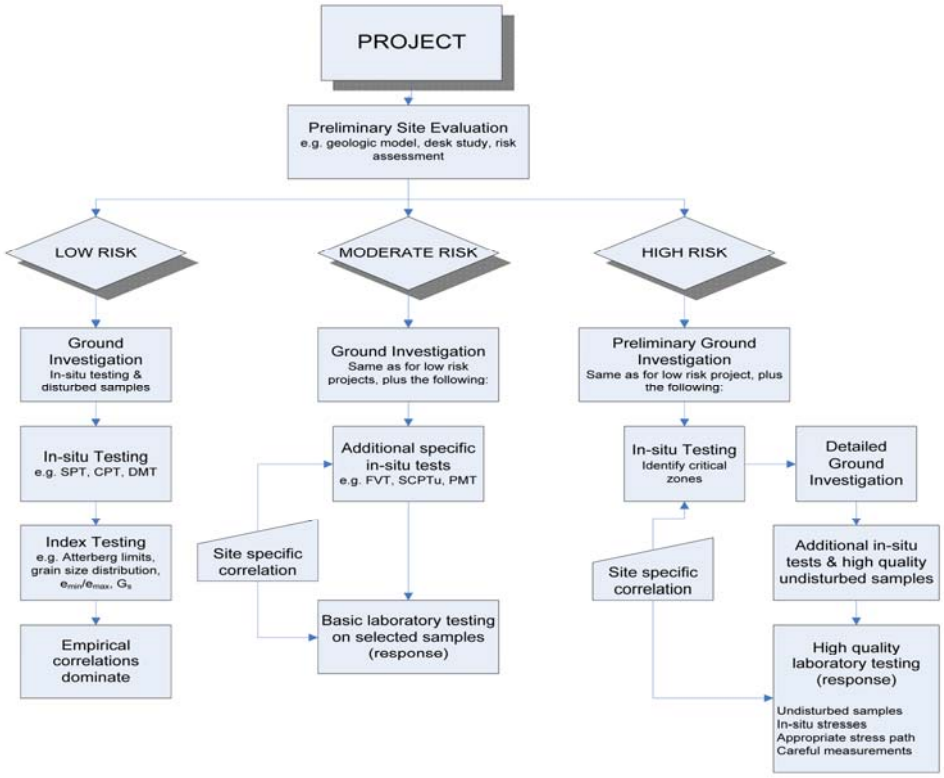

Table 1 Risk-based flowchart for site characterization

Role of the CPT

The objectives of any subsurface investigation are to determine the following:

- Nature and sequence of the subsurface strata (geologic regime)
- Groundwater conditions (hydrologic regime)
- Physical and mechanical properties of the subsurface strata

For geo-environmental site investigations where contaminants are possible, the above objectives have the additional requirement to determine:

- Distribution and composition of contaminants

The above requirements are a function of the proposed project and the associated risks. An ideal investigation program should include a mix of field and laboratory tests depending on the risk of the project.

Table 2 presents a partial list of the major in-situ tests and their perceived applicability for use in different ground conditions.

Group	In-situ Test	Geotechnical Parameter												Ground Type					
		Soil type	Profile	u_0	OCR	D_R-ψ	ϕ'	s_u	G_o - E	σ–ε	M - C_c	k	c_v	hard rock	soft rock	gravel	sand	silt/clay	peat – organic
Penetrometer/ Direct Push	Dy. Probing (DP)	C	B	-	C	C	C	C	C	-	-	-	-	-	C	B	A	B	B
	SPT	B	B	-	C	B	C	C	C	-	-	-	-	-	C	B	A	B	B
	CPT	B	A	-	B	B	B	B	B	C	C	C	-	-	B	B	A	A	A
	CPTu	A	A	A	B	A	B	A	B	C	B	A	A	-	B	B	A	A	A
	SCPTu	A	A	A	A	A	B	A	A	B	B	A	A	-	B	B	A	A	A
	DMT	B	B	B	B	C	B	B	B	C	B	C	B	-	C	C	A	A	A
	SDMT	B	B	B	A	B	B	B	A	B	B	C	B	-	C	C	A	A	A
	Full-flow (T/ball)	C	B	B	B	C	C	A	C	C	C	C	C	-	-	-	C	B	A
	Field vane (FVT)	B	C	-	B	-	-	A	-	-	-	-	-	-	-	-	-	A	B
Pressuremeter	Pre-bored	B	B	-	C	C	C	B	B	C	C	-	C	A	A	B	B	B	B
	Self-bored	B	B	A[1]	B	B	B	B	A	A	B	B	A[1]	-	C	-	B	A	B
	Full-displacement	B	B	B	C	C	C	B	A	A	B	B	A	-	C	-	B	A	A
Other	Screw/plate load	C	-	-	B	C	C	B	B	B	B	C	C	C	A	B	B	B	B
	Borehole shear	C	-	-	-	-	B	C	-	-	-	-	-	C	B	C	C	C	-
	Permeameter	C	-	A	-	-	-	-	-	-	-	A	B	A	A	A	A	A	B
	Borehole seismic	C	C	-	B	C	-	-	A	C	-	-	-	A	A	A	A	A	B
	Surface seismic	-	C	-	B	C	-	-	A	C	-	-	-	A	A	A	A	A	A
	Hydraulic fracture	-	-	B	-	-	-	-	-	-	-	C	C	B	B	-	-	B	C

Applicability: A = high, B = moderate, C = low, - = none

Geotechnical parameters: u_0 = in-situ static pore pressure, OCR = over-consolidation ratio, D_R-ψ = relative density and/or state parameter, ϕ' = peak friction angle, s_u = undrained shear strength (peak and/or remolded), G_o-E = small strain shear and/or Young's modulus, σ–ε = stress-strain relationship, M-C_c = constrained modulus and/or compression index, k = permeability, c_v = coefficient of consolidation

ϕ' will depend on soil type; [1] only when pore pressure sensor fitted.

Table 2. The applicability and usefulness of in-situ tests
(Lunne, Robertson & Powell, 1997, updated by Robertson, 2012)

The Cone Penetration Test (CPT) and its enhanced versions such as the piezocone (CPTu) and seismic (SCPT), have extensive applications in a wide range of soils. Although the CPT is limited primarily to softer soils, with modern large pushing equipment and more robust cones, the CPT can be performed in stiff to very stiff soils, and in some cases soft rock.

Advantages of CPT:

- Fast and continuous profiling
- Repeatable and reliable data (not operator-dependent)
- Economical and productive
- Strong theoretical basis for interpretation

Disadvantage of CPT:

- Relatively high capital investment
- Requires skilled operators
- No soil sample, during a CPT
- Penetration can be restricted in gravel/cemented layers

Although it is not possible to obtain a soil sample during a CPT, it is possible to obtain soil samples using CPT pushing equipment. The continuous nature of CPT results provides a detailed stratigraphic profile to guide in selective sampling appropriate for the project. The recommended approach is to first perform several CPT soundings to define the stratigraphic profile and to provide initial estimates of geotechnical parameters, then follow with selective sampling. The type and amount of sampling will depend on the project requirements and risk as well as the stratigraphic profile. Typically sampling will be focused in critical zones as defined by the CPT.

A variety of push-in discrete depth soil samplers are available. Most are based on designs similar to the original Gouda or MOSTAP soil samplers from the Netherlands. The samplers are pushed to the required depth in a closed position. The Gouda type samplers have an inner cone tip that is retracted to the locked position leaving a hollow sampler with small diameter (25mm/1 inch) stainless steel or brass sample tubes. The hollow sampler is then pushed to collect a sample. The filled sampler and push rods are then retrieved to the ground surface. The MOSTAP type samplers contain a wire to fix the position of the inner cone tip before pushing to obtain a sample. Modifications have also been made to include a wireline system so that soil samples can be retrieved at

multiple depths rather than retrieving and re-deploying the sampler and rods at each interval. The wireline systems tend to work better in soft soils. Figure 1 shows a schematic of typical (Gouda-type) CPT-based soil sampler. The speed of sampling depends on the maximum speed of the pushing equipment but is not limited to the standard 2cm/s used for the CPT. Some specialized CPT trucks can take samples at a rate of up to 40cm/s. Hence, push-in soil sampling can be fast and efficient. In very soft soils, special 0.8m (32 in) long push-in piston samplers have been developed to obtain 63mm (2.5 in) diameter undisturbed soil samples.

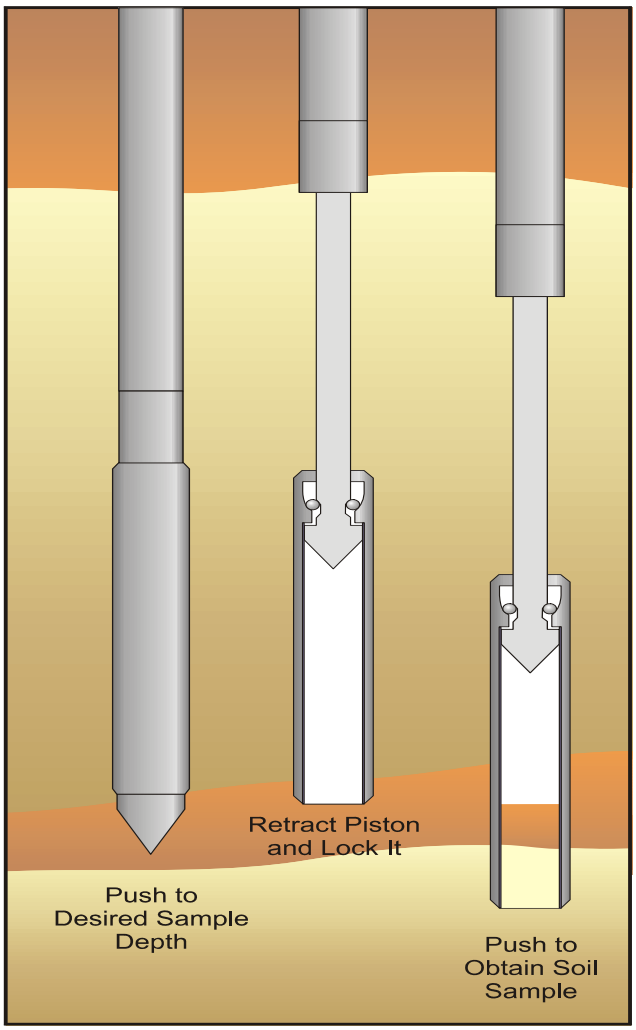

Figure 1 Schematic of simple direct-push (CPT-based) soil sampler (www.greggdrilling.com)

Cone Penetration Test (CPT)

Introduction

In the Cone Penetration Test (CPT), a cone on the end of a series of rods is pushed into the ground at a constant rate and continuous measurements are made of the resistance to penetration of the cone and of a surface sleeve. Figure 2 illustrates the main terminology regarding cone penetrometers.

The total force acting on the cone, Q_c, divided by the projected area of the cone, A_c, produces the cone resistance, q_c. The total force acting on the friction sleeve, F_s, divided by the surface area of the friction sleeve, A_s, produces the sleeve resistance, f_s. In a *piezocone*, pore pressure is also measured, typically behind the cone in the u_2 location, as shown in Figure 2.

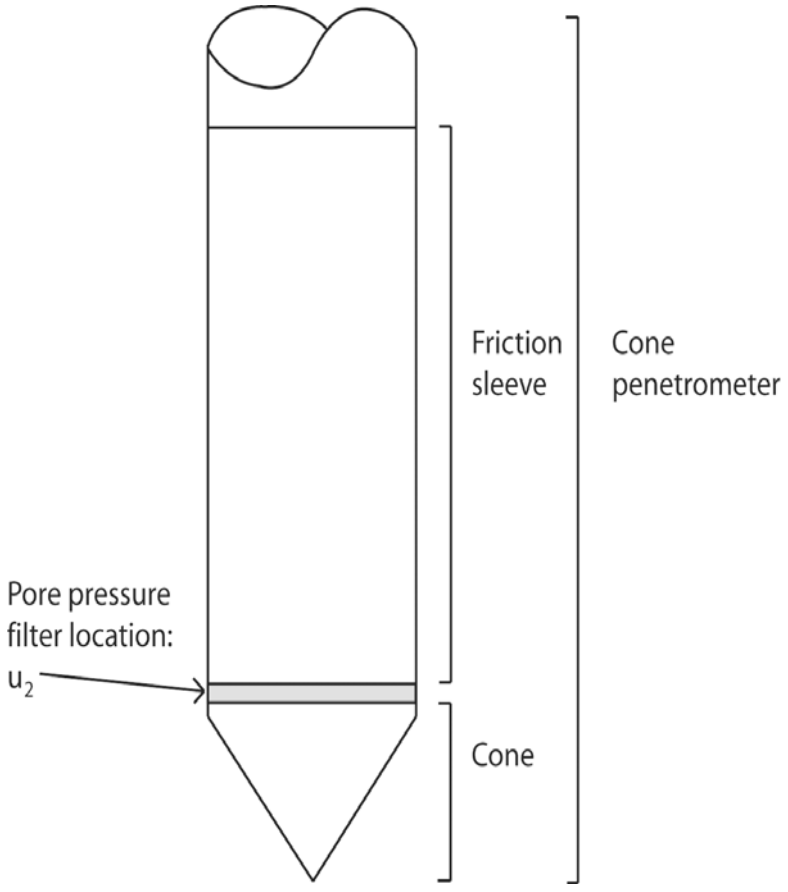

Figure 2 Terminology for cone penetrometers

History

1932

The first cone penetrometer tests were made using a 35 mm outside diameter gas pipe with a 15 mm steel inner push rod. A cone tip with a 10 cm^2 projected area and a 60° apex angle was attached to the steel inner push rods, as shown in Figure 3.

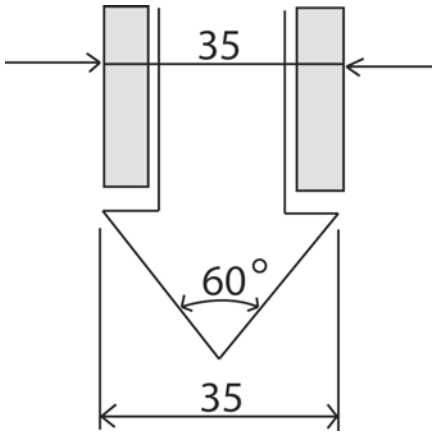

Figure 3 Early Dutch mechanical cone (after Sanglerat, 1972)

1935

Delf Soil Mechanics Laboratory designed the first manually operated 10ton (100kN) cone penetration push machine, see Figure 4.

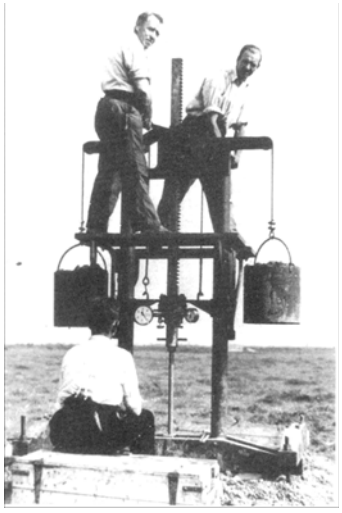

Figure 4 Early Dutch mechanical cone (after Delft Geotechnics)

1948

The original Dutch mechanical cone was improved by adding a conical part just above the cone. The purpose of the geometry was to prevent soil from entering the gap between the casing and inner rods. The basic Dutch mechanical cones, shown in Figure 5, are still in use in some parts of the world.

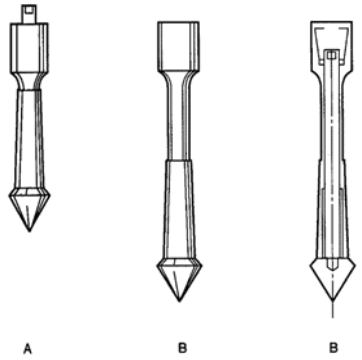

Figure 5 Dutch mechanical cone penetrometer with conical mantle

1953

A friction sleeve ('adhesion jacket') was added behind the cone to include measurement of the local sleeve friction (Begemann, 1953), see Figure 6. Measurements were made every 20 cm, (8 inches) and for the first time, friction ratio was used to classify soil type (see Figure 7).

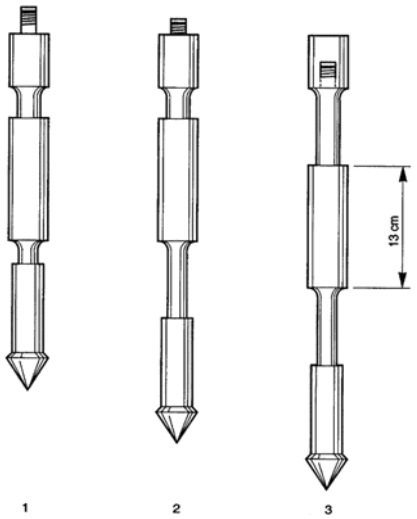

Figure 6 Begemann type cone with friction sleeve

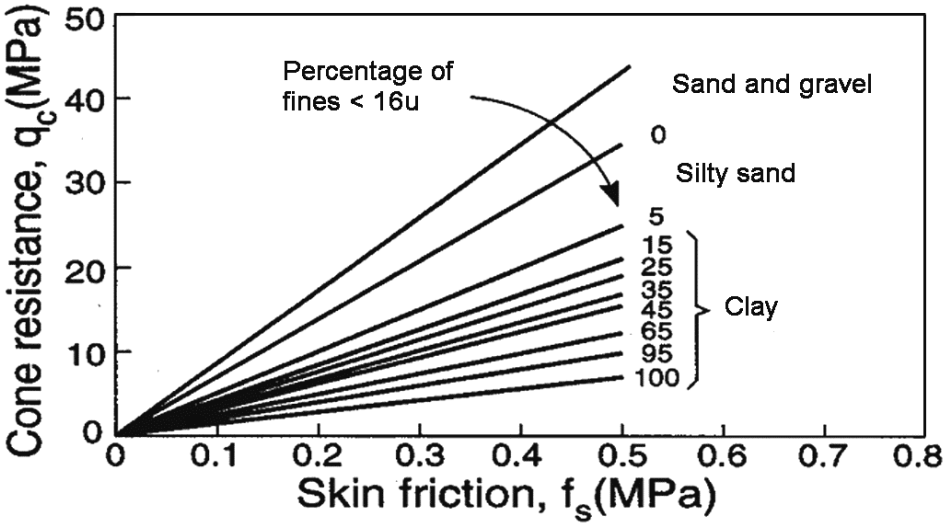

Figure 7 First CPT-based soil classification for Begemann mechanical cone

1965

Fugro developed an electric cone, of which the shape and dimensions formed the basis for the modern cones and the International Reference Test and ASTM procedure. The main improvements relative to the mechanical cone penetrometers were:

- Elimination of incorrect readings due to friction between inner rods and outer rods and weight of inner rods.
- Continuous testing with continuous rate of penetration without the need for alternate movements of different parts of the penetrometer and no undesirable soil movements influencing the cone resistance.
- Simpler and more reliable electrical measurement of cone resistance and sleeve friction resistance.

1974

Cone penetrometers that could also measure pore pressure (*piezocones*) were introduced. Early designs had various shapes and pore pressure filter locations. Gradually the practice has become more standardized so that the recommended position of the filter element is close behind the cone at the u_2 location. With the measurement of pore water pressure it became apparent that it was necessary to correct the cone resistance for pore water pressure effects (q_t), especially in soft clay.

Test Equipment and Procedures

Cone Penetrometers

Cone penetrometers come in a range of sizes with the 10 cm^2 and 15 cm^2 probes the most common and specified in most standards. Figure 8 shows a range of cones from a mini-cone at 2 cm^2 to a large cone at 40 cm^2. The mini cones are used for shallow investigations, whereas the large cones can be used in gravely soils.

Figure 8 Range of CPT probes (from left: 2 cm^2, 10 cm^2, 15 cm^2, 40 cm^2)

Additional Sensors/Modules

Since the introduction of the electric cone in the early 1960's, many additional sensors have been added to the cone, such as;

- Temperature
- Geophones/accelerometers (seismic wave velocity)
- Pressuremeter (cone pressuremeter)
- Camera (visible light)
- Radioisotope (gamma/neutron)
- Electrical resistivity/conductivity
- Dielectric
- pH
- Oxygen exchange (redox)
- Laser/ultraviolet induced fluorescence (LIF/UVOST)
- Membrane interface probe (MIP)

The latter items are primarily for geo-environmental applications.
One of the more common additional sensors is a geophone or accelerometer to allow the measurement of seismic wave velocities. A schematic of the seismic CPT (SCPT) procedure is shown in Figure 9.

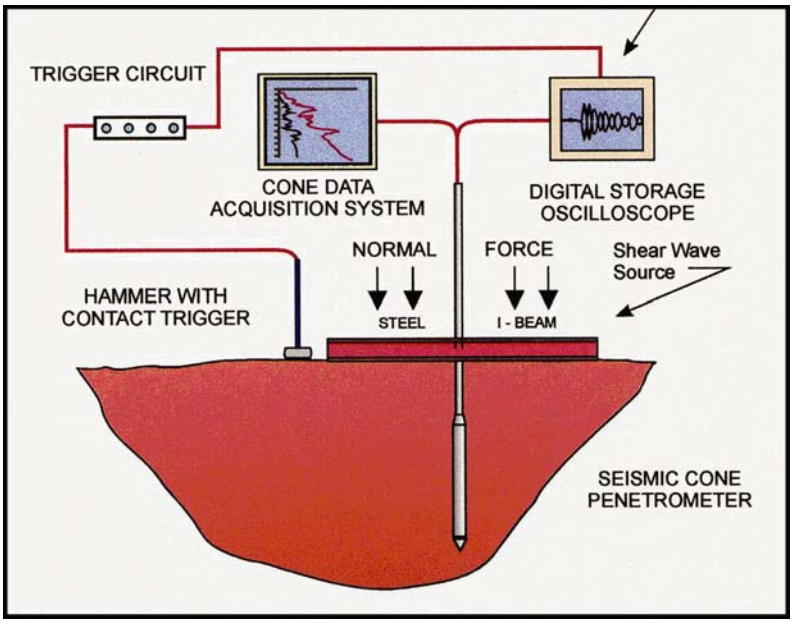

Figure 9 Schematic of Seismic CPT (SCPT) test procedure

Pushing Equipment

Pushing equipment consists of push rods, a thrust mechanism and a reaction frame.

On Land

Pushing equipment for land applications generally consist of specially built units that are either truck or track mounted. CPT's can also be carried out using an anchored drill-rig. Figures 10 to 13 show a range of on land pushing equipment.

Figure 10 Truck mounted 25 ton CPT unit

Figure 11 Track mounted 20 ton CPT unit

Figure 12 Small anchored drill-rig unit

Figure 13 Portable ramset for CPT inside buildings or limited access

Figure 14 Mini-CPT system attached to small track mounted auger rig

Over Water

There is a variety of pushing equipment for over water investigations depending on the depth of water. Floating or jack-up barges are common in shallow water (depth less than 30m/100 ft), see Figures 15 and 16.

Figure 15 Mid-size jack-up boat

Figure 16 Quinn Delta (Gregg) ship with spuds

In deeper water (>100m, 350ft) it is common to place the CPT pushing equipment on the seafloor using specially designed underwater systems, such as shown in Figure 17. Seabed systems can push full size cones (10 and 15cm^2 cones) and smaller systems for mini-cones (2 and 5cm^2 cones) using continuous pushing systems.

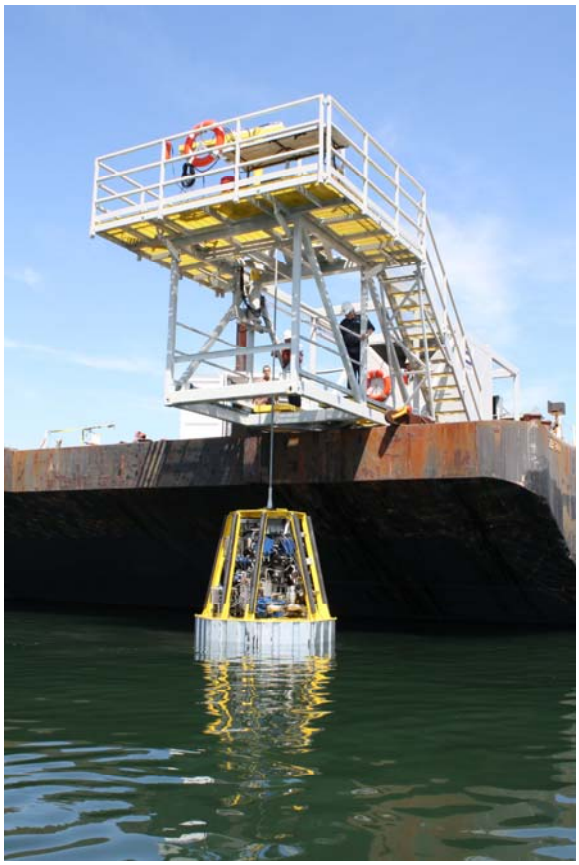

Figure 17 (Gregg) Seafloor CPT system for pushing full size cones in very deep water (up to 4,000msw)

Alternatively, it is also possible to push the CPT from the bottom of a borehole using down-hole equipment. The advantage of down-hole CPT in a drilled borehole is that much deeper penetration can be achieved and hard layers can be drilled through. Down-hole methods can be applied both on-shore and off-shore. Recently, remotely controlled seabed drill rigs have been developed that can drill and sample and push CPT in up to 4,000m (13,000 ft) of water (e.g. Lunne, 2010).

Depth of Penetration

CPT's can be performed to depths exceeding 100m (300ft) in soft soils and with large capacity pushing equipment. To improve the depth of penetration, the friction along the push rods should be reduced. This can be done using an expanded coupling (i.e. friction reducer) a short distance, typically 1m (3ft), behind the cone. Penetration will be limited if, very hard soils, gravel layers or rock are encountered. It is common to use $15cm^2$ cones to increase penetration depth, since $15cm^2$ cones are more robust and have a slightly larger diameter than the standard $10cm^2$ push rods. The push rods can also be lubricated with drilling mud to remove rod friction for deep soundings. Depth of penetration can also be increased using down-hole techniques with a drill rig.

Test Procedures

Pre-drilling

For penetration in fills or hard soils it may be necessary to pre-drill in order to avoid damaging the cone. Pre-drilling, in certain cases, may be replaced by first pre-punching a hole through the upper problem material with a solid steel 'dummy' probe with a diameter slightly larger than the cone. It is also common to hand auger the first 1.5m (5ft) in urban areas to avoid underground utilities.

Verticality

The thrust machine should be set up so as to obtain a thrust direction as near as possible to vertical. The deviation of the initial thrust direction from vertical should not exceed 2 degrees and push rods should be checked for straightness. Modern cones have simple slope sensors incorporated to enable a measure of the non-verticality of the sounding. This is useful to avoid damage to equipment and breaking of push rods. For depths less than 15m (50ft), significant non-verticality is unusual, provided the initial thrust direction is vertical.

Reference Measurements

Modern cones have the potential for a high degree of accuracy and repeatability (~0.1% of full-scale output). Tests have shown that the output of the sensors at zero load can be sensitive to changes in temperature, although most cones now include some temperature compensation. It is common practice to record zero load readings of all sensors to track these changes. Zero load readings should be monitored and recorded at the start and end of each CPT.

Rate of Penetration

The standard rate of penetration is 2cm/s (approximately 1in/s). Hence, a 20m (60ft) sounding can be completed (start to finish) in about 30 minutes. The CPT results are generally not sensitive to slight variations in the rate of penetration.

Interval of readings

Electric cones produce continuous analogue data. However, most systems convert the data to digital form at selected intervals. Most standards require the interval to be no more than 200mm (8in). In general, most systems collect data at intervals of between 10 - 50mm, with 20 mm (~1in) being the more common.

Dissipation Tests

During a pause in penetration, any excess pore pressure generated around the cone will start to dissipate. The rate of dissipation depends upon the coefficient of consolidation, which in turn, depends on the compressibility and permeability of the soil. The rate of dissipation also depends on the diameter of the probe. A dissipation test can be performed at any required depth by stopping the penetration and measuring the decay of pore pressure with time. It is common to record the time to reach 50% dissipation (t_{50}), as shown in Figure 18. If the equilibrium pore pressure is required, the dissipation test should continue until no further dissipation is observed. This can occur rapidly in sands, but may take many hours in plastic clays. Dissipation rate increases as probe size decreases.

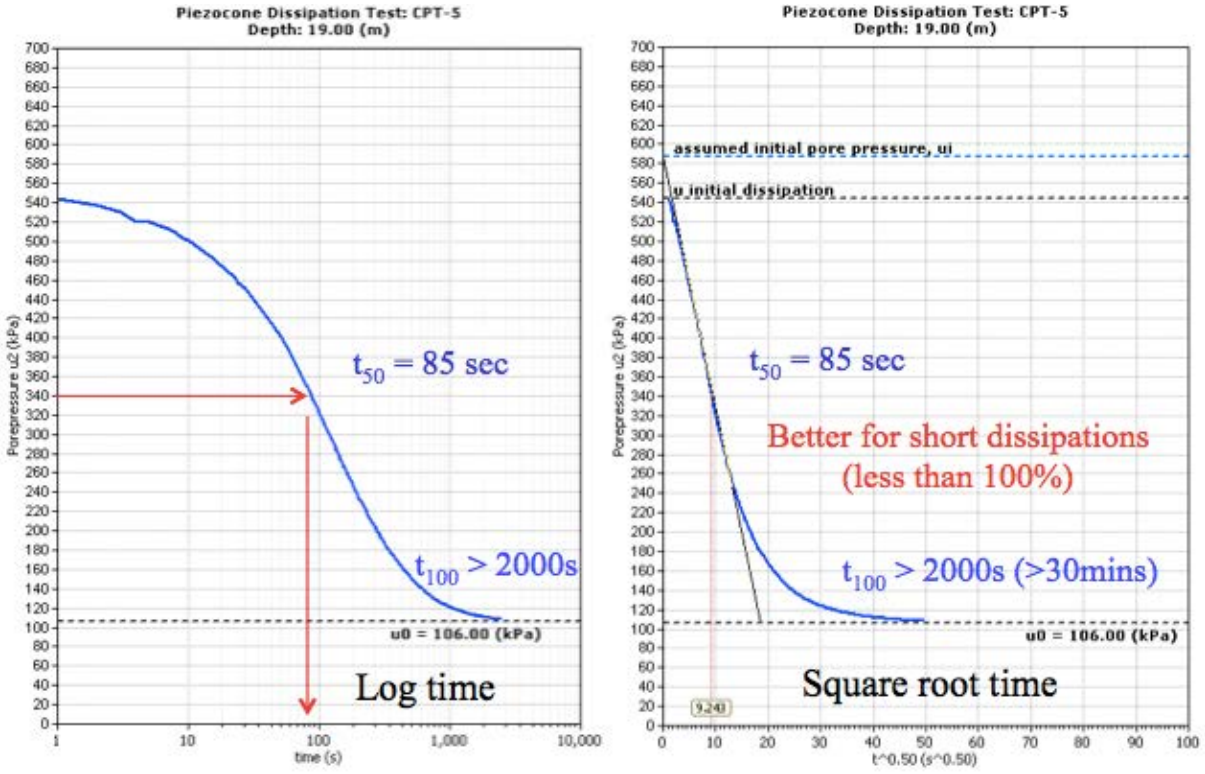

Figure 18 Example dissipation test to determine t_{50}

Calibration and Maintenance

Calibrations should be carried out at intervals based on the stability of the zero load readings. Typically, if the zero load readings remain stable, the load cells do not require a check calibration. For major projects, check calibrations can be carried out before and after the field work, with functional checks during the work. Functional checks should include recording and evaluating the zero load measurements (baseline readings).

With careful design, calibration, and maintenance, strain gauge load cells and pressure transducers can have an accuracy and repeatability of better than +/- 0.1% of full-scale reading.

Table 3 shows a summary of checks and recalibrations for the CPT.

Maintenance	*Start of Project*	*Start of Test*	*End of Test*	*End of Day*	*Once a Month*	*Every 3 months**
Wear	***x***	***x***			***x***	
O-ring seals	***x***			***x***		
Push-rods		***x***			***x***	
Pore pressure-filter	***x***	***x***				
Calibration						***x****
Computer					***x***	
Cone					***x***	
Zero-load		***x***	***x***			
Cables	***x***				***x***	

Table 3 Summary of checks and recalibrations for the CPT

*Note: recalibrations are normally carried out only when the zero-load readings drift outside manufactures recommended range

Cone Design

Penetrometers use strain gauge load cells to measure the resistance to penetration. Basic cone designs use either separate load cells or subtraction load cells to measure the tip resistance (q_c) and sleeve resistance (f_s). In subtraction cones the sleeve friction is derived by 'subtracting' the tip load from the tip + friction load. Figure 19 illustrates the general principle behind load cell designs using either separated load cells or subtraction load cells.

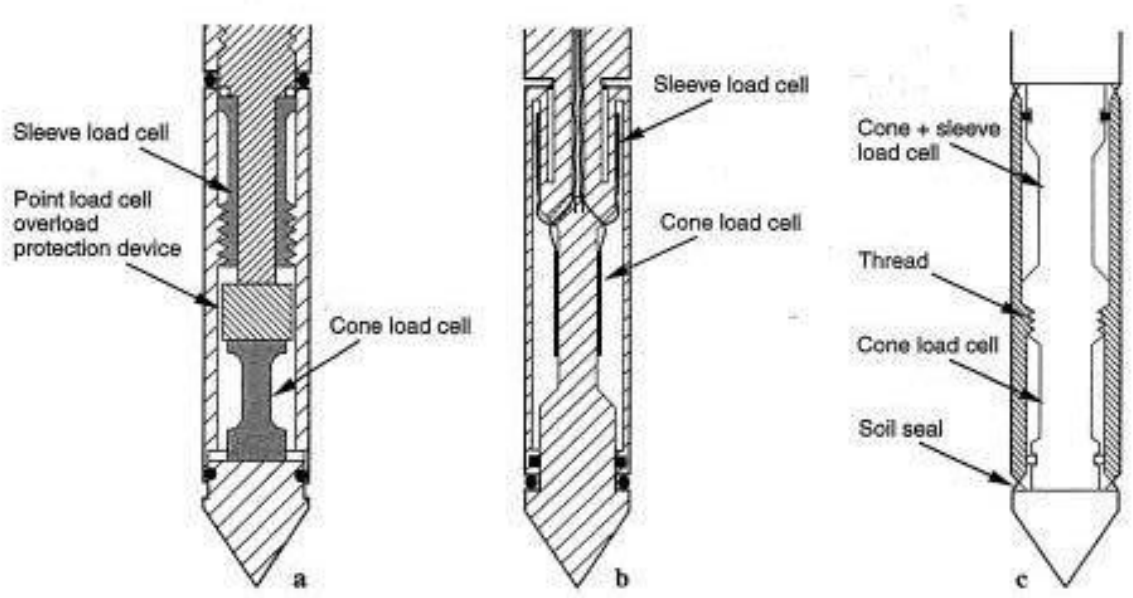

Figure 19 Designs for cone penetrometers (a) tip and sleeve friction load cells in compression, (b) tip load cell in compression and sleeve friction load cell in tension, (c) subtraction type load cell design (after Lunne et al., 1997)

In the 1980's subtraction cones became popular because of the overall robustness of the penetrometer. However, in soft soils, subtraction cone designs suffer from a lack of accuracy in the determination of sleeve resistance due primarily to variable zero load stability of the two load cells. In subtraction cone designs, different zero load errors can produce cumulative errors in the derived sleeve resistance values. For accurate sleeve resistance measurements in soft sediments, it is recommended that cones have separate (compression) load cells.

With good design (separate load cells, equal end area friction sleeve) and quality control (zero load measurements, tolerances and surface roughness) it is possible to obtain repeatable tip and sleeve resistance measurements. However, f_s measurements, in general, will be less accurate than tip resistance, q_c, in most soft fine-grained soils.

Pore pressure (water) effects

Due to the inner geometry of the cone the ambient water pressure acts on the shoulder behind the cone and on the ends of the friction sleeve. This effect is often referred to as the unequal end area effect (Campanella et al., 1982). Figure 20 illustrates the key features for water pressure acting behind the cone and on the end areas of the friction sleeve. In soft clays and silts and in over water work, the measured q_c must be corrected for pore water pressures acting on the cone geometry, thus obtaining the corrected cone resistance, q_t:

$$q_t = q_c + u_2 (1 - a)$$

Where 'a' is the net area ratio determined from laboratory calibration with a typical value between 0.70 and 0.85. In sandy soils $q_c = q_t$.

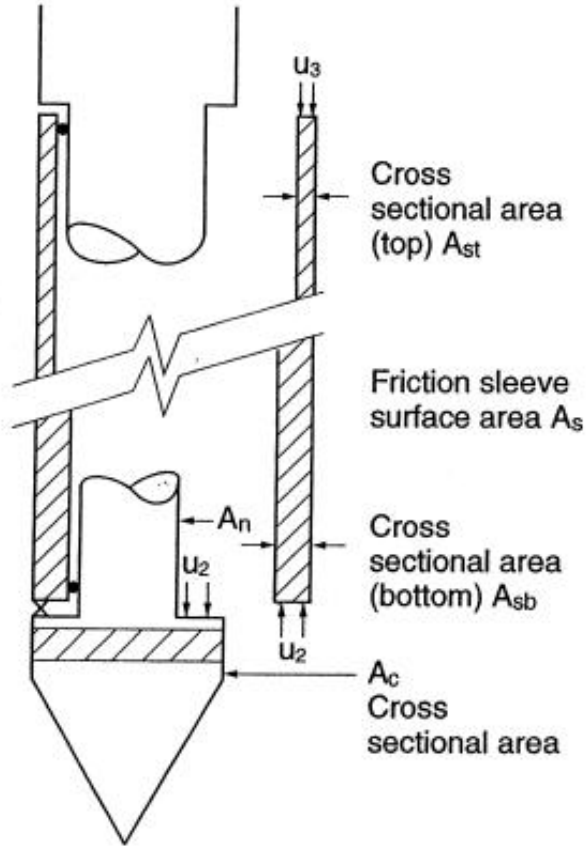

Figure 20 Unequal end area effects on cone tip and friction sleeve

A similar correction should be applied to the sleeve friction.

$$f_t = f_s - (u_2A_{sb} - u_3A_{st})/A_s$$

where: f_s = measured sleeve friction
u_2 = water pressure at base of sleeve
u_3 = water pressure at top of sleeve
A_s = surface area of sleeve
A_{sb} = cross-section area of sleeve at base
A_{st} = cross-sectional area of sleeve at top

However, the ASTM standard requires that cones have an equal end area friction sleeve (i.e. $A_{st} = A_{sb}$) that reduces the need for such a correction. For 15cm^2 cones, where A_s is large compared to A_{sb} and A_{st}, (and $A_{st} = A_{sb}$) the correction is generally small. All cones should have equal end area friction sleeves to minimize the effect of water pressure on the sleeve friction measurements. Careful monitoring of the zero load readings is also required.

In the offshore industry, where CPT can be carried out in very deep water (> 1,000m), cones are sometimes compensated (filled with oil) so that the pressure inside the cone is equal to the hydrostatic water pressure outside the cone. For compensated cones the correction for cone geometry to obtain q_t is slightly different than shown above, since the cone can record zero q_c at the mudline.

CPT Interpretation

Numerous semi-empirical correlations have been developed to estimate geotechnical parameters from the CPT for a wide range of soils. These correlations vary in their reliability and applicability. Because the CPT has additional sensors (e.g. pore pressure, CPTu and seismic, SCPT), the applicability to estimate soil parameters varies. Since CPT with pore pressure measurements (CPTu) is commonly available, Table 4 shows an estimate of the perceived applicability of the CPTu to estimate soil parameters. If seismic is added, the ability to estimate soil stiffness (E, G & G_o) improves further.

Soil Type	D_r	Ψ	K_o	OCR	S_t	s_u	ϕ'	E, G*	M	G_0*	k	c_h
Coarse-gained (sand)	2-3	2-3	5	5			2-3	2-3	2-3	2-3	3-4	3-4
Fine-grained (clay)			2	1	2	1-2	4	2-4	2-3	2-4	2-3	2-3

Table 4 Perceived applicability of CPTu for deriving soil parameters

1=high, 2=high to moderate, 3=moderate, 4=moderate to low, 5=low reliability, Blank=no applicability, * improved with SCPT

Where:

D_r	Relative density	ϕ'	Peak friction angle
Ψ	State Parameter	K_0	In-situ stress ratio
E, G	Young's and Shear moduli	G_0	Small strain shear moduli
OCR	Over consolidation ratio	M	1-D Compressibility
s_u	Undrained shear strength	S_t	Sensitivity
c_h	Coefficient of consolidation	k	Permeability

Most semi-empirical correlations apply primarily to relatively young, uncemented, silica-based soils.

Soil Profiling and Soil Type

One of the major applications of the CPT is for *soil profiling and soil type*. Typically, the cone resistance, (q_t) is high in sands and low in clays, and the friction ratio ($R_f = f_s/q_t$) is low in sands and high in clays. The CPT cannot be expected to provide accurate predictions of soil type based on *physical characteristics,* such as, grain size distribution but provide a guide to the *mechanical characteristics* (strength, stiffness, compressibility) of the soil, or the *soil behavior type* (SBT). CPT data provides a repeatable index of the aggregate behavior of the in-situ soil in the immediate area of the probe. Hence, prediction of soil type based on CPT is referred to as ***Soil Behavior Type (SBT).***

Non-Normalized SBT Charts

The most commonly used CPT soil behavior type (SBT) chart was suggested by Robertson et al. (1986), the updated, dimensionless version (Robertson, 2010) is shown in Figure 21. This chart uses the basic CPT parameters of cone resistance, q_t and friction ratio, R_f. The chart is global in nature and can provide reasonable predictions of soil behavior type for CPT soundings up to about 20m (60ft) in depth. Overlap in some zones should be expected and the zones can be modified somewhat based on local experience.

Normalized SBT_n Charts

Since both the penetration resistance and sleeve resistance increase with depth due to the increase in effective overburden stress, the CPT data requires normalization for overburden stress for very shallow and/or very deep soundings.

A popular CPT soil behavior chart based on normalized CPT data is that first proposed by Robertson (1990) and shown in Figure 22. A zone has been identified in which the CPT results for most young, un-cemented, insensitive, normally consolidated soils will plot. The chart identifies general trends in ground response, such as, increasing soil density, OCR, age and cementation for sandy soils, increasing stress history (OCR) and soil sensitivity (S_t) for cohesive soils. Again the chart is global in nature and provides only a guide to soil behavior type (SBT). Overlap in some zones should be expected and the zones can be modified somewhat based on local experience.

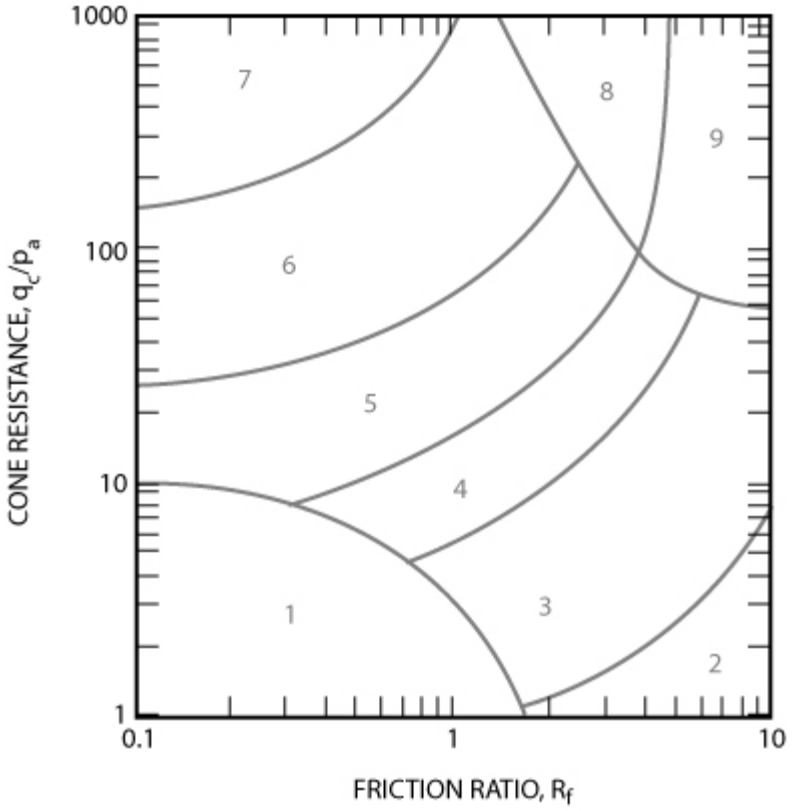

Zone	*Soil Behavior Type*
1	*Sensitive, fine grained*
2	*Organic soils - clay*
3	*Clay – silty clay to clay*
4	*Silt mixtures – clayey silt to silty clay*
5	*Sand mixtures – silty sand to sandy silt*
6	*Sands – clean sand to silty sand*
7	*Gravelly sand to dense sand*
8	*Very stiff sand to clayey sand**
9	*Very stiff fine grained**

** Heavily overconsolidated or cemented*

P_a = atmospheric pressure = 100 kPa = 1 tsf

Figure 21 Non-normalized CPT Soil Behavior Type (SBT) chart (Robertson et al., 1986, updated by Robertson, 2010).

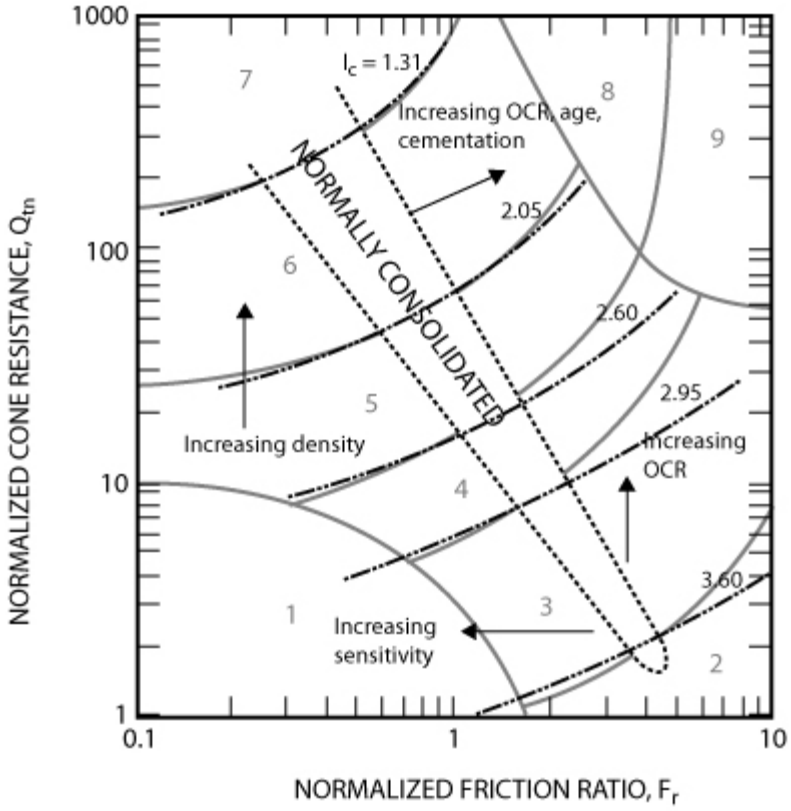

Zone	***Soil Behavior Type***	***I_c***
1	*Sensitive, fine grained*	N/A
2	*Organic soils – clay*	> 3.6
3	*Clays – silty clay to clay*	2.95 – 3.6
4	*Silt mixtures – clayey silt to silty clay*	2.60 – 2.95
5	*Sand mixtures – silty sand to sandy silt*	2.05 – 2.6
6	*Sands – clean sand to silty sand*	1.31 – 2.05
7	*Gravelly sand to dense sand*	< 1.31
8	*Very stiff sand to clayey sand**	N/A
9	*Very stiff, fine grained**	N/A

** Heavily overconsolidated or cemented*

Figure 22 Normalized CPT Soil Behavior Type (SBT_n) chart, Q_t - F (Robertson, 1990, updated by Robertson, 2010).

The full normalized SBT_n charts suggested by Robertson (1990) also included an additional chart based on normalized pore pressure parameter, B_q, as shown on Figure 23, where;

$$B_q = \Delta u / q_n$$

and; excess pore pressure, $\Delta u = u_2 - u_0$
net cone resistance, $q_n = q_t - \sigma_{vo}$

The $Q_t - B_q$ chart can aid in the identification of soft, saturated fine-grained soils where excess CPT penetration pore pressures can be large. In general, the Q_t - B_q chart is not commonly used for onshore CPT due to the lack of repeatability of the pore pressure results (e.g. poor saturation or loss of saturation of the filter element, etc.).

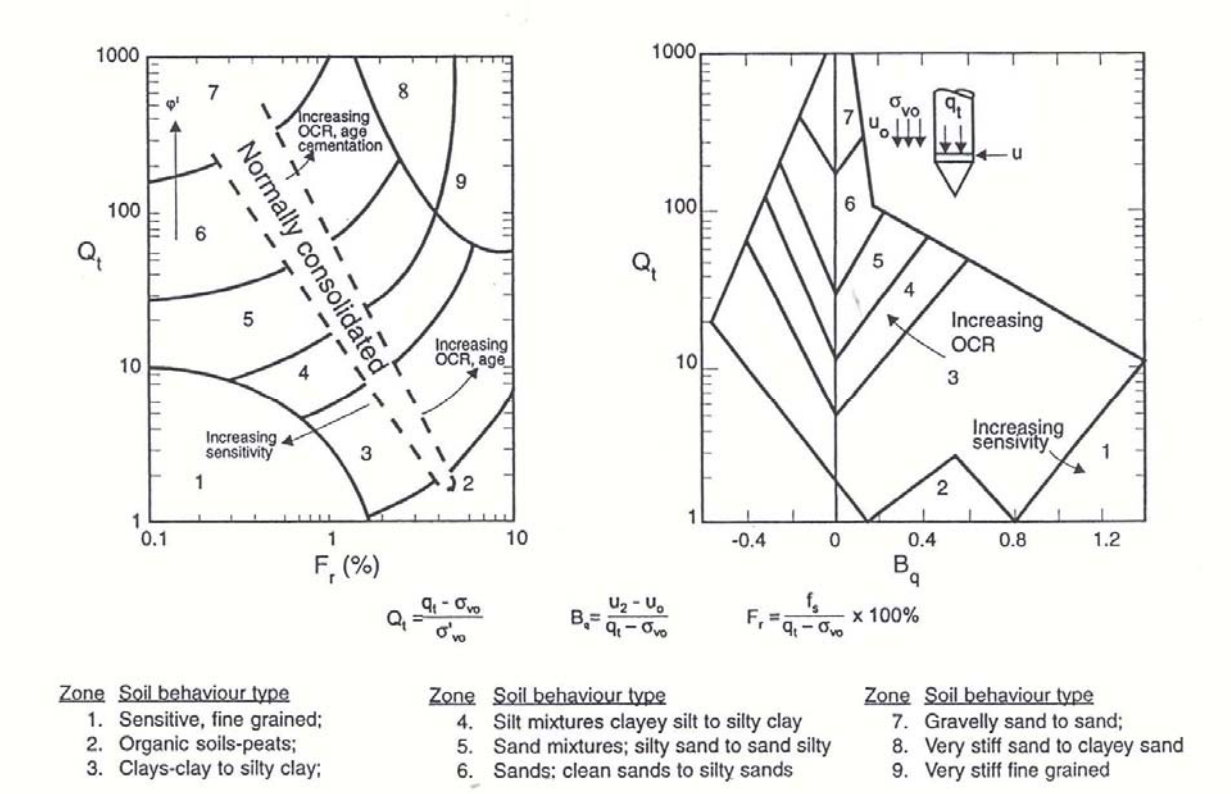

Figure 23 Normalized CPT Soil Behavior Type (SBT_n) charts $Q_t - F_r$ and Q_t - B_q (after Robertson, 1990).

If no prior CPT experience exists in a given geologic environment it is advisable to obtain samples from appropriate locations to verify the soil type. If significant CPT experience is available and the charts have been evaluated based on this experience, samples may not always be required.

Soil behavior type can be improved if pore pressure measurements are also collected, as shown on Figure 23. In soft clays and silts the penetration pore pressures can be very large, whereas, in stiff heavily over-consolidated clays or dense silts and silty sands the penetration pore pressures (u_2) can be small and sometimes negative relative to the equilibrium pore pressures (u_0). The rate of pore pressure dissipation during a pause in penetration can also guide in the soil type. In sandy soils any excess pore pressures will dissipate very quickly, whereas, in clays the rate of dissipation can be very slow.

To simplify the application of the CPT SBT_n chart shown in Figure 22, the normalized cone parameters Q_t and F_r can be combined into one Soil Behavior Type index, I_c, where I_c is the radius of the essentially concentric circles that represent the boundaries between each SBT_n zone. I_c can be defined as follows;

$$I_c = ((3.47 - \log Q_t)^2 + (\log F_r + 1.22)^2)^{0.5}$$

where:

Q_t = normalized cone penetration resistance (dimensionless)
= $(q_t - \sigma_{vo})/\sigma'_{vo}$
F_r = normalized friction ratio, in %
= $(f_s/(q_t - \sigma_{vo})) \times 100\%$

The term Q_t represents the simple normalization with a stress exponent (n) of 1.0, which applies well to clay-like soils. Robertson (2009) suggested that the normalized SBT_n charts shown in Figures 22 and 23 should be used with the normalized cone resistance (Q_{tn}) calculated using a stress exponent that varies with soil type via I_c (i.e. Q_{tn}, see Figure 46 for details).

The approximate boundaries of soil behavior types are then given in terms of the SBT_n index, I_c, as shown in Figure 22. The soil behavior type index does not apply to zones 1, 8 and 9. Profiles of I_c provide a simple guide to the continuous variation of soil behavior type in a given soil profile based on CPT results. Independent studies have shown that the normalized SBT_n chart shown in Figure 22 typically has greater than 80% reliability when compared with samples.

Schneider et al (2008) proposed a CPT-based soil type chart based on normalized cone resistance (Q_t) and normalized excess pore pressure ($\Delta u_2/\sigma'_{vo}$), as shown on Figure 24. Superimposed on the Schneider et al chart are contours of B_q to illustrate the link with $\Delta u_2/\sigma'_{vo}$. Also shown on the Schneider et al chart are approximate contours of OCR (dashed lines). Application of the Schneider et al chart can be problematic for some onshore projects where the CPTu pore pressure results may not be reliable, due to loss of saturation. However, for offshore projects, where CPTu sensor saturation is more reliable, and onshore projects in soft fine-grained soils with high groundwater, the chart can be very helpful. The Schneider et al chart is focused primarily on fine-grained soils were excess pore pressures are recorded and Q_t is small.

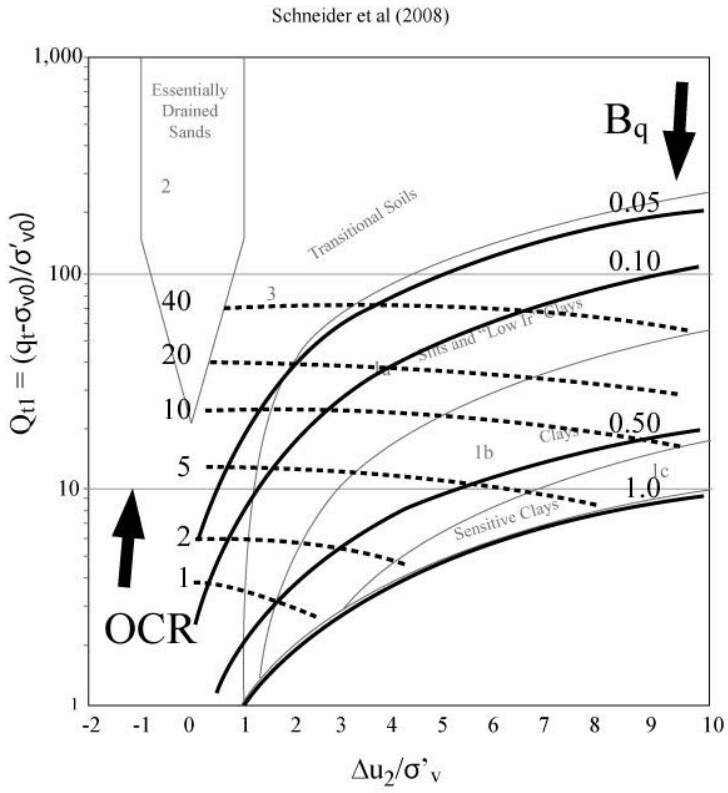

Figure 24 CPT classification chart from Schneider et al (2008) based on ($\Delta u_2/\sigma'_{vo}$) with contours of B_q and OCR

In recent years, the SBT charts have been color coded to aid in the visual presentation of SBT on a CPT profile. An example CPTu profile is shown in Figure 25.

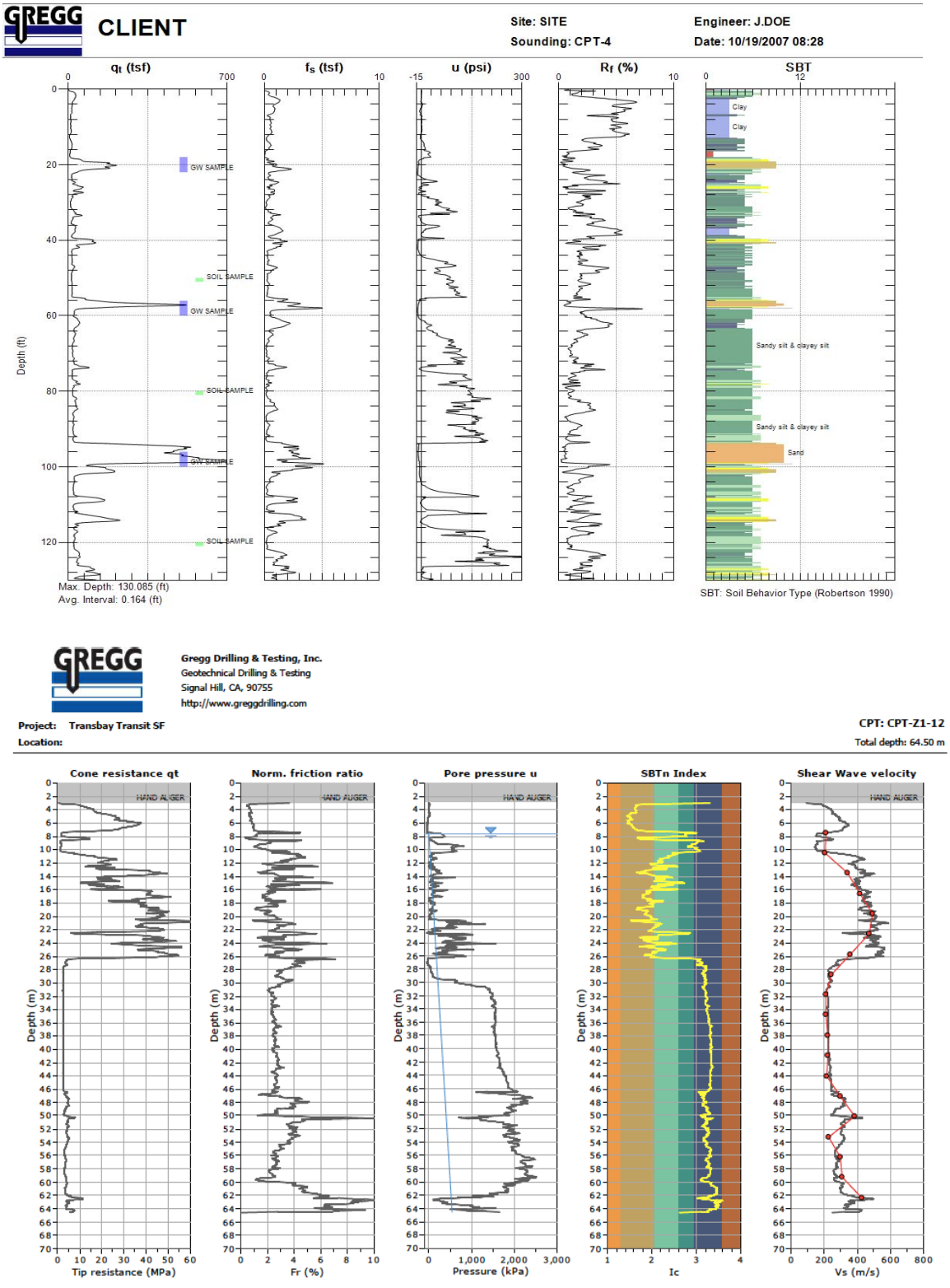

Figure 25 Examples of (a) CPTu and (b) SCPTu
(1 tsf ~ 0.1 MPa, 14.5 psi = 100kPa, 1ft = 0.3048m)

A more general normalized CPT SBT chart, using large strain '*soil behavior*' descriptions, is shown in Figure 26.

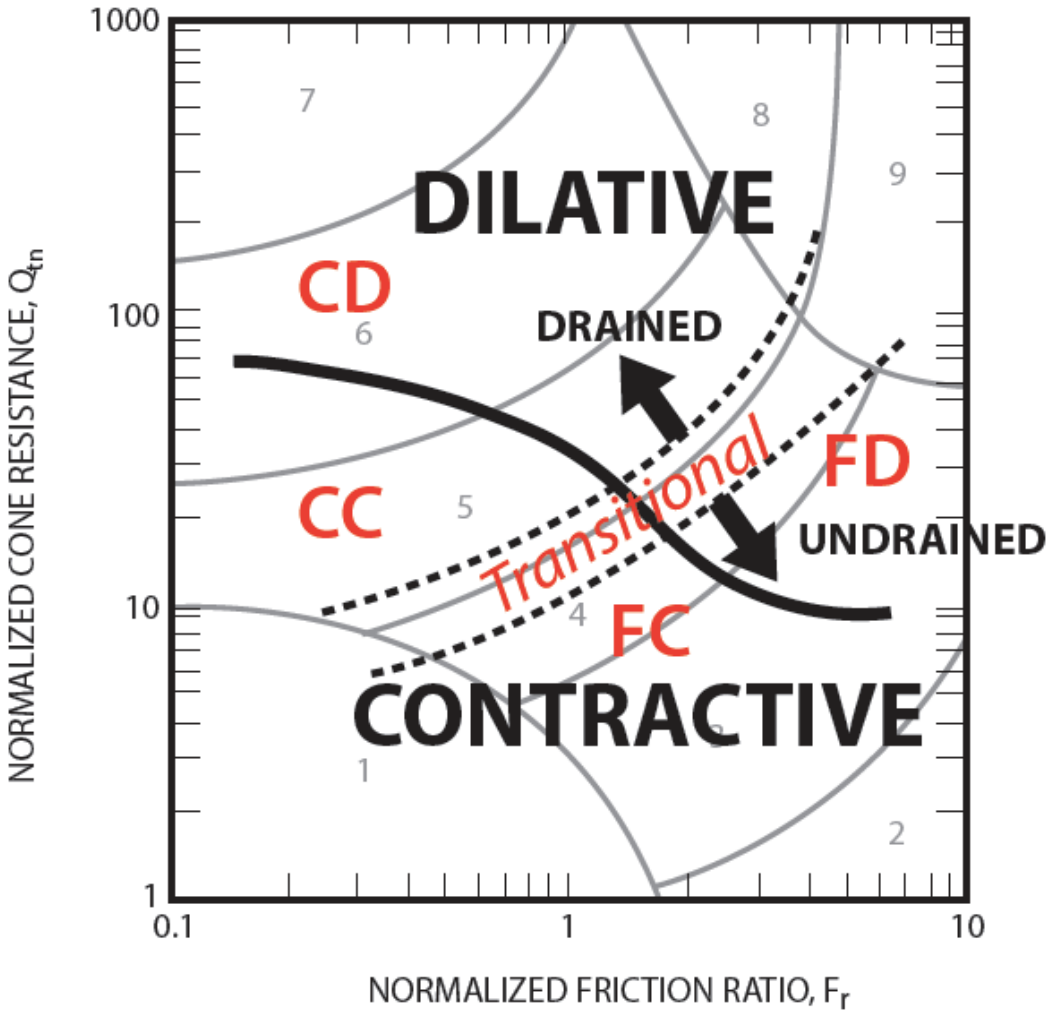

Figure 26 Normalized CPT Soil Behavior Type (SBT_n) chart, Q_t - F using general large strain '*soil behavior*' descriptors

(Modified from Robertson, 2012)

CD	Coarse-grained Dilative soil – predominately drained CPT
CC	Coarse-grained Contractive soil – predominately drained CPT
FD	Fine-grained Dilative soil – predominately undrained CPT
FC	Fine-grained Contractive – predominately undrained CPT

Equivalent SPT N_{60} Profiles

The Standard Penetration Test (SPT) is one of the most commonly used in-situ tests in many parts of the world, especially North and South America. Despite continued efforts to standardize the SPT procedure and equipment there are still problems associated with its repeatability and reliability. However, many geotechnical engineers have developed considerable experience with design methods based on local SPT correlations. When these engineers are first introduced to the CPT they initially prefer to see CPT results in the form of equivalent SPT N-values. Hence, there is a need for reliable CPT/SPT correlations so that CPT data can be used in existing SPT-based design approaches.

There are many factors affecting the SPT results, such as borehole preparation and size, sampler details, rod length and energy efficiency of the hammer-anvil-operator system. One of the most significant factors is the energy efficiency of the SPT system. This is normally expressed in terms of the rod energy ratio (ER_r). An energy ratio of about 60% has generally been accepted as the reference value that represents the approximate historical average SPT energy.

A number of studies have been presented over the years to relate the SPT N value to the CPT cone penetration resistance, q_c. Robertson et al. (1983) reviewed these correlations and presented the relationship shown in Figure 26 relating the ratio $(q_c/p_a)/N_{60}$ with mean grain size, D_{50} (varying between 0.001mm to 1mm). Values of q_c are made dimensionless when dividing by the atmospheric pressure (p_a) in the same units as q_c. It is observed that the ratio increases with increasing grain size.

The values of N used by Robertson et al. correspond to an average energy ratio of about 60%. Hence, the ratio applies to $N_{60,}$ as shown on Figure 27. Other studies have linked the ratio between the CPT and SPT with fines content for sandy soils.

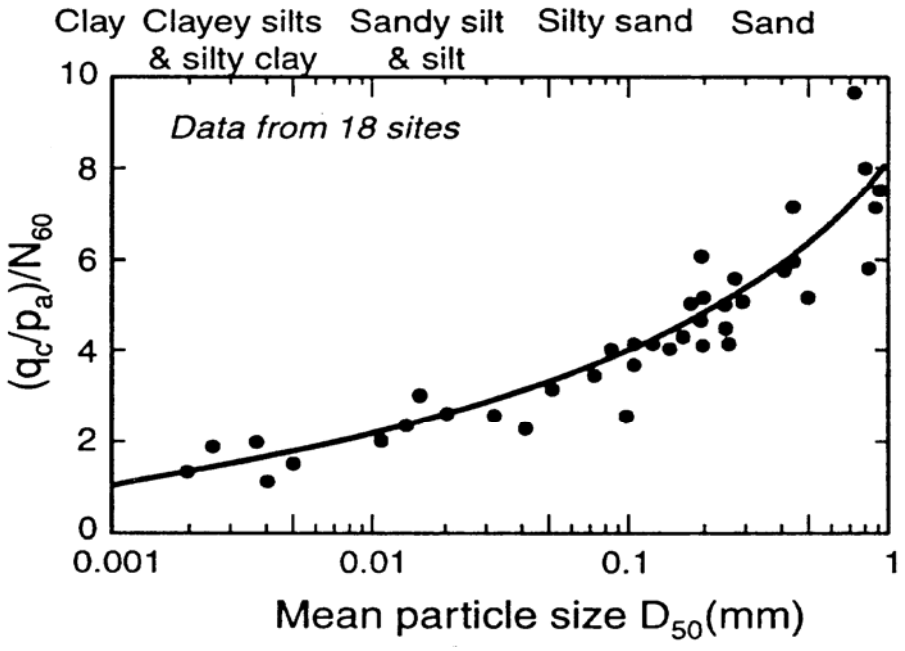

Figure 27 CPT-SPT correlations with mean grain size
(Robertson et al., 1983)

The above correlations require the soil grain size information to determine the mean grain size (or fines content). Grain characteristics can be estimated directly from CPT results using soil behavior type (SBT) charts. The CPT SBT charts show a clear trend of increasing friction ratio with increasing fines content and decreasing grain size. Robertson et al. (1986) suggested $(q_c/p_a)/N_{60}$ ratios for each soil behavior type zone using the non-normalized CPT chart.

The suggested $(q_c/p_a)/N_{60}$ ratio for each soil behavior type is given in Table 5.

These values provide a reasonable estimate of SPT N_{60} values from CPT data. For simplicity the above correlations are given in terms of q_c. For fine grained soft soils the correlations should be applied to total cone resistance, q_t. Note that in sandy soils $q_c = q_t$.

One disadvantage of this simplified approach is the somewhat discontinuous nature of the conversion. Often a soil will have CPT data that cover different SBT zones and hence produces discontinuous changes in predicted SPT N_{60} values.

Zone	*Soil Behavior Type (SBT)*	$\frac{(q_c/p_a)}{N_{60}}$
1	*Sensitive fine grained*	2.0
2	*Organic soils – clay*	1.0
3	*Clays: clay to silty clay*	1.5
4	*Silt mixtures: clayey silt & silty clay*	2.0
5	*Sand mixtures: silty sand to sandy silt*	3.0
6	*Sands: clean sands to silty sands*	5.0
7	*Dense sand to gravelly sand*	6.0
8	*Very stiff sand to clayey sand**	5.0
9	*Very stiff fine-grained**	1.0

Table 5 Suggested $(q_c/p_a)/N_{60}$ ratios

Jefferies and Davies (1993) suggested the application of the soil behavior type index, I_c to link with the CPT-SPT correlation. The soil behavior type index, I_c, can be combined with the CPT-SPT ratios to give the following simple relationship:

$$\frac{(q_t/p_a)}{N_{60}} = 8.5\left(1 - \frac{I_c}{4.6}\right)$$

Robertson (2012) suggested an update of the above relationship that provides improved estimates of N_{60} for insensitive clays:

$$\frac{(q_t/p_a)}{N_{60}} = 10^{(1.1268 - 0.2817Ic)}$$

Jefferies and Davies (1993) suggested that the above approach can provide better estimates of the SPT N_{60}-values than the actual SPT test due to the poor repeatability of the SPT. In fine-grained soils with high sensitivity, the above relationship may overestimate the equivalent N_{60}.

In very loose soils with $(N_1)_{60} < 10$, the weight of the rods and hammer can dominate the SPT penetration resistance and produce very low N-values, which can result in high $(q_t/p_a)/N_{60}$ ratios due to the low SPT N-values measured.

Soil Unit Weight (γ)

Soil total unit weights (γ) are best obtained by obtaining relatively undisturbed samples (e.g., thin-walled Shelby tubes; piston samples) and weighing a known volume of soil. When this is not feasible, the total unit weight can be estimated from CPT results, such as Figure 28 and the following relationship (Robertson, 2010):

$$\gamma/\gamma_w = 0.27\ [\log R_f] + 0.36\ [\log(q_t/p_a)] + 1.236$$

where R_f = friction ratio = $(f_s/q_t)100$ %
γ_w = unit weight of water in same units as γ
p_a = atmospheric pressure in same units as q_t

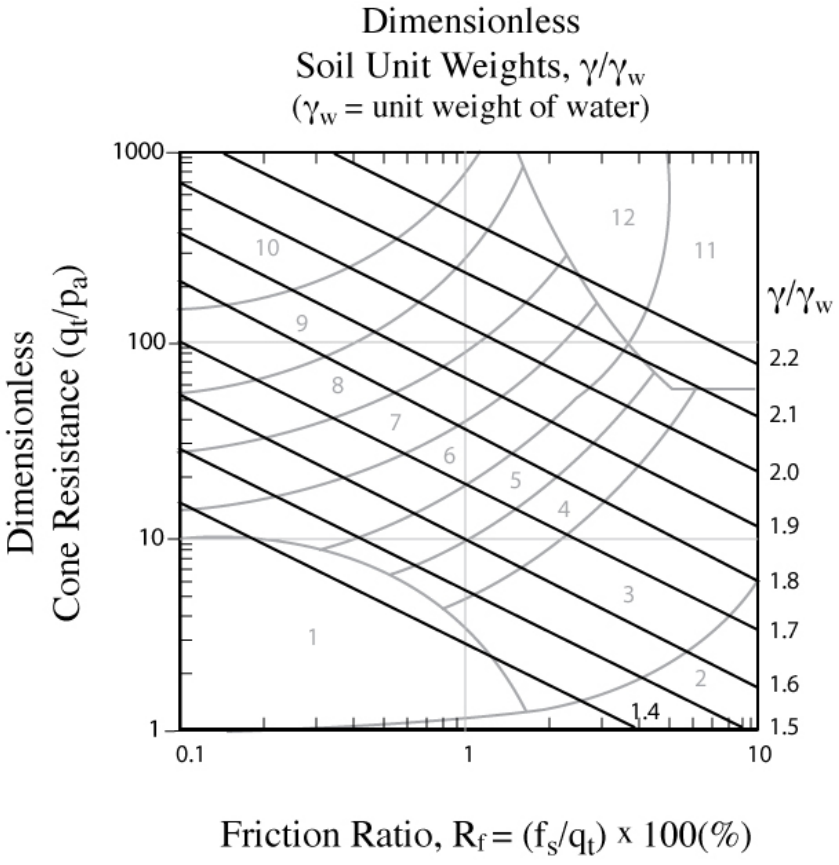

Figure 28 Dimensionless soil unit weight, γ/γ_w based on CPT

Undrained Shear Strength (s_u)

No single value of undrained shear strength, s_u, exists, since the undrained response of soil depends on the direction of loading, soil anisotropy, strain rate, and stress history. Typically the undrained strength in tri-axial compression is larger than in simple shear that is larger than tri-axial extension ($s_{uTC} > s_{uSS} > s_{uTE}$). The value of s_u to be used in analysis therefore depends on the design problem. In general, the simple shear direction of loading often represents the average undrained strength ($s_{uSS} \sim s_{u(ave)}$).

Since anisotropy and strain rate will inevitably influence the results of all in-situ tests, their interpretation will necessarily require some empirical content to account for these factors, as well as possible effects of sample disturbance.

Theoretical solutions have provided valuable insight into the form of the relationship between cone resistance and s_u. All theories result in a relationship between corrected cone resistance, q_t, and s_u of the form:

$$s_u = \frac{q_t - \sigma_v}{N_{kt}}$$

Typically N_{kt} varies from 10 to 18, with 14 as an average for $s_{u(ave)}$. N_{kt} tends to increase with increasing plasticity and decrease with increasing soil sensitivity. Lunne et al., 1997 showed that N_{kt} decreases as B_q increases. In very sensitive fine-grained soil, where $B_q \sim 1.0$, N_{kt} can be as low as 6.

For deposits where little experience is available, estimate s_u using the corrected cone resistance (q_t) and preliminary cone factor values (N_{kt}) from 14 to 16. For a more conservative estimate, select a value close to the upper limit.

In very soft clays, where there may be some uncertainty with the accuracy in q_t, estimates of s_u can be made from the excess pore pressure (Δu) measured behind the cone (u_2) using the following:

$$s_u = \frac{\Delta u}{N_{\Delta u}}$$

Where $N_{\Delta u}$ varies from 4 to 10. For a more conservative estimate, select a value close to the upper limit. Note that $N_{\Delta u}$ is linked to N_{kt}, via B_q, where:

$$N_{\Delta u} = B_q N_{kt}$$

If previous experience is available in the same deposit, the values suggested above should be adjusted to reflect this experience.

For larger, moderate to high risk projects, where high quality field and laboratory data may be available, site-specific correlations should be developed based on appropriate and reliable values of s_u.

Soil Sensitivity

The sensitivity (S_t) of clay is defined as the ratio of undisturbed peak undrained shear strength to totally remolded undrained shear strength.

The remolded undrained shear strength, $s_{u(Rem)}$, can be assumed equal to the sleeve resistance, f_s. Therefore, the sensitivity of a clay can be estimated by calculating the peak s_u from either site specific or general correlations with q_t or Δu and $s_{u(Rem)}$ from f_s, and can be approximated using the following:

$$S_t = \frac{s_u}{s_{u(Rem)}} = \frac{q_t - \sigma_v}{N_{kt}} (1 / f_s) = 7 / F_r$$

For relatively sensitive clays ($S_t > 10$), the value of f_s can be very low with inherent difficulties in accuracy. Hence, the estimate of sensitivity (and remolded strength) should be used as a guide only.

Undrained Shear Strength Ratio (s_u/σ'_{vo})

It is often useful to estimate the undrained shear strength ratio from the CPT, since this relates directly to overconsolidation ratio (OCR). Critical State Soil Mechanics presents a relationship between the undrained shear strength ratio for normally consolidated clays under different directions of loading and the effective stress friction angle, ϕ'. Hence, a better estimate of undrained shear strength ratio can be obtained with knowledge of the friction angle [$(s_u/\sigma'_{vo})_{NC}$ increases with increasing ϕ']. For normally consolidated clays:

$$(s_u/\sigma'_{vo})_{NC} \sim 0.22 \quad \text{in direct simple shear } (\phi' = 26^o)$$

From the CPT:

$$(s_u/\sigma'_{vo}) = \left(\frac{q_t - \sigma_{vo}}{\sigma'_{vo}}\right)(1/N_{kt}) = Q_t / N_{kt}$$

Since $N_{kt} \sim 14$ $\qquad (s_u/\sigma'_{vo}) \sim 0.071\ Q_t$

For a normally consolidated clay where $(s_u/\sigma'_{vo})_{NC} \sim 0.22$;

$$Q_t = 3 \text{ to } 4 \quad \text{for NC insensitive clay}$$

Based on the assumption that the sleeve resistance, f_s, is a direct measure of the remolded shear strength, $s_{u(Rem)} = f_s$

Therefore:

$$s_{u(Rem)}/\sigma'_{vo} = f_s/\sigma'_{vo} = (F \,.\, Q_t)/100$$

Hence, it is possible to represent $(s_{u(Rem)}/\sigma'_{vo})$ contours on the normalized SBT_n chart (Robertson, 2009). These contours also represent OCR for insensitive clays with high values of (s_u/σ'_{vo}) and sensitivity for low values of (s_u/σ'_{vo}).

Stress History - Overconsolidation Ratio (OCR)

Overconsolidation ratio (OCR) is defined as the ratio of the maximum past effective consolidation stress and the present effective overburden stress:

$$OCR = \frac{\sigma'_p}{\sigma'_{vo}}$$

For mechanically overconsolidated soils where the only change has been the removal of overburden stress, this definition is appropriate. However, for cemented and/or aged soils the OCR may represent the ratio of the yield stress and the present effective overburden stress. The yield stress ratio (YSR) will also depend on the direction and type of loading. For overconsolidated clays:

$$(s_u/\sigma'_{vo})_{OC} = (s_u/\sigma'_{vo})_{NC} (OCR)^{0.8}$$

Based on this, Robertson (2009) suggested:

$$OCR = 0.25 (Q_t)^{1.25}$$

Kulhawy and Mayne (1990) suggested a simpler method:

$$OCR = k \left(\frac{q_t - \sigma_{vo}}{\sigma'_{vo}} \right) = k\, Q_t \qquad \text{or} \qquad \sigma'_p = k\,(q_t - \sigma_{vo})$$

An average value of k = 0.33 can be assumed, with an expected range of 0.2 to 0.5. Higher values of k are recommended in aged, heavily overconsolidated clays. If previous experience is available in the same deposit, the values of k should be adjusted to reflect this experience and to provide a more reliable profile of OCR. The simpler Kulhawy and Mayne approach is valid for $Q_t < 20$. For larger, moderate to high-risk projects, where additional high quality field and laboratory data may be available, site-specific correlations should be developed based on consistent and relevant values of OCR.

Mayne (2012) suggested an extension of this approach that can be applied to all soils based on the following: $\sigma'_p = 0.33(q_t - \sigma_{vo})^m (p_a/100)^{1-m}$

where m is a function of SBT I_c ($m \sim 0.72$ in young, uncemented silica sand and $m \sim 1.0$ in intact clay).

In-Situ Stress Ratio (K_o)

There is no reliable method to determine K_o from CPT. However, an estimate can be made in fine-grained soils based on an estimate of OCR, as shown in Figure 29.

Kulhawy and Mayne (1990) suggested a simpler approach, using:

$$K_o = (1 - \sin\phi') (OCR)^{\sin\phi'}$$

That can be approximated (for low plastic fine-grained soils) to:

$$K_o \sim 0.5 (OCR)^{0.5}$$

These approaches are generally limited to mechanically overconsolidated, fine-grained soils. Considerable scatter exists in the database used for these correlations and therefore they must be considered only as a guide.

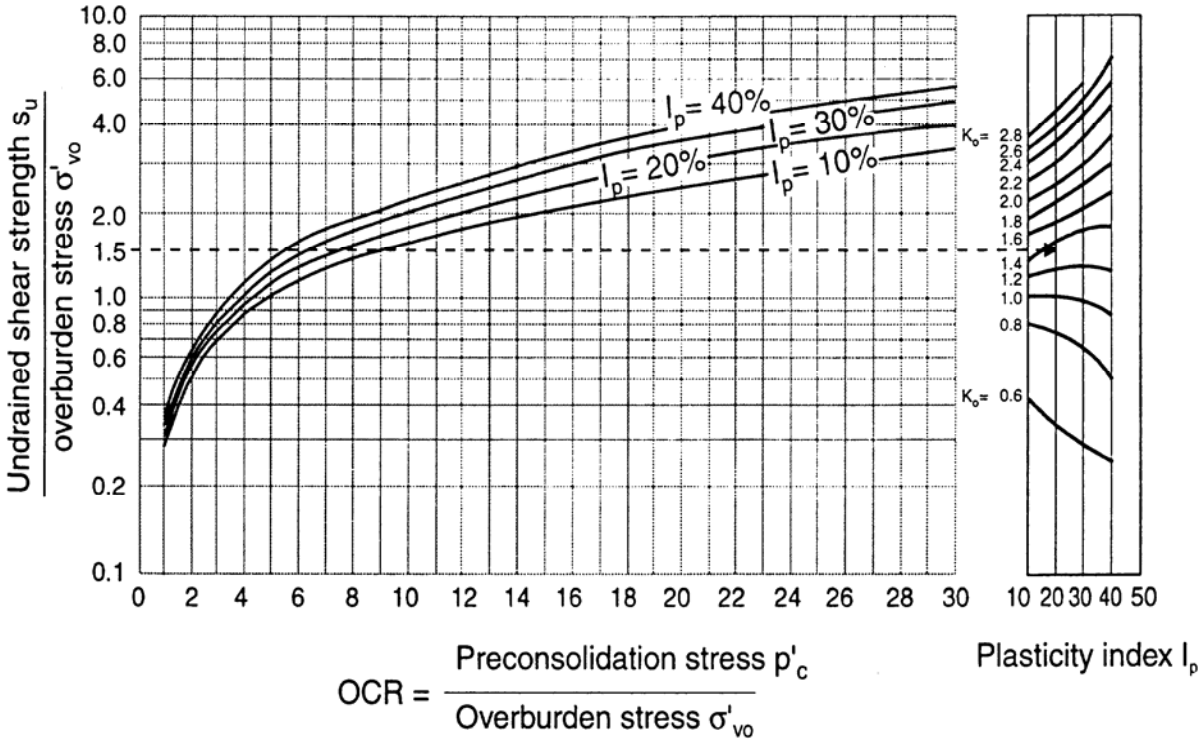

Figure 29 OCR and K_o from s_u/σ'_{vo} and Plasticity Index, I_p (after Andresen et al., 1979)

Relative Density (D_r)

For coarse-grained soils, the density, or more commonly, the relative density or density index, is often used as an intermediate soil parameter. Relative density, D_r, or density index, I_D, is defined as:

$$I_D = D_r = \frac{e_{max} - e}{e_{max} - e_{min}}$$

where:

> e_{max} and e_{min} are the maximum and minimum void ratios and e is the in-situ void ratio.

The problems associated with the determination of e_{max} and e_{min} are well known. Also, research has shown that the stress strain and strength behavior of coarse-grained soils is too complicated to be represented by only the relative density of the soil. However, for many years relative density has been used by engineers as a parameter to describe sand deposits.

Research using large calibration chambers has provided numerous correlations between CPT penetration resistance and relative density for clean, predominantly quartz sands. The calibration chamber studies have shown that the CPT resistance is controlled by sand density, in-situ vertical and horizontal effective stress and sand compressibility. Sand compressibility is controlled by grain characteristics, such as grain size, shape and mineralogy. Angular sands tend to be more compressible than rounded sands as do sands with high mica and/or carbonate compared with clean quartz sands. More compressible sands give a lower penetration resistance for a given relative density then less compressible sands.

Based on extensive calibration chamber testing on Ticino sand, Baldi et al. (1986) recommended a formula to estimate relative density from q_c. A modified version of this formula, to obtain D_r from q_{c1} is as follows:

$$D_r = \left(\frac{1}{C_2}\right) \ln\left(\frac{Q_{cn}}{C_0}\right)$$

where:

C_0 and C_2 are soil constants

σ'_{vo} = effective vertical stress

Q_{cn} = $(q_c / p_a) / (\sigma'_{vo}/p_a)^{0.5}$
= normalized CPT resistance, corrected for overburden pressure (more recently defined as Q_{tn}, using net cone resistance, q_n)

p_a = reference pressure of 1 tsf (100kPa), in same units as q_c and σ'_{vo}

q_c = cone penetration resistance (more correctly, q_t)

For moderately compressible, normally consolidated, unaged and uncemented, predominantly quartz sands the constants are: $C_o = 15.7$ and $C_2 = 2.41$.

Kulhawy and Mayne (1990) suggested a simpler relationship for estimating relative density:

$$D_r^2 = \frac{Q_{cn}}{305\, Q_C\, Q_{OCR}\, Q_A}$$

where:

Q_{cn} and p_a are as defined above

Q_C = Compressibility factor ranges from 0.90 (low compress.) to 1.10 (high compress.)

Q_{OCR} = Overconsolidation factor = $OCR^{0.18}$

Q_A = Aging factor = $1.2 + 0.05 \log(t/100)$

A constant of 350 is more reasonable for medium, clean, uncemented, unaged quartz sands that are about 1,000 years old. The constant can be closer to 300 for fine sands and closer to 400 for coarse sands. The constant increases with age and increases significantly when age exceeds 10,000 years. The relationship can then be simplified for most young, uncemented silica-based sands to:

$$D_r^2 = Q_{tn} / 350$$

State Parameter (ψ)

The state parameter (ψ) is defined as the difference between the current void ratio, e and the void ratio at critical state $e_{cs,}$ at the same mean effective stress for coarse-grained (sandy) soils. Based on critical state concepts, Jefferies and Been (2006) provide a detailed description of the evaluation of soil state using the CPT. They describe in detail that the problem of evaluating state from CPT response is complex and depends on several soil parameters. The main parameters are essentially the shear stiffness, shear strength, compressibility and plastic hardening. Jefferies and Been (2006) provide a description of how state can be evaluated using a combination of laboratory and in-situ tests. They stress the importance of determining the in-situ horizontal effective stress and shear modulus using in-situ tests and determining the shear strength, compressibility and plastic hardening parameters from laboratory testing on reconstituted samples. They also show how the problem can be assisted using numerical modeling. For high-risk projects a detailed interpretation of CPT results using laboratory results and numerical modeling can be appropriate (e.g. Shuttle and Cunning, 2007), although soil variability can complicate the interpretation procedure. Some unresolved concerns with the Jefferies and Been (2006) approach relate to the stress normalization using n = 1.0 for all soils, and the influence of soil fabric in sands with high fines content.

For low risk projects and in the initial screening for high-risk projects there is a need for a simple estimate of soil state. Plewes et al (1992) provided a means to estimate soil state using the normalized soil behavior type (SBT_n) chart suggested by Jefferies and Davies (1991). Jefferies and Been (2006) updated this approach using the normalized SBT_n chart based on the parameter $Q_t (1-B_q) +1$. Robertson (2009) expressed concerns about the accuracy and precision of the Jefferies and Been (2006) normalized parameter in soft soils. In sands, where $B_q = 0$, the normalization suggested by Jefferies and Been (2006) is the same as Robertson (1990).

Based on the data presented by Jefferies and Been (2006) and Shuttle and Cunning (2007) as well the measurements from the CANLEX project (Wride et al, 2000) for predominantly, coarse-grained uncemented young soils, combined with the link between OCR and state parameter in fine-grained soil, Robertson (2009) developed contours of state parameter (ψ) on the updated SBT_n $Q_{tn} - F$ chart for uncemented, Holocene-age soils. The contours of ψ, that are shown on Figure 30, are approximate since stress state and plastic hardening will also

influence the estimate of in-situ soil state in the coarse-grained region of the chart (i.e. when $I_c < 2.60$) and soil sensitivity for fine-grained soils. Jefferies and Been (2006) suggested that soils with a state parameter less than -0.05 (i.e. $\psi < -0.05$) are dilative at large strains.

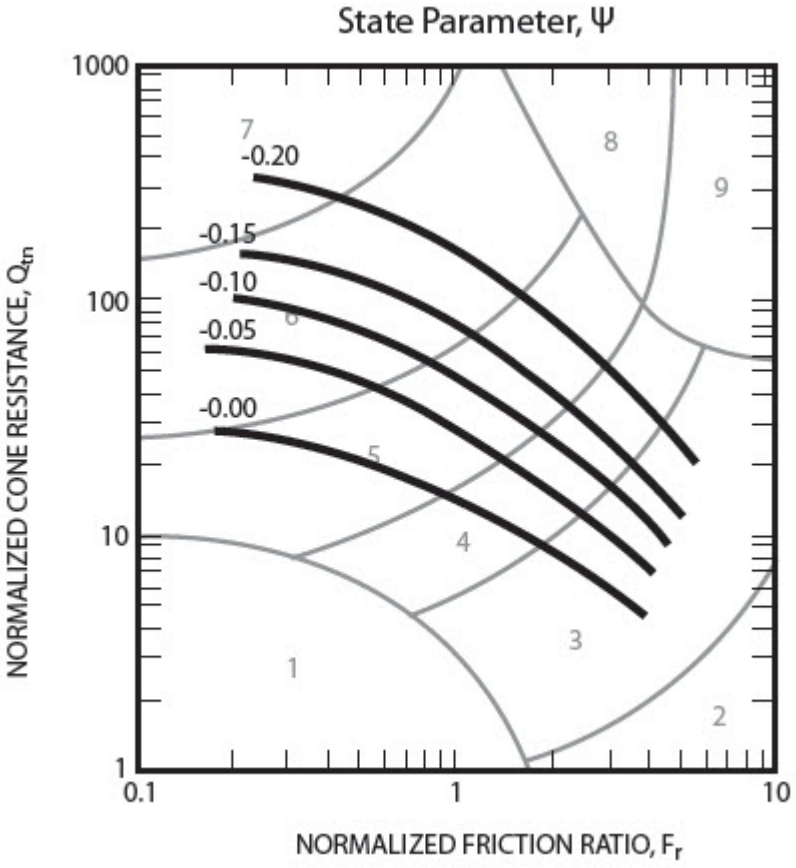

Figure 30 Contours of estimated state parameter, ψ (thick lines), on normalized SBT_n $Q_{tn} - F_r$ chart for uncemented Holocene-age soils (after Robertson, 2009)

Robertson (2010) suggested a simplified and approximate relationship between ψ and the clean sand equivalent normalized cone resistance, $Q_{tn,cs}$, as follows:

$$\psi = 0.56 - 0.33 \log Q_{tn,cs}$$

The clean sand equivalent normalized cone resistance, $Q_{tn,cs}$ evolved from the study of liquefaction case histories and details are provided in a later section on "*Seismic Design – Liquefaction*" (see Figure 46).

Friction Angle (ϕ')

The shear strength of uncemented, coarse-grained soils is usually expressed in terms of a peak secant friction angle, ϕ'.

Significant advances have been made in the development of theories to model the cone penetration process in sands (Yu and Mitchell, 1998). Cavity expansion models show the most promise since they are relatively simple and can incorporate many of the important features of soil response. However, empirical correlations based on calibration chamber test results and field results are still the most commonly used.

Robertson and Campanella (1983) suggested a correlation to estimate the peak friction angle (ϕ') for uncemented, unaged, moderately compressible, predominately quartz sands based on calibration chamber test results. For sands of higher compressibility (i.e. carbonate sands or sands with high mica content), the method will tend to predict low friction angles.

$$\tan \phi' = \frac{1}{2.68}\left[\log\left(\frac{q_c}{\sigma'_{vo}}\right) + 0.29\right]$$

Kulhawy and Mayne (1990) suggested an alternate relationship for clean, rounded, uncemented quartz sands, and evaluated the relationship using high quality field data:

$$\phi' = 17.6 + 11 \log (Q_{tn})$$

Jefferies and Been (2006) showed a strong link between state parameter (ψ) and the peak friction angle (ϕ') for a wide range of sands. Using this link, it is possible to link $Q_{tn,cs}$ with ϕ', using:

$$\phi' = \phi'_{cv} - 48\ \psi$$

Where ϕ'_{cv} = constant volume (or critical state) friction angle depending on mineralogy (Bolton, 1986), typically about 33 degrees for quartz sands but can be as high as 40 degrees for felspathic and carbonate sands.

Hence, the relationship between normalized clean sand equivalent cone resistance, $Q_{tn,cs}$ and ϕ' becomes:

$$\phi' = \phi'_{cv} + 15.84\ [\log Q_{tn,cs}] - 26.88$$

The above relationship produces estimates of peak friction angle for clean quartz sands that are similar to those by Kulhawy and Mayne (1990). However, the above relationship based on state parameter has the advantage that it includes the importance of grain characteristics and mineralogy that are reflected in both ϕ'_{cv}, as well as soil type through $Q_{tn,cs}$. The above relationship tends to predict ϕ' values closer to measured values in calcareous sands where the CPT tip resistance can be low for high values of ϕ'.

For fine-grained soils, the best means for defining the effective stress peak friction angle is from consolidated triaxial tests on high quality undisturbed samples. An assumed value of $\phi' = 28°$ for clays and 32° for silts is often sufficient for many low-risk projects. Alternatively, an effective stress limit plasticity solution for undrained cone penetration developed at the Norwegian Institute of Technology (NTH: Senneset et al., 1989) allows the approximate evaluation of effective stress parameters (c' and ϕ') from piezocone (u_2) measurements. In a simplified approach for normally- to lightly-overconsolidated clays and silts (c' = 0), the NTH solution can be approximated for the following ranges of parameters: $20^o \leq \phi' \leq 40^o$ and $0.1 \leq B_q \leq 1.0$ (Mayne 2006):

$$\phi' \text{ (deg)} = 29.5^o \cdot B_q^{0.121}\ [0.256 + 0.336 \cdot B_q + \log Q_t]$$

For heavily overconsolidated soils, fissured geomaterials, and highly cemented or structured clays, the above will not provide reliable results and should be determined by laboratory testing on high quality undisturbed samples. The above approach is only valid when positive (u_2) pore pressures are recorded (i.e. $B_q > 0.1$).

Stiffness and Modulus

CPT data can be used to estimate modulus in soils for subsequent use in elastic or semi-empirical settlement prediction methods. However, correlations between q_c and Young's moduli (E) are sensitive to stress and strain history, aging and soil mineralogy.

A useful guide for estimating Young's moduli for young, uncemented predominantly silica sands is given in Figure 31. The modulus has been defined as that mobilized at about 0.1% strain. For more heavily loaded conditions (i.e. larger strain) the modulus would decrease (see "*Applications*" section).

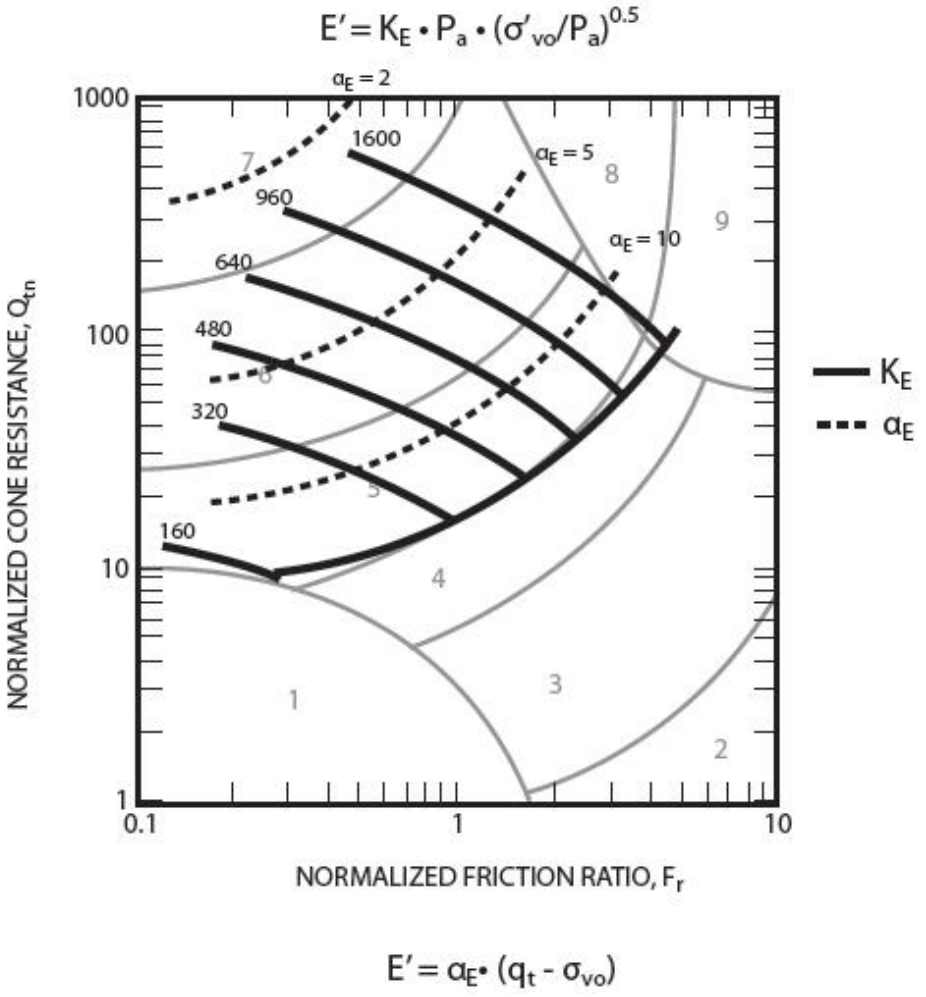

Figure 31 Evaluation of drained Young's modulus (at ~ 0.1% strain) from CPT for young, uncemented silica sands, $E = \alpha_E (q_t - \sigma_{vo})$
where: $\alpha_E = 0.015 [10^{(0.55Ic + 1.68)}]$

Modulus from Shear Wave Velocity

A major advantage of the seismic CPT (SCPT) is the additional measurement of the shear wave velocity, V_s. The shear wave velocity is measured using a downhole technique during pauses in the CPT resulting in a continuous profile of V_s. Elastic theory states that the small strain shear modulus, G_o can be determined from:

$$G_o = \rho V_s^2$$

Where: ρ is the mass density of the soil ($\rho = \gamma/g$) and G_o is the small strain shear modulus (shear strain, $\gamma < 10^{-4}$ %).

Hence, the addition of shear wave velocity during the CPT provides a direct measure of small strain soil stiffness.

The small strain shear modulus represents the elastic stiffness of the soil at shear strains (γ) less than 10^{-4} percent. Elastic theory also states that the small strain Young's modulus, E_o is linked to G_o, as follows;

$$E_o = 2(1 + \upsilon)G_o$$

where: υ is Poisson's ratio, which ranges from 0.1 to 0.3 for most soils.

Application to engineering problems requires that the small strain modulus be softened to the appropriate strain level. For most well designed structures the degree of softening is often close to a factor of about 2.5. Hence, for many applications the equivalent Young's modulus (E') can be estimated from:

$$E' \sim G_o = \rho V_s^2$$

Further details regarding appropriate use of soil modulus for design is given in the section on *Applications of CPT Results*.

The shear wave velocity can also be used directly for the evaluation of liquefaction potential. Hence, the SCPT provides two independent methods to evaluate liquefaction potential.

Estimating Shear Wave Velocity from CPT

Shear wave velocity can be correlated to CPT cone resistance as a function of soil type and SBT I_c. Shear wave velocity is sensitive to age and cementation, where older deposits of the same soil have higher shear wave velocity (i.e. higher stiffness) than younger deposits. Based on SCPT data, Figure 32 shows a relationship between normalized CPT data (Q_{tn} and F_r) and normalized shear wave velocity, V_{s1}, for uncemented Holocene to Pleistocene age soils, where:

$$V_{s1} = V_s \, (p_a / \sigma'_{vo})^{0.25}$$

V_{s1} is in the same units as V_s (e.g. either m/s or ft/s). Younger Holocene age soils tend to plot toward the center and lower left of the SBT_n chart whereas older Pleistocene age soil tend to plot toward the upper right part of the chart.

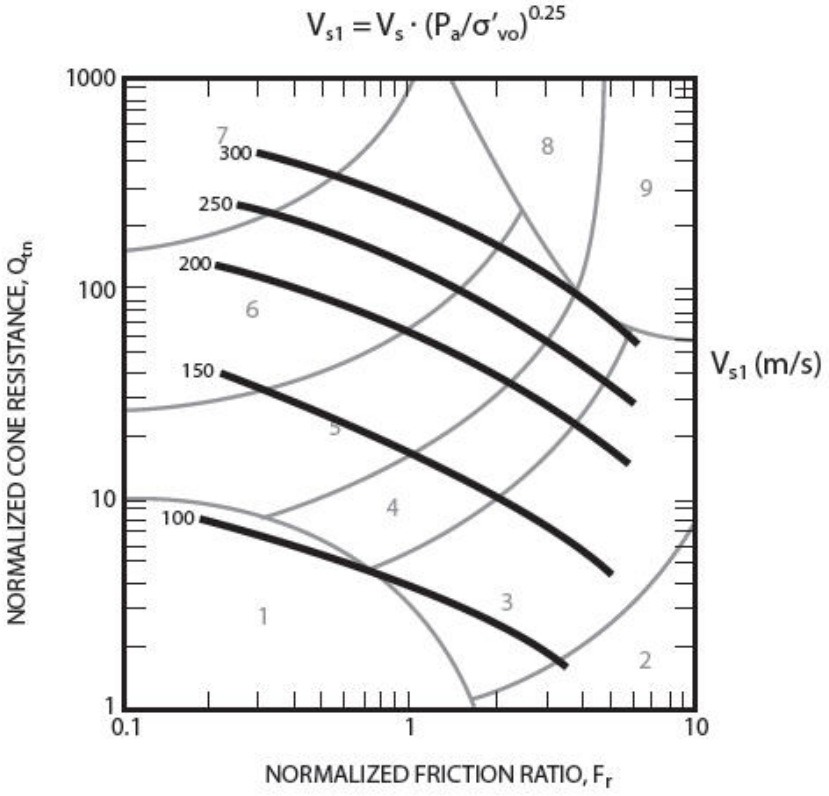

Figure 32 Evaluation of normalized shear wave velocity, V_{s1}, from CPT for uncemented Holocene and Pleistocene age soils (1m/s = 3.28 ft/sec)

$$V_s = [\alpha_{vs} \; (q_t - \sigma_v)/p_a]^{0.5} \; \text{(m/s)}; \; \text{where } \alpha_{vs} = 10^{(0.55\, Ic + 1.68)}$$

Identification of soils with unusual characteristics using the SCPT

Almost all available empirical correlations to interpret in-situ tests assume that the soil is '*well behaved*' with no microstructure, i.e. similar to soils in which the correlation was based. Most existing correlations apply to silica-based soils that are young and uncemented. Application of existing empirical correlations in soils that are not young and uncemented can produce incorrect interpretations. Hence, it is important to be able to identify soils with *'unusual'* characteristics (i.e. microstructure). The cone resistance (q_t) is a measure of large strain soil strength and the shear wave velocity (V_s) is a measure of small strain soil stiffness (G_o). Research has shown that young uncemented sands have data that fall within a narrow range of combined q_t and G_o, as shown in Figure 33. Most young (Holocene-age), uncemented, coarse-grained soils (Schneider and Moss, 2011) have a modulus number, $K_G < 330$, where:

$$K_G = [G_o/q_t]\, Q_{tn}^{0.75}$$

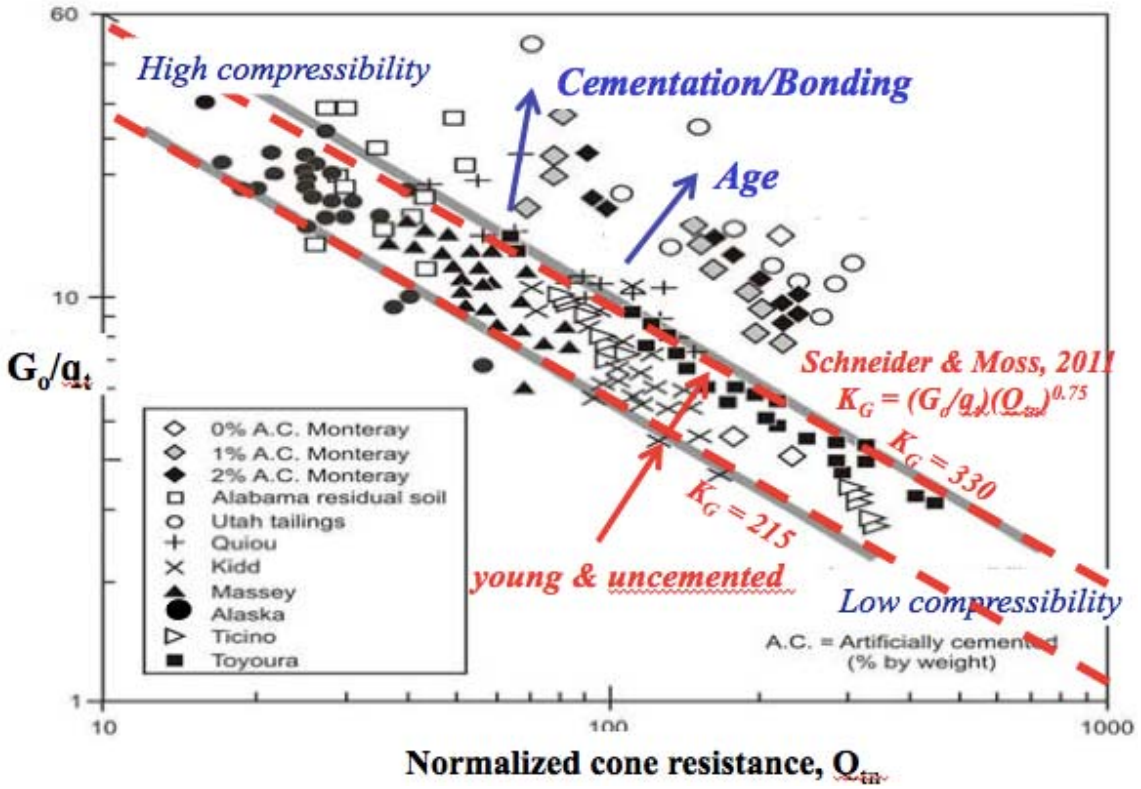

Figure 33 Characterization of uncemented, unaged sands
(modified from Eslaamizaad and Robertson, 1997)

Hydraulic Conductivity (k)

An approximate estimate of soil hydraulic conductivity or coefficient of permeability, *k*, can be made from an estimate of soil behavior type using the CPT SBT charts. Table 6 provides estimates based on the CPT-based SBT charts shown in Figures 21 and 22. These estimates are approximate at best, but can provide a guide to variations of possible permeability.

SBT Zone	SBT	Range of *k* (m/s)	SBT_n I_c
1	Sensitive fine-grained	$3x10^{-10}$ to $3x10^{-8}$	*NA*
2	Organic soils - clay	$1x10^{-10}$ to $1x10^{-8}$	$I_c > 3.60$
3	Clay	$1x10^{-10}$ to $1x10^{-9}$	$2.95 < I_c < 3.60$
4	Silt mixture	$3x10^{-9}$ to $1x10^{-7}$	$2.60 < I_c < 2.95$
5	Sand mixture	$1x10^{-7}$ to $1x10^{-5}$	$2.05 < I_c < 2.60$
6	Sand	$1x10^{-5}$ to $1x10^{-3}$	$1.31 < I_c < 2.05$
7	Dense sand to gravelly sand	$1x10^{-3}$ to 1	$I_c < 1.31$
8	*Very dense/ stiff soil	$1x10^{-8}$ to $1x10^{-3}$	*NA*
9	*Very stiff fine-grained soil	$1x10^{-9}$ to $1x10^{-7}$	*NA*

**Overconsolidated and/or cemented*

Table 6 Estimated soil permeability (k) based on the CPT SBT chart by Robertson (2010) shown in Figures 21 and 22

The average relationship between soil permeability (*k*) and SBT_n I_c, shown in Table 6, can be represented by:

When $1.0 < I_c \leq 3.27$ $\quad k = 10^{(0.952 - 3.04\, Ic)}$ m/s

When $3.27 < I_c < 4.0$ $\quad k = 10^{(-4.52 - 1.37\, Ic)}$ m/s

The above relationships can be used to provide an approximate estimate of soil permeability (*k*) and to show the likely variation of soil permeability with depth from a CPT sounding. Since the normalized CPT parameters (Q_{tn} and F_r) respond to the mechanical behavior of the soil and depend on many soil variables, the suggested relationship between *k* and I_c is approximate and should only be used as a guide.

Robertson et al. (1992) presented a summary of available data to estimate the horizontal coefficient of permeability (k_h) from dissipation tests. Since the relationship is also a function of the soil stiffness, Robertson (2010) updated the relationship as shown in Figure 34.

Jamiolkowski et al. (1985) suggested a range of possible values of k_h/k_v for soft clays as shown in Table 7.

Nature of clay	k_h/k_v
No macrofabric, or only slightly developed macrofabric, essentially homogeneous deposits	1 to 1.5
From fairly well- to well-developed macrofabric, e.g. sedimentary clays with discontinuous lenses and layers of more permeable material	2 to 4
Varved clays and other deposits containing embedded and more or less continuous permeable layers	3 to 10

Table 7 Range of possible field values of k_h/k_v for soft clays
(modified from Jamiolkowski et al., 1985)

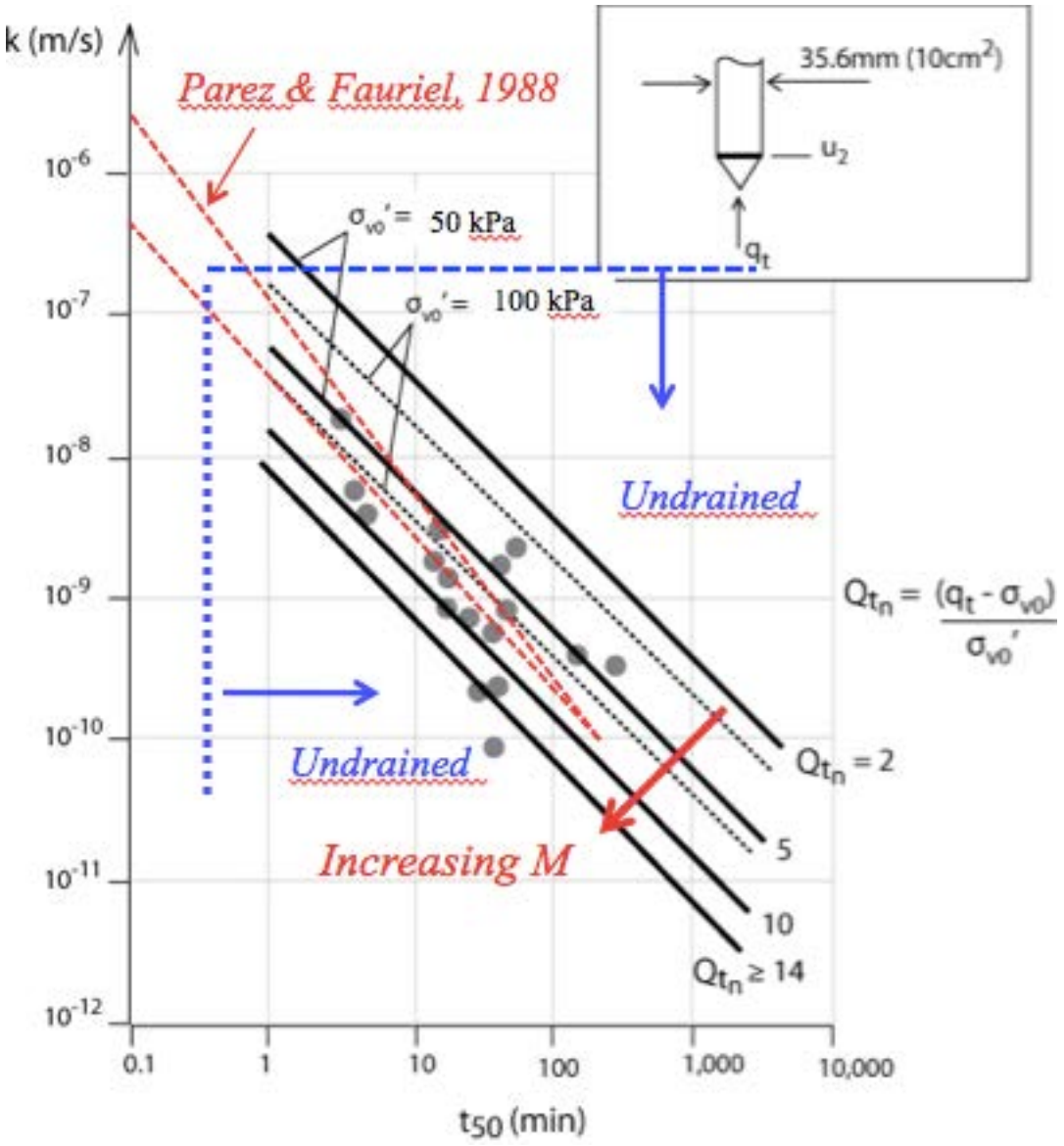

Figure 34 Relationship between CPTu t_{50} (in minutes), based on u_2 pore pressure sensor location and 10cm^2 cone, and soil permeability (k_h) as a function of normalized cone resistance, Q_{tn} (after Robertson 2010)

Consolidation Characteristics

Flow and consolidation characteristics of a soil are normally expressed in terms of the coefficient of consolidation, c, and hydraulic conductivity, k. They are inter-linked through the formula:

$$c = \frac{k\ \mathrm{M}}{\gamma_w}$$

Where: M is the 1-D constrained modulus relevant to the problem (i.e. unloading, reloading, virgin loading).

The parameters c and k vary over many orders of magnitude and are some of the most difficult parameters to measure in geotechnical engineering. It is often considered that accuracy within one order of magnitude is acceptable. Due to soil anisotropy, both c and k have different values in the horizontal (c_h, k_h) and vertical (c_v, k_v) direction. The relevant design values depend on drainage and loading direction.

Details on how to estimate k from CPT soil behavior type charts are given in the previous section.

The coefficient of consolidation can be estimated by measuring the dissipation or rate of decay of pore pressure with time after a stop in CPT penetration. Many theoretical solutions have been developed for deriving the coefficient of consolidation from CPT pore pressure dissipation data. The coefficient of consolidation should be interpreted at 50% dissipation, using the following formula:

$$c = \left(\frac{\mathrm{T_{50}}}{\mathrm{t_{50}}}\right) \mathrm{r_o}^2$$

where:

$\mathrm{T_{50}}$ = theoretical time factor
$\mathrm{t_{50}}$ = measured time for 50% dissipation
$\mathrm{r_o}$ = penetrometer radius

It is clear from this formula that the dissipation time is inversely proportional to the radius of the probe. Hence, in soils of very low permeability, the time for dissipation can be decreased by using smaller diameter probes. Robertson et al. (1992) reviewed dissipation data from around the world and compared the results with the leading theoretical solution by Teh and Houlsby (1991), as shown in Figure 35.

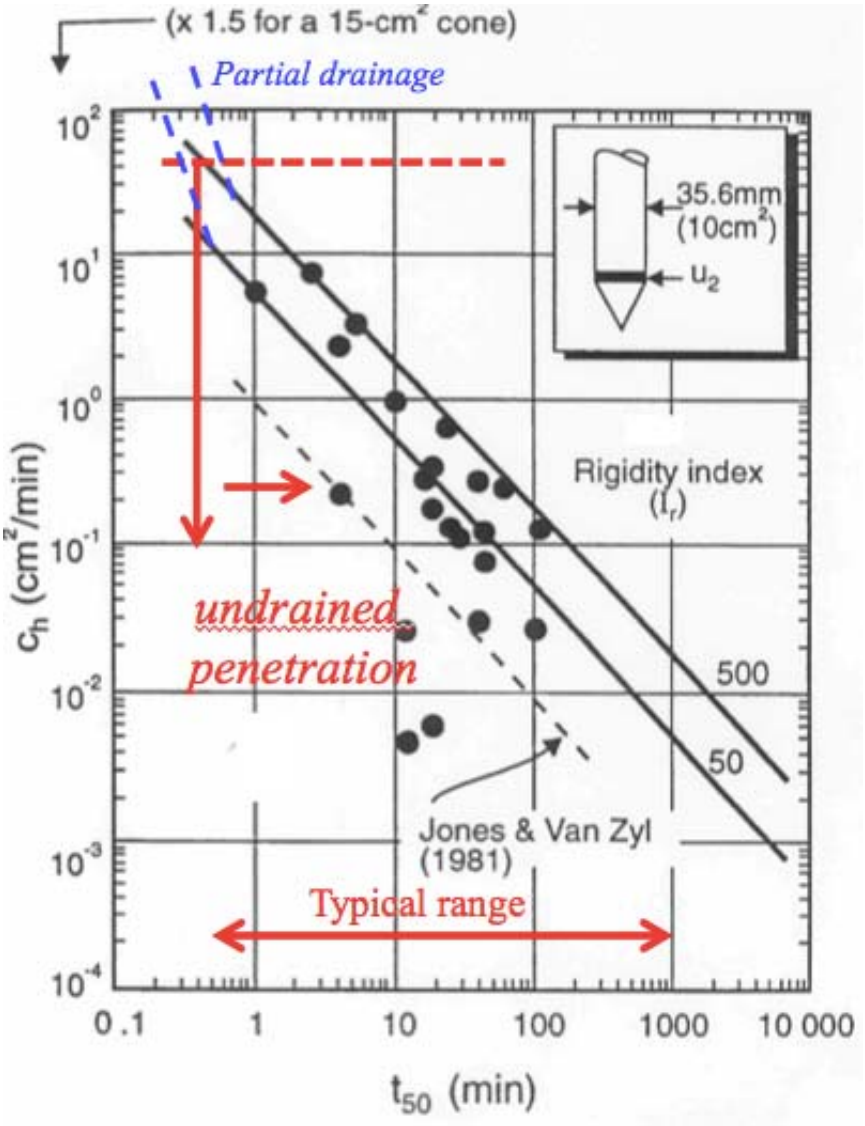

Figure 35 Average laboratory c_h values and CPTU results
(after Robertson et al., 1992, Teh and Houlsby theory shown as solid lines for I_r = 50 and 500).

The review showed that the theoretical solution provided reasonable estimates of c_h. The solution and data shown in Figure 35 apply to a pore pressure sensor located just behind the cone tip (i.e. u_2).

The ability to estimate c_h from CPT dissipation results is controlled by soil stress history, sensitivity, anisotropy, rigidity index (relative stiffness), fabric and structure. In overconsolidated soils, the pore pressure behind the cone tip can be low or negative, resulting in dissipation data that can initially rise before decreasing to the equilibrium value. Care is required to ensure that the dissipation is continued to the correct equilibrium and not stopped prematurely after the initial rise. In these cases, the pore pressure sensor can be moved to the face of the cone or the t_{50} time can be estimated using the maximum pore pressure as the initial value.

Based on available experience, the CPT dissipation method should provide estimates of c_h to within + or – half an order of magnitude. However, the technique is repeatable and provides an accurate measure of changes in consolidation characteristics within a given soil profile.

An approximate estimate of the coefficient of consolidation in the vertical direction can be obtained using the ratios of permeability in the horizontal and vertical direction given in the section on hydraulic conductivity, since:

$$c_v = c_h \left(\frac{k_v}{k_h} \right)$$

Table 7 can be used to provide an estimate of the ratio of hydraulic conductivities.

For relatively short dissipations, the dissipation results can be plotted on a square-root time scale. The gradient of the initial straight line is *m*, where;

$$c_h = (m/M_T)^2 \; r^2 \; (I_r)^{0.5}$$

$M_T = 1.15$ for u_2 position and $10cm^2$ cone (i.e. r = 1.78 cm).

Constrained Modulus

Consolidation settlements can be estimated using the 1-D Constrained Modulus, M, where;

$$M = 1/ m_v = \delta\sigma_v / \delta\varepsilon = 2.3\ (1+e_0)\ \sigma'_{vo} / C_c$$

Where m_v = equivalent oedometer coefficient of compressibility.

Constrained modulus can be estimated from CPT results using the following empirical relationship;

$$M = \alpha_M\ (q_t - \sigma_{vo})$$

Sangrelat (1970) suggested that α_M varies with soil plasticity and natural water content for a wide range of fine-grained soils and organic soils, although the data were based on q_c. Meigh (1987) suggested that α_M lies in the range 2 – 8, whereas Mayne (2001) suggested a general value of 5. Robertson (2009) suggested that α_M varies with Q_t, such that;

When $I_c > 2.2$ (fine-grained soils) use:

$\alpha_M = Q_t$ when $Q_t < 14$

$\alpha_M = 14$ when $Q_t > 14$

When $I_c < 2.2$ (coarse-grained soils) use:

$$\alpha_M = 0.0188\ [10^{(0.55Ic + 1.68)}]$$

Estimates of drained 1-D constrained modulus from undrained cone penetration will be approximate. Estimates can be improved with additional information about the soil, such as plasticity index and natural water content, where α_M can be lower in organic soils and soils with high water content.

Applications of CPT Results

The previous sections have described how CPT results can be used to estimate geotechnical parameters that can be used as input in analyses. An alternate approach is to apply the in-situ test results directly to an engineering problem. A typical example of this approach is the evaluation of pile capacity directly from CPT results without the need for soil parameters.

As a guide, Table 8 shows a summary of the applicability of the CPT for direct design applications. The ratings shown in the table have been assigned based on current experience and represent a qualitative evaluation of the confidence level assessed to each design problem and general soil type. Details of ground conditions and project requirements can influence these ratings.

In the following sections a number of direct applications of CPT/CPTu results are described. These sections are not intended to provide full details of geotechnical design, since this is beyond the scope of this guide. However, they do provide some guidelines on how the CPT can be applied to many geotechnical engineering applications. A good reference for foundation design is the Canadian Foundation Engineering Manual (CFEM, 2007, www.bitech.ca).

Type of soil	Pile design	Bearing capacity	Settlement*	Compaction control	Liquefaction
Sand	1 – 2	1 – 2	2 – 3	1 – 2	1 – 2
Clay	1 – 2	1 – 2	2 – 3	3 – 4	1 – 2
Intermediate soils	1 – 2	2 – 3	2 – 4	2 – 3	1 – 2

Reliability rating: 1=High; 2=High to moderate; 3=Moderate; 4=Moderate to low; 5=low
* improves with SCPT data

Table 8 Perceived applicability of the CPT/CPTU for various direct design problems

Shallow Foundation Design

General Design Principles

Typical Design Sequence:

1. Select minimum depth to protect against:
    - external agents: e.g. frost, erosion, trees
    - poor soil: e.g. fill, organic soils, etc.

2. Define minimum area necessary to protect against soil failure:
    - perform bearing capacity analyses

2. Compute settlement and check if acceptable

3. Modify selected foundation if required.

Typical Shallow Foundation Problems

Study of 1200 cases of foundation problems in Europe showed that the problems could be attributed to the following causes:

- 25% footings on recent fill (mainly poor engineering judgment)
- 20% differential settlement (50% could have been avoided with good design)
- 20% effect of groundwater
- 10% failure in weak layer
- 10% nearby work (excavations, tunnels, etc.)
- 15% miscellaneous causes (earthquake, blasting, etc.)

In design, ***settlement*** is generally the ***critical*** issue. Bearing capacity is generally not of prime importance.

Construction

Construction details can significantly alter the conditions assumed in the design.

Examples are provided in the following list:

- During Excavation
  - bottom heave
  - slaking, swelling, and softening of expansive clays or rock
  - piping in sands and silts
  - remolding of silts and sensitive clays
  - disturbance of granular soils
- Adjacent construction activity
  - groundwater lowering
  - excavation
  - pile driving
  - blasting
- Other effects during or following construction
  - reversal of bottom heave
  - scour, erosion and flooding
  - frost action

Shallow Foundation - Bearing Capacity

General Principles

Load-settlement relationships for typical footings (Vesic, 1972):

1. Approximate elastic response
2. Progressive development of local shear failure
3. General shear failure

In dense coarse-grained soils failure typically occurs along a well-defined failure surface. In loose coarse-grained soils, volumetric compression dominates and punching failures are common. Increased depth of overburden can change a dense sand to behave more like loose sand. In (homogeneous) fine-grained cohesive soils, failure occurs along an approximately circular surface.

Significant parameters are:

- nature of soils
- density and resistance of soils
- width and shape of footing
- depth of footing
- position of load.

A given soil does not have a unique bearing capacity; the bearing capacity is a function of the footing shape, depth and width as well as load eccentricity.

General Bearing Capacity Theory

Initially developed by Terzaghi (1936); there are now over 30 theories with the same general form, as follows:

Ultimate bearing capacity, (q_f):

$$q_f = 0.5\,\gamma\,B\,N_\gamma\,s_\gamma\,i_\gamma + c\,N_c\,s_c\,i_c + \gamma\,D\,N_q\,s_q\,i_q$$

where:

$N_\gamma\ N_c\ N_q$ = bearing capacity coefficients (function of ϕ')

$s_\gamma\ s_c\ s_q$ = shape factors (function of B/L)

$i_\gamma\ i_c\ i_q$ = load inclination factors
B = width of footing
D = depth of footing
L = length of footing

Complete rigorous solutions are impossible since stress fields are unknown. All theories differ in simplifying assumptions made to write the equations of equilibrium. No single solution is correct for all cases.

Shape Factors

Shape factors are applied to account for 3-D effects. Based on limited theoretical ideas and some model tests, recommended factors are as follows:

$$s_c = s_q = 1 + \left(\frac{B}{L}\right)\left(\frac{N_q}{N_c}\right)$$

$$s_\gamma = 1 - 0.4\left(\frac{B}{L}\right)$$

Load Inclination Factors

When load is inclined (δ), the shape of a failure surface changes and reduces the area of failure, and hence, a reduced resistance. At the limit of inclination, $\delta = \phi$, $q_f = 0$, since slippage can occur along the footing-soil interface.

In general:

$$i_c = i_q = \left(1 - \frac{\delta}{90^o}\right)^2$$

$$i_\gamma = \left(1 - \frac{\delta}{\phi}\right)^2$$

For an eccentric load, Terzaghi proposed a simplified concept of an equivalent footing width, B'.

$$B' = B - 2\,e$$

where 'e' is the eccentricity. For combined inclined and eccentric load, use B' and relevant values of shape factors. For footings near a slope, use modified bearing capacity factors (e.g. Bowles, 1982). They will be small for clay but large for granular soils.

Effect of Groundwater

The bearing capacity is based on effective stress analysis hence position of the groundwater table affects the value of the soil unit weight.

- If depth to the water table, $d_w = 0$, use γ' in both terms
- If $d_w = D$ (depth of footing), use γ' in width term and γ in depth term.

In general, install drainage to keep $d_w > D$.

Indirect Methods Based on Soil Parameters

Granular, coarse-grained soils

Bearing capacity is generally not calculated, since settlements control, except for very narrow footings.

Cohesive, fine-grained soils

Short-term stability generally controls, hence application of undrained shear strength, s_u.

$$q_f = N_c s_u + \gamma D$$

where:

N_c = function of footing width and shape; for strip footings at the ground surface, $N_c = (\pi + 2)$.

s_u = apply Bjerrum's correction, based on past experience, to field vane shear strength or from CPT.

Allowable bearing capacity:

$$q_{all} = (q_f - \gamma D) / FS$$

$$\text{Hence,} \quad q_{all} = \frac{N_c \, s_u}{FS}$$

Where: FS is Factor of Safety, typically = 3.0.

Use a high FS to account for limitations in theory, underestimation of loads, overestimation of soil strength, avoid local yield in soil and keep settlements small.

Direct Approach to estimate Bearing Capacity (In-Situ Tests)

Based on in-situ tests, theory, model tests and past foundation performance.

SPT

- Empirical direct methods
- Limited to granular soils, however, sometimes applied to very stiff clays
- Often linked to allowable settlement of 25mm (Terzaghi & Peck)
- SPT of poor reliability, hence, empirical methods tend to be very conservative

CPT

Empirical direct methods:

Granular, coarse-grained soils:

$$q_f = K_\phi \; q_{c\,(av)}$$

where:
$q_{c\,(av)}$ = average CPT penetration resistance below depth of footing, z = B

Eslaamizaad & Robertson (1996) suggested K_ϕ = 0.16 to 0.30 depending on B/D and shape. In general, assume K_ϕ = 0.16 (see Figure 36). Meyerhof (1956) suggested K_ϕ = 0.30. However, generally settlements will control.

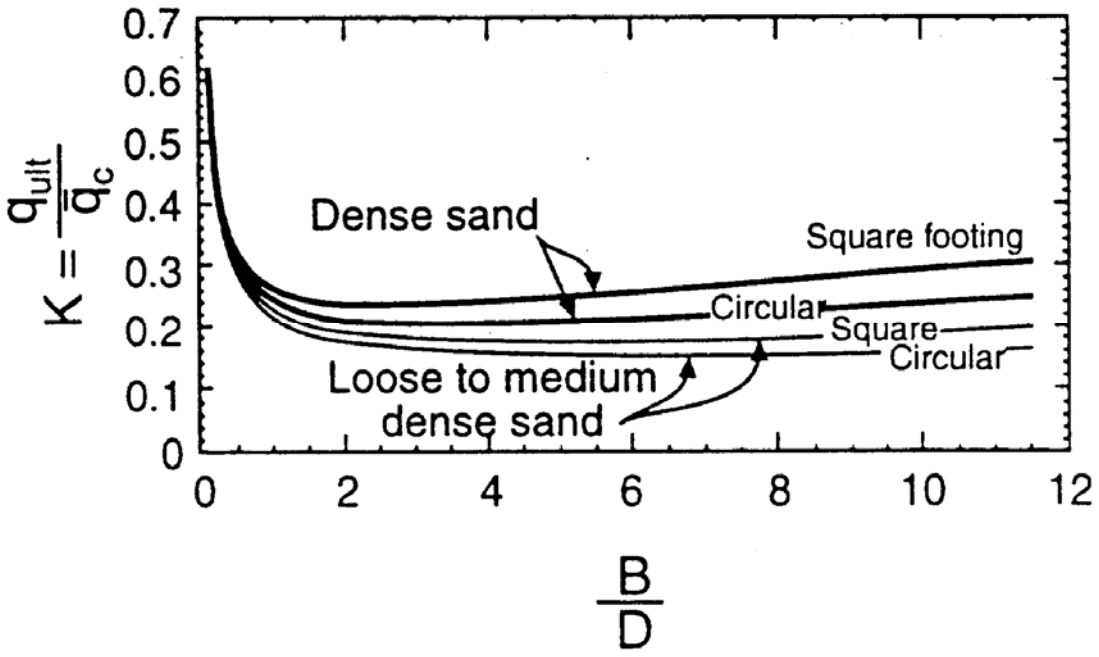

Figure 36 Correlation between bearing capacity of footing on cohesionless soils and average cone resistance
(after Eslaamizaad and Robertson, 1996)

Cohesive, fine-grained soils:

$$q_f = K_{su}\, q_{c\,(av)} + \gamma\, D$$

K_{su} = 0.30 to 0.60 depending on footing B/D and shape and soil OCR and sensitivity. In general, assume K_{su}= 0.30 in clay

Shallow Foundation Design – Settlement

General Design Principles

Requires:

- magnitude of settlement
- rate of settlement
- compatibility with acceptable behavior of building

For well-designed foundations, the magnitude of strains in the ground is generally very small ($\varepsilon < 10^{-1}$ %). Hence, ground response is approximately elastic (non-linear elastic).

Granular coarse-grained soils

Coarse-grained soils have high permeability, thus immediate settlements. However, long term settlements can occur due to submergence, change in water level, blasting, machine vibration or earthquake loading.

Cohesive fine-grained soils

Fine-grained soils have very low permeability, thus the need to consider magnitude and duration of settlement.

In soft, normally to lightly overconsolidated clays, 80% to 90% of settlement is due to primary consolidation. Secondary settlement also can be large. In stiff, overconsolidated clays (OCR > 4), approximately 50% of settlement can be due to immediate distortion settlement and secondary settlement is generally small.

Methods for granular coarse-grained soils

Due to difficulty in sampling, most methods are based on in-situ tests, either direct or via estimate of equivalent elastic modulus (E').

For most tests, the link between test result and modulus is empirical, since it depends on many variables; e.g. mineralogy, stress history, stress state, age, cementation, etc.

CPT

Meyerhof (1974) suggested that the total settlement, s, could be calculated using the following formula:

$$s = \frac{\Delta p\, B}{2 q_{c(av)}}$$

where:

Δp = net footing pressure
B = footing width
$q_{c\,(av)}$ = average CPT penetration resistance below depth of footing,
z = B

Schmertmann (1970) recommended using the following equation:

$$s = C_1\, C_2\, \Delta p \sum \left(\frac{I_z}{C_3 E'} \right) \Delta z$$

where:

C_1 = correction for depth of footing
= $1 - 0.5(\sigma'_1/\Delta p)$
C_2 = correction for creep and cyclic loading
= $1 + 0.2 \log (10\ t_{yr})$
C_3 = correction for shape of footing
= 1.0 for circular footings
= 1.2 for square footings
= 1.75 for strip footings
σ'_1 = effective overburden pressure at footing depth (see Figure 37)
Δp = net footing pressure
t_{yr} = time in years since load application
I_z = strain influence factor (see Figure 37)
Δz = thickness of sublayer
E' = Equivalent Young's modulus = $\alpha_E\, q_c$
α_E = function of degree of loading, soil density, stress history, cementation, age, grain shape and mineralogy (e.g. Figure 38)

= 2 to 4 for very young, normally consolidated sands;
= 4 to 10 for aged (> 1,000years), normally consolidated sands;
= 6 to 20 for overconsolidated sands

q_c = average CPT resistance for sublayer

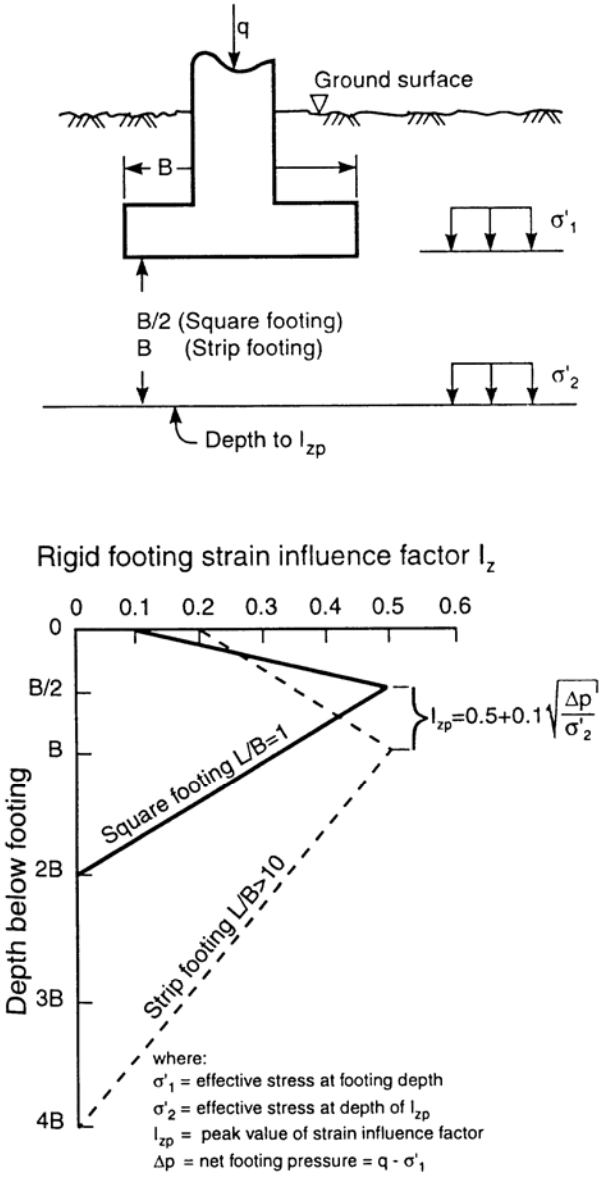

Figure 37 Strain influence method for footings on sand
(Schmertmann, 1970)

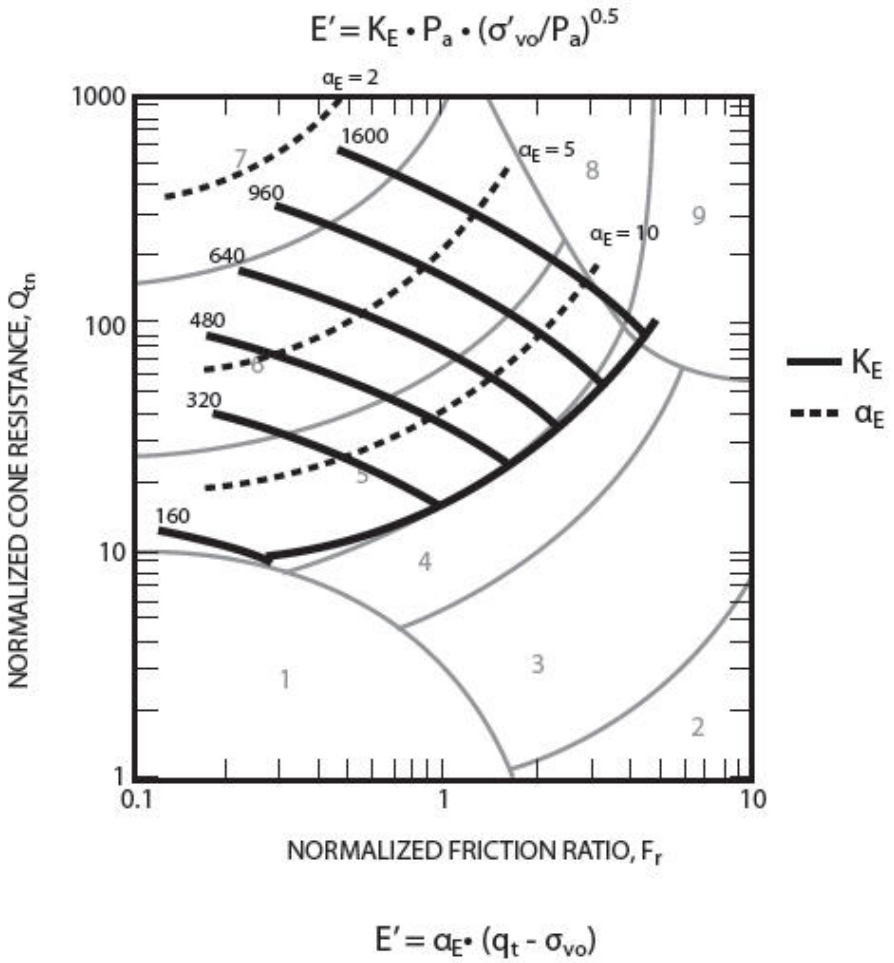

Figure 38 Evaluation of drained Young's modulus from CPT for uncemented sandy soils, $E = \alpha_E (q_t - \sigma_{vo})$

Where: $\alpha_E = 0.015 [10^{(0.55Ic + 1.68)}]$

In this method, (see Figure 39) the sand is divided into a number of layers, n, of thickness, Δz, down to a depth below the base of the footing equal to 2B for a square footing and 4B for a strip footing (length of footing, L > 10B). A value of q_c is assigned to each layer, as illustrated in Figure 39. Note in sandy soils $q_c = q_t$.

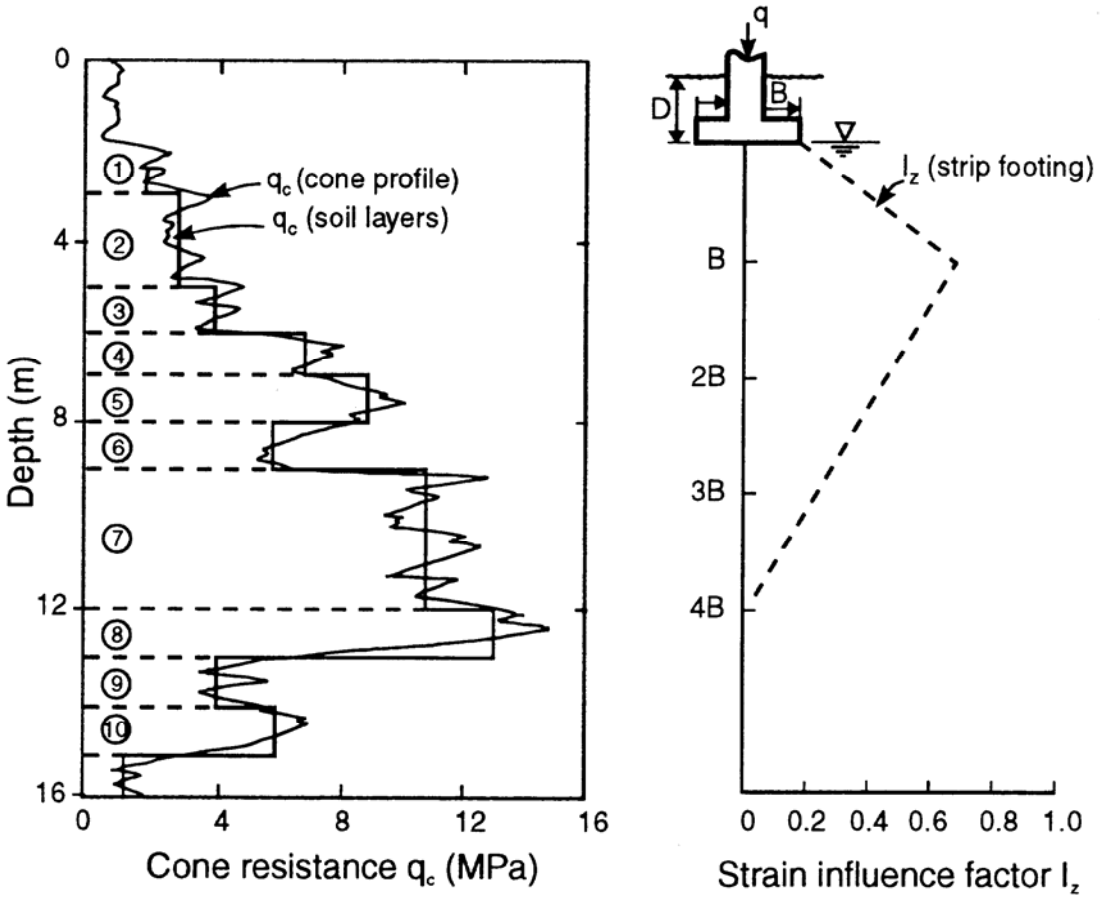

Figure 39 Application of Schmertmann (1970) method for settlement of footings on sand

Based on a review of 30 full-size footing tests on 12 different sands, Mayne and Illingsworth (2010) suggested the following simple relationship:

$$\frac{q_{applied}}{q_c} = \frac{3}{5} \cdot \sqrt{\frac{s}{B}}$$

where:

$q_{applied}$ = applied footing stress

q_c = average cone resistance within 1.5B below footing

Seismic Shear Wave Velocity

Eslaamizaad and Robertson (1996) suggested using shear wave velocity (V_s) to measure small strain stiffness (G_o) directly and applying it to settlement calculations, as follows:

$$G_o = \frac{\gamma}{g} (V_s)^2$$

Then, the equivalent Young's modulus can be estimated as follows:

$$E' = 2(1 + \upsilon)\psi\, G_o \approx 2.6\psi\, G_o$$

where:

Ψ = a function of the degree of loading and stress history (see Figure 40).

Fahey, (1998) suggested that the variation of ψ could be defined by:

$$\psi = G/G_o = 1 - f\,(q/q_{ult})^g$$

Mayne (2005) suggested that values of f = 1 and g = 0.3 are appropriate for uncemented soils that are not highly structured and these values agree well with the NC relationship shown in Figure 40. Hence,

$$E' = 0.047\,[1 - (q/q_{ult})^{0.3}]\,[10^{(0.55Ic + 1.68)}]\,(q_t - \sigma_{vo})$$

Since settlement is a function of degree of loading, it is possible to calculate the load settlement curve, as follows:

$$s = \left(\frac{\Delta p\ B}{E'}\right) i_c$$

where: i_c = influence coefficient

In general, for most well designed shallow foundations, $q/q_{ult} = 0.3$ (i.e. FS > 3), then $\Psi \sim 0.3$, hence, $E' \approx G_o$

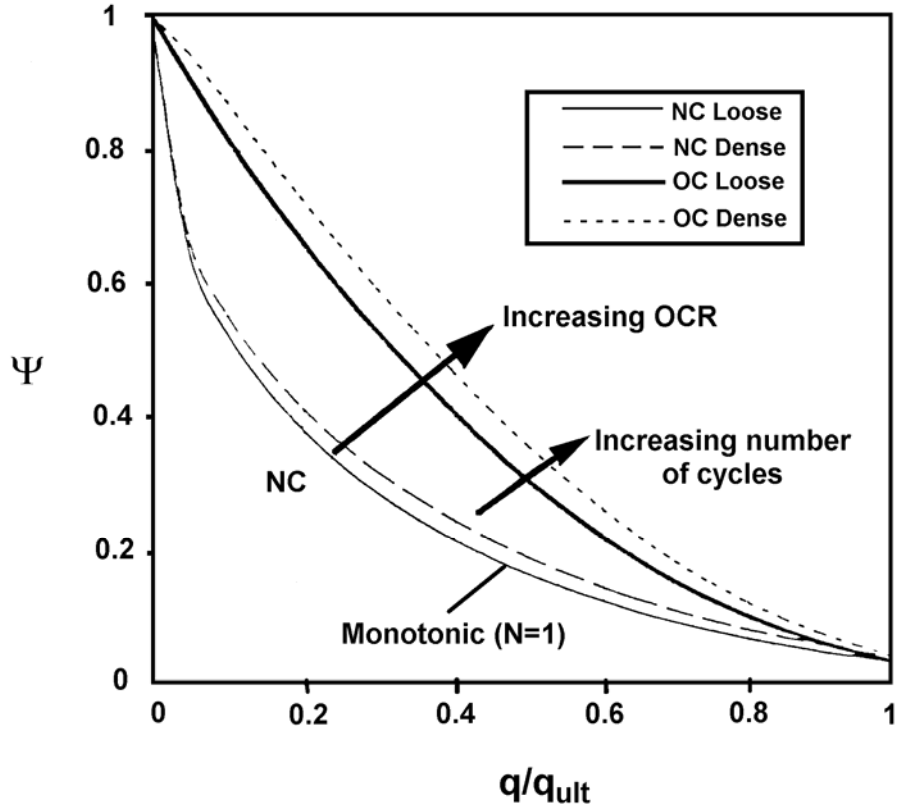

Figure 40 Factor Ψ versus q/q_{ult} for sands with various densities and stress histories

Shear wave velocity has the advantage of providing a direct measure of soil stiffness without an empirical correlation. The only empiricism is to adjust the small strain modulus for effects of stress level and strain level below the footing. The shear wave velocity approach can also be applied to estimate settlements in very stiff clays where consolidation settlements are very small.

Methods for cohesive fine-grained soils

The key parameter is the preconsolidation pressure, σ'_p. This can only be measured accurately in the laboratory on high quality samples. However, OCR and σ'_p profiles can be estimated from the CPT. It is useful to link results from high quality laboratory tests with continuous profiles of the CPT.

In general, to keep settlements small, the applied stress must be $< \sigma'_p$. In soft ground this may require some form of ground improvement.

Components of settlement are:

s_i = immediate (distortion) settlement
s_c = consolidation settlement
s_s = secondary time dependent (creep) settlement

Immediate Settlements

Based on elastic theory, Janbu (1963) proposed:

$$s_i = \left(\frac{\Delta p \; B}{E_u} \right) \mu_o \; \mu_1$$

where:

B = footing width
Δp = net pressure
E_u = soil modulus (undrained)
μ_o, μ_1 = influence factors for depth of footing and thickness of compressible layer

Undrained modulus can be estimated from undrained shear strength (s_u) from either field vane tests and/or the CPT, but requires knowledge of soil plasticity.

$$E_u = n. \; s_u$$

Where: n varies from 40 to 1000, depending on degree of loading and plasticity of soil (see Figure 41).

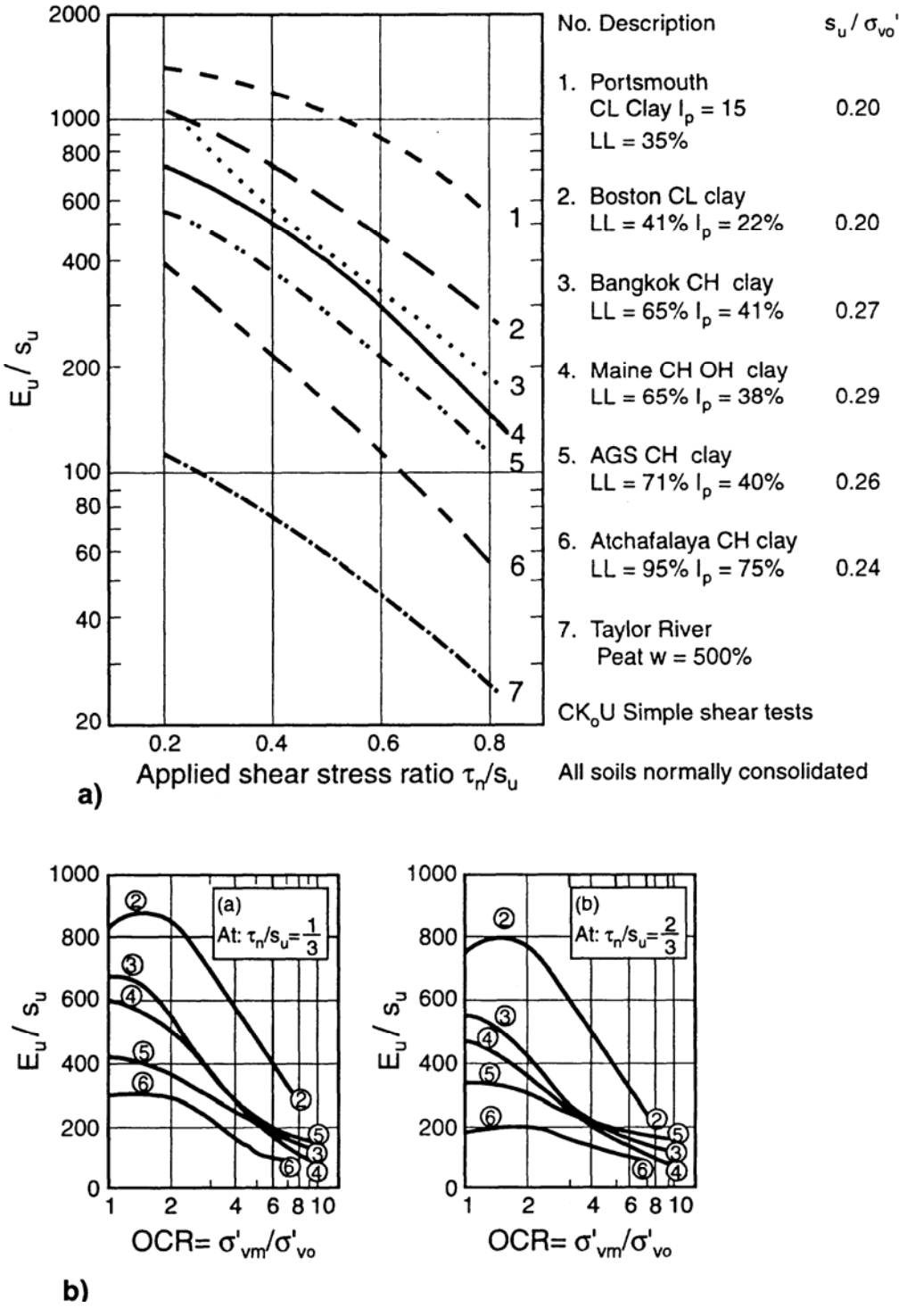

Figure 41 Selection of soil stiffness ratio for clays
(after Ladd et al., 1977)

Consolidation Settlements

Terzaghi's 1-D theory of consolidation often applies, since 2- and 3-D effects are generally small. Settlement for a wide range of footings and soils can be calculated using the 1-D constrained modulus, M, using:

$$\varepsilon_{vol} = (\Delta\sigma'_v / M)$$

Hence, $$s = (\Delta\sigma'_v / M) H$$

The 1-D Constrained Modulus (M) can be estimated from the CPT using:

$$M = \alpha_M (q_t - \sigma_{vo})$$

When $I_c > 2.2$ (fine-grained soils) use:

$$\alpha_M = Q_t \quad \text{when } Q_t < 14$$

$$\alpha_M = 14 \quad \text{when } Q_t > 14$$

When $I_c < 2.2$ (coarse-grained soils) use:

$$\alpha_M = 0.0188\ [10^{(0.55Ic + 1.68)}]$$

The above approach can be applied to all soils, since M can be estimated for a wide range of soils. The above approach is simpler than the Schmertmann (1970) approach that is limited to only sands. When using CPT results, the settlement can be calculated over each depth increment and the total settlement becomes the summation over the full depth. The above approach, based on 1-D constrained modulus, M, is often suitable for many projects. Care is required when applying the above approach to lightly overconsolidated soils if loading will significantly exceed σ'_p.

Rate of settlement is important, hence, the need for coefficient of consolidation, c_v. Experience shows that c_v can be highly variable due to non-linearity of the stress-strain relationship as well as change in permeability as soils compress. Values of c_v can be best estimated either:

1. Separately from 1-D constrained modulus, M (or m_v, since $M = 1/m_v$) from oedometer tests on high quality samples and permeability, k from in-situ tests, using:

$$c_v = \frac{k\,M}{\gamma_w}$$

or

2. Directly from CPTu dissipation tests.

c_v values vary by orders of magnitude, hence, accuracy of the calculation is generally very poor. Drainage conditions play a major role, yet are difficult to identify. The CPTu can provide an excellent picture of the drainage conditions. Avoid a design that *depends* on the time-settlement relationship. For settlement sensitive structures, try to minimize differential settlements (e.g. Osaka Airport - mechanical adjustments due to very large long term settlements).

Secondary Settlements

Time dependent settlements depend on soil mineralogy and degree of loading. Organic soils can have high secondary settlement. In general, avoid soils with high secondary settlements. Mesri, (1994) suggested a simplified approach that links coefficient of secondary consolidation (C_α) and compression index, C_c, for inorganic clays and silts, as follows:

$$C_\alpha = 0.04 \left(\frac{C_c}{1+e_o} \right) \sim 0.1\ (\sigma'_v/M)$$

Long term secondary (creep) settlement, s_s is then:

$$s_s = C_\alpha\ \Delta z \log (t/t_p)$$

where t_p is duration of primary consolidation.

Provided that the applied stress is less than 80% of σ'_p, secondary consolidation is generally small. Constrained Modulus, M can be estimated from the CPT (see earlier section).

Allowable Settlements

Loads considered in settlement analyses depend on nature of soil and time-dependence of settlement. Differential settlements generally control.

Sands

- Load: maximum possible load due to immediate settlement
- Differential settlement: can be up to 100% of maximum settlement due to natural variability of sand. Typically less than or equal to 25mm (1 inch)

Clays

- Load: dead load plus % of live load (LL) depending on duration of live load
  - 50% of LL for buildings
  - 30% of LL for bridges
  - 75% of LL for reservoirs
- Settlements: are more uniform and can be larger than 25mm (1 inch)

Typical Design Sequence

1. Check for possible isolated footing design
2. Check for possible raft foundation
3. Ground improvement
4. Deep foundations

Raft Foundations

Consider a raft when:

- Area of footing > 50% of building area
- Need to provide underground space in location of high groundwater
- Need to reduce magnitude of total settlements (i.e. floating foundation)
- Need to reduce differential settlements

A raft is an inverted slab, designed to distribute structural loads from columns and walls, while keeping deformations within acceptable limits.

The structural characteristics of a raft foundation can be optimized by accounting for the interaction between the raft and supporting ground. Structural engineers usually perform an elastic analysis using elastic (Winkler) springs. Hence, they would like the spring constant, k_s.

k_s = coefficient of subgrade reaction (kN/m^3)

$$k_s = \frac{p}{s}$$

where:

p = net applied stress
s = settlement resulting from applied stress, p

The process is governed by the relative stiffness of the structure and the ground. The coefficient of subgrade reaction is not a soil parameter, since it depends on the size of the footing and degree of loading. Often estimates are made from global tables (Terzaghi; see Table 9).

Soil type	Subgrade reaction (kN/m^3)
Loose sand	5,000 – 16,000
Medium dense sand	10,000 – 80,000
Dense sand	60,000 – 125,000
Clayey sand	30,000 – 80,000
Silty sand	20,000 – 50,000
Clayey soil: s_u < 50 kPa	10,000 – 20,000
50kPa < s_u < 100kPa	20,000 – 50,000
100 kPa < s_u	>50,000

Table 9 Recommended coeffiecient of subgrade reaction (k_s) for different soil types (Terzaghi, 1955)

It is best to obtain estimates based on in-situ testing.

Plate Load Tests (PLT)

Plate load tests can provide a direct measure of the relationship between p and s, but size effects can dominate results. Terzaghi (1955) suggested a link between a 1-foot square plate (k_{s1}) and the width of footing B, as follows:

$$k_s = k_{s1}\left(\frac{B+1}{2B}\right)^2$$

However, there is very large scatter in the results, due to variability in ground stiffness with depth.

Shear Wave Velocity (V_s)

Based on work by Vesic (1961) and elastic theory, the modulus of subgrade reaction is:

$$k'_s = 0.65 \sqrt[12]{\frac{E\,B^4}{E_f I_f}} \left(\frac{E}{1-\nu^2} \right)$$

where:

E	=	modulus of elasticity of soil
E_f	=	modulus of elasticity of footing
B	=	footing width
I_f	=	moment of inertia
ν	=	Poisson's ratio for soil
k'_s	=	modulus of subgrade reaction:

$$k'_s = k_s B$$

For most values of E_s and E_f, the expression simplifies to:

$$k'_s \approx \left(\frac{E}{1-\nu^2} \right)$$

Bowles (1974) suggested:

$$k_s = 120\ q_{all}$$

where q_{all} is in kPa and k_s is in kN/m^3.

It is possible to estimate E from shear wave velocity, V_s. The small strain shear modulus is given by the following:

$$G_o = \frac{\gamma}{g} (V_s)^2$$

In addition:

$$G_{eq} = \Psi\, G_o$$

and

$$E = 2(1 + \upsilon)\, G_{eq}$$

Since $\nu \approx 0.2$ to 0.3,

$$k'_s = k_s\, B \approx 2.9\, \Psi\, G_o$$

Hence:

$$k_s \approx 2.9\, \Psi\, \frac{\frac{\gamma}{g}(V_s)^2}{B}$$

where**:**

$\Psi =$ a function of the degree of loading and stress history (see Figure 40).

Fahey, (1998) suggested that the variation of ψ could be defined by:

$$\psi = G/G_o = 1 - f\,(q/q_{ult})^g$$

Mayne (2005) suggested that values of $f = 1$ and $g = 0.3$ are appropriate for most uncemented soils that are not highly structured and these values agree well with the NC relationship shown in Figure 40. The value of g increases toward a value of 1.0 when the soil is overconsolidated or under increasing number of load cycles.

For most well designed foundations, $q/q_{ult} = 0.3$ (i.e. FS > 3) and hence, $\Psi = 0.3$, then:

$$k_s \approx G_o / B$$

Deep Foundation Design

Piles

Piles can be used to:

- Transfer high surface loads, through soft layers down to stronger layers
- Transfer loads by friction over significant length of soil
- Resist lateral loads
- Protect against scour, etc.
- Protect against swelling soils, etc

Piles are generally much more expensive than shallow footings.

Types of Piles

Generally classified based on installation method (Weltman & Little, 1977):

- Displacement
    - Preformed
    - Driven Cast-in-place
    - High pressure grouted
- Non/low-displacement
    - Mud bored
    - Cased bored
    - Cast-in-place screwed (auger)
    - Helical (screw)

Contractors are developing new pile types and installation techniques constantly to achieve increased capacity and improved cost effectiveness for different ground conditions. Hence, it is difficult to predict capacity and load-settlement response for all piles using simple analytical techniques, since the capacity and load response characteristics can be dominated by the method of installation.

Selection of Pile Type

1. Assess foundation loads
2. Assess ground conditions
3. Are piles necessary?
4. Technical considerations:
    - Ground conditions
    - Loading conditions
    - Environmental considerations
    - Site and equipment constraints
    - Safety
5. List all technically feasible pile types and rank in order of suitability based on technical considerations
6. Assess cost of each suitable pile type and rank based on cost considerations
7. Assess construction program for each suitable pile type and rank
8. Make overall ranking based on technical, cost and program considerations

General Design Principles

Axial Capacity

The total ultimate pile axial capacity, Q_{ult}, consists of two components: end bearing load (or point resistance), Q_b, and side friction load (sometimes referred to as the shaft or skin friction), Q_s, as follows:

$$Q_{ult} = Q_s + Q_b$$

In sands, the end bearing, Q_b, tends to dominate, whereas in soft clays, the side friction, Q_s, tends to dominate. The end bearing, Q_b, is calculated as the product between the pile end area, A_p, and the unit end bearing, q_p. The friction load, Q_s, is the product between the outer pile shaft area, A_s, by the unit side friction, f_p.

$$Q_{ult} = f_p A_s + q_p A_p$$

Obviously, different f_p values are mobilized along different parts of the pile, so that, in practice, the calculation is performed as a summation of small components. For open-ended piles, some consideration should be made

regarding whether the pile is plugged or unplugged (de Ruiter and Beringen, 1979), but the procedure is essentially as outlined above. In general, most pipe piles behave plugged (closed-ended) at working loads, but become unplugged (open-ended) at failure. The allowable or design pile load, Q_{all} will be then given by the total ultimate axial capacity divided by a factor of safety. Sometimes separate factors of safety are applied to Q_b and Q_s.

Basic approaches are:

- Static Methods
- Pile Dynamics
- Pile Load Tests

Static Methods

Pseudo-theoretical Approach

Pseudo-theoretical methods are based on shear strength parameters.

Similar to bearing capacity calculations for shallow foundations - there are over 20 different bearing capacity theories. No single solution is applicable to all piles and most cannot account for installation technique. Hence, there has been extensive application of in-situ test techniques applied via empirical direct design methods.

The most notable is the application of the CPT, since the CPT is a close model of the pile process. Detailed analysis is generally limited to high-risk pile design, such as large offshore piles.

Effective Stress Approach (β)

The effective stress (β) approach (Burland, 1973), has been very useful in providing insight of pile performance.

Unit side friction, $f_p = \beta \sigma_v'$

Unit end bearing, $q_p = N_t \sigma_b'$

Soil Type	Cast-in-place Piles	Driven Piles
Silt	0.2 - 0.3	0.3 - 0.5
Loose sand	0.2 - 0.4	0.3 - 0.8
Medium sand	0.3 - 0.5	0.6 - 1.0
Dense sand	0.4 - 0.6	0.8 - 1.2
Gravel	0.4 - 0.7	0.8 - 1.5

Table 10 Range of β coefficients: cohesionless soils

Soil Type	Cast-in-place Piles	Driven Piles
Silt	10 - 30	20 - 40
Loose sand	20 - 30	30 - 80
Medium sand	30 - 60	50 - 120
Dense sand	50 - 100	100 - 120
Gravel	80 - 150	150 - 300

Table 11 Range of N_t factors: cohesionless soils

The above coefficients are approximate since they depend on ground characteristics and pile installation details. In the absence of pile load tests assume FS = 3.

Randolph and Wroth (1982) related β to the overconsolidation ratio (OCR) for cohesive soils and produced tentative design charts. In general, for cohesive soils:

$$\beta = 0.25 - 0.32, \text{ and } N_t = 3 - 10$$

Effective stress concepts may not radically change empirical based design rules, but can increase confidence in these rules and allow extrapolation to new situations.

Total Stress Approach (α)

It has been common to design piles in cohesive soils based on total stress and undrained shear strength, s_u.

$$\text{Unit side friction, } f_p = \alpha\, s_u$$

$$\text{Unit end bearing, } q_p = N_t\, s_u$$

Where α varies from 0.5 - 1.0 depending on OCR and N_t varies from 6 to 9 depending on depth of embedment and pile size.

Empirical Approach

CPT Method

Research has shown (Robertson et al., 1988; Briaud and Tucker, 1988; Tand and Funegard, 1989; Sharp et al., 1988) that CPT methods generally give superior predictions of axial pile capacity compared to most conventional methods. The main reason for this is that the CPT provides a continuous profile of soil response. Almost all CPT methods use reduction factors to measured CPT values. The need for such reduction factors is due to a combination of the following influences: scale effect, rate of loading effects, difference of insertion technique, position of the CPT friction sleeve and differences in horizontal soil displacements. The early work by DeBeer (1963) identified the importance of scale effects. Despite these differences, the CPT is still the test that gives the closest simulation of a pile. Superiority of CPT methods over non-CPT methods has been confirmed in other studies (e.g. O'Neill, 1986).

The main CPT method by Bustamante and Gianeselli (1982 - LCPC Method) is outlined below. The LCPC CPT method is recommended since it provides simple guidance to account for many different pile installation methods and generally provides good estimates of axial capacity of single piles.

LCPC CPT Method (Bustamante and Gianeselli, 1982)

The method by Bustamante and Gianeselli was based on the analysis of 197 pile load (and extraction) tests with a wide range of pile and soil types, which may partly explain the good results obtained with the method. The method, also known as the LCPC method, is summarized in Table 12 and Table 13. The LCPC method was updated with small changes by Bustamante and Frank, (1997)

Nature of soil	q_c (MPa)	Factors k_c Group I	Group II
Soft clay and mud	< 1	0.4	0.5
Moderately compact clay	1 to 5	0.35	0.45
Silt and loose sand	≤ 5	0.4	0.5
Compact to stiff clay and compact silt	> 5	0.45	0.55
Soft chalk	≤ 5	0.2	0.3
Moderately compact sand and gravel	5 to 12	0.4	0.5
Weathered to fragmented chalk	> 5	0.2	0.4
Compact to very compact sand and gravel	> 12	0.3	0.4

Group I: plain bored piles; mud bored piles; micro piles (grouted under low pressure); cased bored piles; hollow auger bored piles; piers; barrettes.
Group II: cast screwed piles; driven precast piles; prestressed tubular piles; driven cast piles; jacked metal piles; micropiles (small diameter piles grouted under high pressure with diameter < 250 mm); driven grouted piles (low pressure grouting); driven metal piles; driven rammed piles; jacket concrete piles; high pressure grouted piles of large diameter.

Table 12 Bearing capacity factors, k_c
(Bustamante and Gianeselli, 1982)

The pile unit end bearing, q_p, is calculated from the calculated equivalent average cone resistance, q_{ca}, multiplied by an end bearing coefficient, k_c (Table 12). The pile unit side friction, f_p, is calculated from measured q_c values divided by a friction coefficient, α_{LCPC} (Table 13).

$$q_p = k_c \, q_{ca}$$

$$f_p = \frac{q_c}{\alpha_{LCPC}}$$

Maximum f_p values are also recommended based on pile and soil type. Only the measured CPT q_c is used for the calculation of both side friction and pile end bearing resistance. This is considered an advantage by many due to the difficulties associated in interpreting sleeve friction (f_s) in CPT data.

Nature of soil	q_c (MPa)	Category: Coefficients, α — I A	I B	II A	II B	Maximum limit of f_p (MPa) — I A	I B	II A	II B	III A	III B
Soft clay and mud	< 1	30	30	30	30	0.015	0.015	0.015	0.015	0.035	
Moderately compact clay	1 to 5	40	80	40	80	0.035 (0.08)	0.035 (0.08)	0.035 (0.08)	0.035	0.08	≥ 0.12
Silt and loose sand	≤ 5	60	150	60	120	0.035	0.035	0.035	0.035	0.08	–
Compact to stiff clay and compact silt	> 5	60	120	60	120	0.035 (0.08)	0.035 (0.08)	0.035 (0.08)	0.035	0.08	≥ 0.20
Soft chalk	≤ 5	100	120	100	120	0.035	0.035	0.035	0.035	0.08	–
Moderately compact sand and gravel	5 to 12	100	200	100	200	0.08 (0.12)	0.035 (0.08)	0.08 (0.12)	0.08	0.12	≥ 0.20
Weathered to fragmented chalk	> 5	60	80	60	80	0.12 (0.15)	0.08 (0.12)	0.12 (0.15)	0.12	0.15	≥ 0.20
Compact to very compact sand and gravel	> 12	150	300	150	200	0.12 (0.15)	0.08 (0.12)	0.12 (0.15)	0.12	0.15	≥ 0.20

Category – IA: plain bored piles; mud bored piles; hollow auger bored piles; micropiles (grouted under low pressure); cast screwed piles; piers; barrettes. IB: cased bored piles; driven cast piles. IIA: driven precast piles; prestressed tubular piles; jacket concrete piles. IIB: driven metal piles; jacked metal piles. IIIA: driven grouted piles; driven rammed piles. IIIB: high pressure grouted piles of large diameter > 250 mm; micropiles (grouted under high pressure).
Note: Maximum limit unit skin friction, f_p: bracket values apply to careful execution and minimum disturbance of soil due to construction.

Table 13 Friction coefficient, α
(Bustamante and Gianeselli, 1982)

The equivalent average cone resistance, q_{ca}, at the base of the pile used to compute the pile unit end bearing, q_p, is the mean q_c value measured along two fixed distances, a, (a = 1.5D, where D is the pile diameter) above (-a) and below (+a) the pile tip. The authors suggest that q_{ca} be calculated in three steps, as shown in Figure 42. The first step is to calculate q'_{ca}, the mean q_c between -a and +a. The second step is to eliminate values higher than $1.3q'_{ca}$ along the length -a to +a, and the values lower than $0.7q'_{ca}$ along the length -a, which generates the thick curve shown in Figure 42. The third step is to calculate q_{ca}, the mean value of the thick curve.

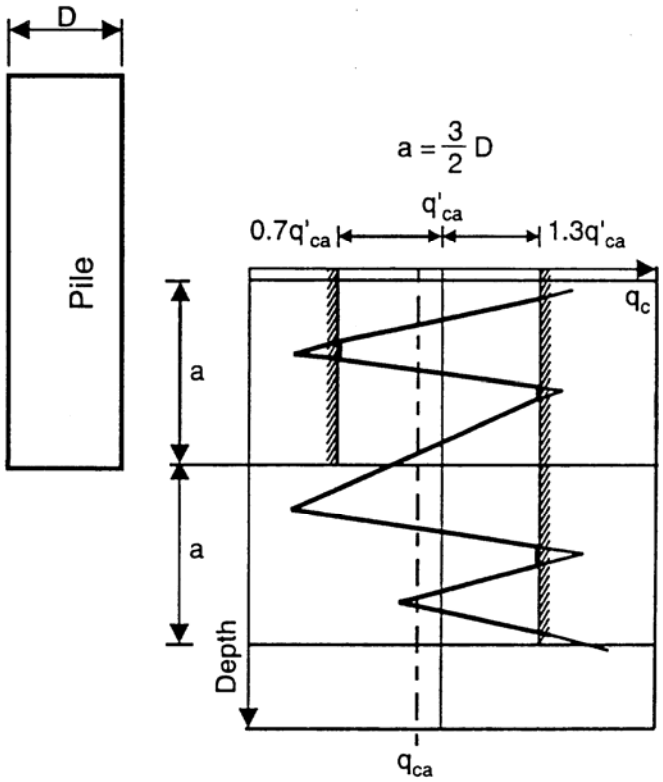

Figure 42 Calculation of equivalent average cone resistance
(Bustamante and Gianeselli, 1982).

Other Design Considerations

Factor of Safety

In order to obtain the design load, factors of safety are applied to the ultimate load and a deterministic approach is usually adopted to define these values. The selection of an appropriate factor of safety depends on many factors, such as

reliability and sufficiency of the site investigation data, confidence in the method of calculation, previous experience with similar piles in similar soils and whether or not pile load test results are available.

Factors of safety are generally of the order of 2, although real values are sometimes greater, as partial factors of safety are sometimes applied during calculations (particularly to soil strengths) before arriving to the ultimate pile capacity.

Recommended factors of safety for calculating the axial capacity of piles from the CPT are given in Table 14.

Method	Factor of safety (FS)
Bustamante and Gianeselli (1982)	2.0 (Q_s) 3.0 (Q_b)
de Ruiter and Beringen (1979)	2.0 (static loads) 1.5 (static + storm loads)

Table 14 Recommended factors of safety for axial capacity of piles from CPT

The design of high capacity large diameter bored piles in stiff clay or dense sand can be difficult due to the fact that settlement criteria usually control rather than capacity. Hence, very high factors of safety are often applied to limit settlement.

Pile Dynamics

The objective of methods that rely on pile dynamics is to relate the dynamic pile behavior to the ultimate static pile resistance. Hence, pile dynamics can work well in drained soils (sands, gravels, etc.) but can be difficult in undrained soils (silts, clays, etc.).

The early approach was to use simple pile driving equations (Hiley, Engineering News, etc.) based on equating the available energy of the hammer to the work performed by the pile. However, these were based on a rigid pile concept, which is fundamentally incorrect. Current approaches are based on 1-D wave-equation analyses (Goble et al., 1970). This method takes into account the

characteristics of the hammer, driving cap, pile and soil. The method is commonly applied using commercial software (i.e. WEAP). This method is good to assist in selection of hammers and prediction of driving stresses and the choice of driving criteria. It is also useful for dynamic monitoring during construction.

Pile Load Tests

Since there is much uncertainty in the prediction of pile capacity and response, it is common to perform pile load tests on major projects.

For major projects, it is common to apply static methods (i.e. LCPC CPT method) to obtain a first estimate of capacity, apply pile dynamics if driven piles selected (aid in hammer selection, driving stresses, driving criteria) and perform a small number of pile load tests to evaluate pile response and to calibrate the static method. Results from the pile load tests can be used to modify the static prediction (i.e. CPT prediction) of pile capacity and the modified method applied across the site. For low-risk projects, pile load tests may not be warranted and a slightly conservative prediction should be applied using the static (CPT) method.

Group Capacity

The capacity of a group of piles is influenced by the spacing, pile installation and ground conditions. The group efficiency is defined as the ratio of the group capacity to the sum of the individual pile capacities.

Driven piles in coarse-grained soils develop larger individual capacities when installed as a group since lateral earth pressures and soil density increase due to pile driving. Hence, it is conservative to use the sum of the individual pile capacities.

For bored pile groups, the individual capacity can reduce due to reduced lateral stresses. Meyerhof (1976) suggested a reduction factor of 0.67.

For piles in fine-grained soils the capacity of the pile group should be estimated based on the ‘block’ of piles since the soil between the piles may move with the pile group.

Design of Piles in Rock

Piles can be placed on or socketed into rock to carry high loads. The exact area of contact with rock, depth of penetration into rock and quality of rock are largely unknown, hence, there is much uncertainty. The capacity is often confirmed based on driving or installation details, local experience and test loading. End bearing capacity can be based on pressuremeter test results or strength from rock cores. Shaft resistance should be estimated with caution, due to possible poor contact between rock and pile, possible stress concentration and resulting progressive failure.

Pile Settlement

Although the installation of piles changes the deformation and compressibility characteristics of the soil mass governing the behavior of single piles under load, this influence usually extends only a few pile diameters below the pile base. Meyerhof (1976) suggested that the total settlement of a group of piles at working load can generally be estimated assuming an equivalent foundation. For a group of predominately friction piles (i.e. $Q_s > Q_b$), the equivalent foundation is assumed to act on the soil at an effective depth of 2/3 of the pile embedment. For a group of piles that are predominately end bearing (i.e. $Q_b > Q_s$), the equivalent foundation is taken at or close to the base of the piles. The resulting settlement is calculated in a manner similar to that of shallow foundations.

Sometimes large capacity piles are installed and used as single piles and the load settlement response of a single pile is required. The load settlement response of a single pile is controlled by the combined behavior of the side resistance (Q_s) and base resistance (Q_b). The side resistance is usually developed at a small settlement of about 0.5 percent of the shaft diameter and generally between 5 to 10mm. In contrast to the side resistance, the base resistance requires much larger movements to develop fully, usually about 10 to 20 percent of the base diameter. An estimate of the load settlement response of a single pile can be made by combining the two components of resistance according to the above guidelines. In this way, a friction pile (i.e. $Q_s >> Q_b$), will show a clear plunging failure at a small settlement of about 0.5% of the pile diameter. On the other hand, an end bearing pile (i.e. $Q_b >> Q_s$), will not show a clear plunging failure

until very large settlements have taken place and usually settlement criteria control before failure can occur. In both cases, the side friction is almost fully mobilized at working loads. Hence, it is often important to correctly define the proportions of resistance (Q_b/Q_s).

Methods have been developed to estimate the load-transfer (t-z) curves (Verbrugge, 1988). However, these methods are approximate at best and are strongly influenced by pile installation and soil type. The recommended method for estimating load settlement response for single piles is to follow the general guidelines above regarding the development of each component of resistance.

Negative Shaft Friction and Down Drag on Piles

When the ground around a pile settles, the resulting downward movement can induce downward forces on the pile.

The magnitude of the settlement can be very small to develop these downward forces. For end bearing piles, the negative shaft friction plus the dead load can result in structural failure of the pile. For friction piles, the negative shaft friction can result in greater settlements. No pile subject to down drag will settle more than the surrounding ground.

Lateral Response of Piles

Vertical piles can resist lateral loads by deflecting and mobilizing resistance in the surrounding ground. The response depends on the relative stiffness of the pile and the ground. In general, the response is controlled by the stiffness of the ground near the surface, since most long piles are relatively flexible.

A common approach is to simulate the ground by a series of horizontal springs. The spring stiffness can be estimated based on a simple subgrade modulus approach (assumes the ground to be linear and homogeneous) or as non-linear springs (p-y curves) (Matlock, 1970). The p-y curves can be estimated using empirical relationships based on lab results or in-situ tests (e.g. pressuremeter, DMT, SCPT) (Baguelin et al., 1978; Robertson et al., 1986). The initial stiffness of the p-y curves is controlled by the small strain stiffness (G_o) that can be determined by measuring (or estimating) the shear wave velocity (V_s) using the SCPT.

Another approach is to simulate the ground as an elastic continuum. Poulos and Davis, (1980) and Randolph, (1981) suggested design charts that require estimates of equivalent ground modulus for uniform homogeneous ground profiles.

The above approaches apply to single piles. When piles are installed in groups, interaction occurs and lateral deformations can increase. These can be estimated using simplified theoretical solutions (Poulos and Davis, 1980, Randolph, 1981). The direction of the applied load relative to the group is important for laterally loaded pile groups.

Seismic Design - Liquefaction

(see Robertson & Wride, 1998; Zhang et al., 2002 & 2004; Robertson, 2009 for details)

Soil liquefaction is a major concern for structures constructed with or on sand or sandy soils. The major earthquakes of Niigata (1964), Kobe (1995) and Christchurch (2010/11) have illustrated the significance and extent of damage caused by soil liquefaction. Soil liquefaction is also a major design problem for large sand structures such as mine tailings impoundment and earth dams.

To evaluate the potential for soil liquefaction, it is important to determine the soil stratigraphy and in-situ state of the deposits. The CPT is an ideal in-situ test to evaluate the potential for soil liquefaction because of its repeatability, reliability, continuous data and cost effectiveness. This section presents a summary of the application of the CPT to evaluate soil liquefaction. Full details are contained in a report prepared for NCEER (Youd et al., 2001) as a result of workshops on liquefaction held in 1996/97 and in a paper by Robertson and Wride (1998) and updated by Robertson (2009).

Liquefaction Definitions

Several phenomena are described as soil liquefaction, hence, the following definitions are provided to aid in the understanding of the phenomena.

Flow (*static*) Liquefaction

- Applies to strain softening soils only (i.e. susceptible to strength loss).
- Requires a strain softening response in undrained loading resulting in approximately constant shear stress and effective stress.
- Requires in-situ shear stresses to be greater than the residual or minimum undrained shear strength.
- Either static or cyclic loading can trigger flow liquefaction.
- For failure of a soil structure to occur, such as a slope, a sufficient volume of material must strain soften. The resulting failure can be a slide or a flow depending on the material characteristics and ground geometry. The resulting movements are due to internal causes and often occur after the trigger mechanism.

- Can occur in any strain-softening saturated (or near-saturated) soil, such as very loose coarse-grained (sand) deposits, very sensitive fine-grained (clay), and loose loess (silt) deposits.

Cyclic (softening) Liquefaction

- Requires undrained cyclic loading during which shear stress reversal occurs or zero shear stress can develop.
- Requires sufficient undrained cyclic loading to allow effective stresses to essentially reach zero.
- Deformations during cyclic loading can accumulate to large values, but generally stabilize shortly after cyclic loading stops. The resulting movements are due to external causes and occur mainly during the cyclic loading.
- Can occur in almost all saturated coarse-grained soil (sand) provided that the cyclic loading is sufficiently large in magnitude and duration.
- Fine-grained (clay) soils can experience cyclic softening when the applied cyclic shear stress is close to the undrained shear strength. Deformations are generally small due to the cohesive strength at low effective stress. Rate effects (creep) often control deformations in cohesive soils.

Note that strain softening soils can also experience cyclic liquefaction depending on ground geometry. Figure 43 presents a flow chart to clarify the phenomena of soil liquefaction.

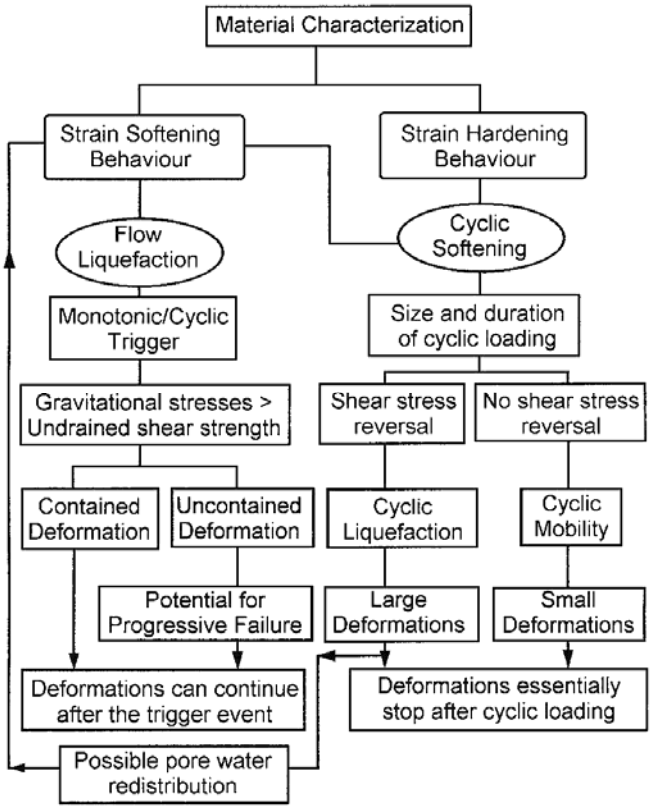

Figure 43 Flow chart to evaluate liquefaction of soils (after Robertson and Wride, 1998)

If a soil is strain softening (i.e. can experience strength loss), flow liquefaction is possible if the soil can be triggered to strain-soften and if the gravitational shear stresses are larger than the minimum undrained shear strength. The trigger can be either monotonic or cyclic. Whether a slope or soil structure will fail and slide will depend on the amount of strain softening soil relative to strain hardening soil within the structure, the brittleness of the strain softening soil and the geometry of the ground. The resulting deformations of a soil structure with both strain softening and strain hardening soils will depend on many factors, such as distribution of soils, ground geometry, amount and type of trigger mechanism, brittleness of the strain softening soil and drainage conditions. Examples of flow liquefaction failures are the Aberfan flow slide (Bishop, 1973), Zealand submarine flow slides (Koppejan et al., 1948) and the Stava tailings dam failure. In general, flow liquefaction failures are not common, however, when they occur, they typically take place rapidly with little warning and are usually catastrophic. Hence, the design against flow liquefaction should be carried out cautiously.

If a soil is strain hardening, flow liquefaction will not occur. However, cyclic (softening) liquefaction can occur due to cyclic undrained loading. The amount and extent of deformations during cyclic loading will depend on the state (density/OCR) of the soils, the magnitude and duration of the cyclic loading and the extent to which shear stress reversal occurs. If extensive shear stress reversal occurs and the magnitude and duration of cyclic loading are sufficiently large, it is possible for the effective stresses to essentially reach zero in sand-like soils resulting in large deformations. Examples of cyclic liquefaction were common in the major earthquakes in Niigata (1964) and Christchurch (2010/11) and manifest in the form of sand boils, damaged lifelines (pipelines, etc.) lateral spreads, slumping of embankments, ground settlements, and ground surface cracks.

If cyclic liquefaction occurs and drainage paths are restricted due to overlying less permeable layers, the sand immediately beneath the less permeable soil can become looser due to pore water redistribution, resulting in possible subsequent flow liquefaction, given the right geometry. In cases where drainage is restricted, caution is required to allow for possible void redistribution.

CPT for Cyclic Liquefaction – Level Ground Sites

(see Robertson & Wride, 1998; Zhang et al., 2002 & 2004; Robertson, 2009 for details)

Most of the existing work on cyclic liquefaction has been primarily for earthquakes. The late Prof. H.B. Seed and his co-workers developed a comprehensive methodology to estimate the potential for cyclic liquefaction for level ground sites due to earthquake loading. The methodology requires an estimate of the cyclic stress ratio (CSR) profile caused by the design earthquake and the cyclic resistance ratio (CRR) of the ground. If the CSR is greater than the CRR cyclic liquefaction can occur. The CSR is usually estimated based on a probability of occurrence for a given earthquake. A site-specific seismicity analysis can be carried out to determine the design CSR profile with depth. A simplified method to estimate CSR was also developed by Seed and Idriss (1971) based on the peak ground surface acceleration (a_{max}) at the site. The simplified approach can be summarized as follows:

$$CSR = \frac{\tau_{av}}{\sigma'_{vo}} = 0.65\left[\frac{a_{max}}{g}\right]\left(\frac{\sigma_{vo}}{\sigma'_{vo}}\right) r_d$$

where τ_{av} is the average cyclic shear stress; a_{max} is the maximum horizontal acceleration at the ground surface; g is the acceleration due to gravity; σ_{vo} and σ'_{vo} are the total and effective vertical overburden stresses, respectively, and r_d is a stress reduction factor which is dependent on depth. The factor r_d can be estimating using the following tri-linear function, which provides a good fit to the average of the suggested range in r_d originally proposed by Seed and Idriss (1971):

$$r_d = 1.0 - 0.00765z \quad \text{if } z < 9.15 \text{ m}$$

$$= 1.174 - 0.0267z \quad \text{if } z = 9.15 \text{ to } 23 \text{ m}$$

$$= 0.744 - 0.008z \quad \text{if } z = 23 \text{ to } 30 \text{ m}$$

$$= 0.5 \quad \text{if } z > 30 \text{ m}$$

Where z is the depth in meters. These formulae are approximate at best and represent only average values since r_d shows considerable variation with depth. Recently Idriss and Boulanger (2008) suggested alternate values for r_d, but these are associated with alternate values of CRR.

The sequence to evaluate cyclic liquefaction for level ground sites is:

1. Evaluate susceptibility to cyclic liquefaction
2. Evaluate triggering of cyclic liquefaction
3. Evaluate post-earthquake deformations.

1. Evaluate Susceptibility to Cyclic Liquefaction

The response of soil to seismic loading varies with soil type and state (void ratio, effective confining stress, stress history, etc.). Boulanger and Idriss (2004) correctly distinguished between *sand-like* and *clay-like* behavior. The following criteria can be used to identify soil behavior:

Sand-like Behavior: Sand-like soils are susceptible to cyclic liquefaction when their behavior is typically characterized by Plasticity Index (PI) < 10 and Liquid Limit (LL) < 37 and natural water content (w_c) > 0.85 (LL). More emphasis should be placed on PI, since both LL and w_c tend to be less reliable.

- Low risk projects: Assume soils are susceptible to cyclic liquefaction based on above criteria unless previous local experience shows otherwise.
- High risk projects: Either assume soils are susceptible to cyclic liquefaction or obtain high quality samples and evaluate susceptibility based on appropriate laboratory testing, unless previous local experience exists.

Clay-like Behavior: Clay-like soils are generally not susceptible to cyclic liquefaction when their behavior is characterized by PI > 15 but they can experience cyclic softening.

- Low risk projects: Assume soils are not susceptible to cyclic liquefaction based on above criteria unless previous local experience shows otherwise. Check for cyclic softening.
- High risk projects: Obtain high quality samples and evaluate susceptibility to either cyclic liquefaction and/or cyclic softening based on appropriate laboratory testing, unless previous local experience exists.

Figure 44 shows the criteria suggested by Bray and Sancio (2006) that includes a transition from sand-like to clay-like behavior between 12 < PI < 18.

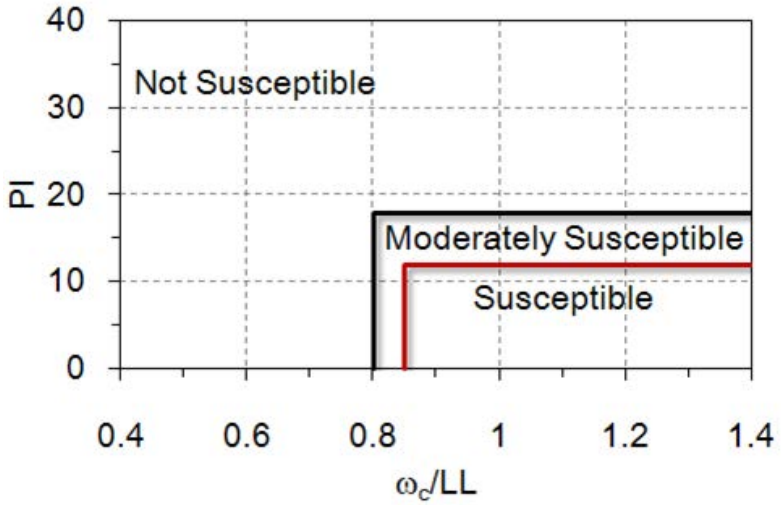

Figure 44 Liquefaction susceptibility criteria (after Bray and Sancio, 2006)

These criteria are generally conservative. Boulanger and Idriss (2004) suggested that sand-like behavior is limited to PI < 7. Use the criteria shown in Figure 44, unless local experience in the same geology unit shows that a lower PI is more appropriate.

Fine-grained soils transition from a behavior that is more fundamentally like sands to behavior that is more fundamentally like clays over a range of Atterberg Limits and moisture contents, as shown in Figure 44. The transition from more sand-like to more clay-like behavior has a direct correspondence to the types of engineering procedures that are best suited to evaluate their seismic behavior. The transition from sand-like to clay-like behavior generally occurs when the SBT_n 2.5 < I_c < 2.7, as illustrated in Figures 26 & 49. For soils that plot in or close to this transition region samples should be obtained to verify behavior.

2. Evaluate Triggering of Cyclic Liquefaction

Sand-like Materials

Seed et al., (1985) developed a method to estimate the cyclic resistance ratio (CRR) for clean sand with level ground conditions based on the Standard Penetration Test (SPT). The CPT has become more popular to estimate CRR, due to the continuous, reliable and repeatable nature of the data (Youd et al., 2001; Robertson, 2009) and a larger database.

Apply the simplified (NCEER) approach as described by Youd et al (2001) using generally conservative assumptions. The simplified approach should be used for low- to medium-risk projects and for preliminary screening for high-risk projects. For low-risk projects, where the simplified approach is the only method applied, conservative criteria should be used. The recommended CPT correlation for sand-like soils is shown in Figure 45 and can be estimated using the following simplified equations suggested by Robertson and Wride, (1998):

$$CRR_{7.5} = 93\left[\frac{(Q_{tn,cs})}{1000}\right]^3 + 0.08$$

if $50 \le Q_{tn,cs} \le 160$

$$CRR_{7.5} = 0.833\left[\frac{(Q_{tn,cs})}{1000}\right] + 0.05$$

if $Q_{tn,cs} < 50$

The field observations, used to compile the curve in Figure 45, were based primarily on the following conditions:

- Holocene-age, uncemented silica-based sand deposits with $K_o < 0.7$
- Level or gently sloping ground
- Cyclic stress ratio $(CSR)_{7.5}$ adjusted to magnitude M = 7.5 earthquake
- Depth range from 1 to 15 m (3 to 50 ft), 85% for depths < 10 m (30 ft)
- Earthquakes with magnitude mostly between 6 < M < 8
- Representative average CPT values for the layer considered to have experienced cyclic liquefaction.

Caution should be exercised when extrapolating the CPT correlation to conditions outside the above range. An important feature to recognize is that the correlation is based primarily on average values for the inferred liquefied layers. However, the correlation is often applied to all measured CPT values, which include low values below the average. Therefore, the correlation can be conservative in variable deposits where a small part of the CPT data can indicate possible liquefaction.

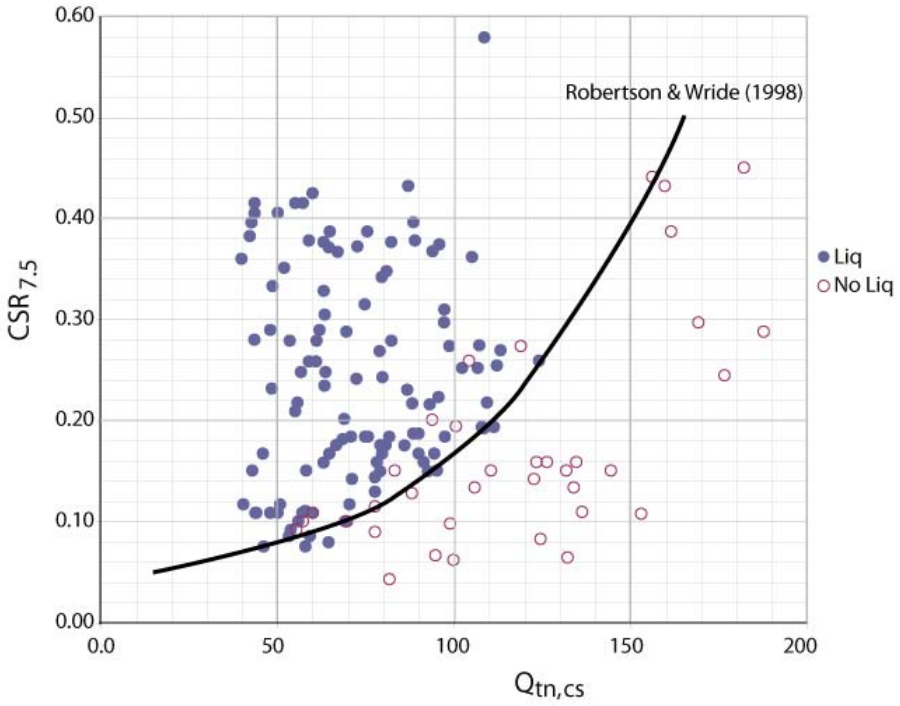

Figure 45 Cyclic resistance ratio ($CRR_{7.5}$) from CPT normalized clean sand equivalent cone resistance ($Q_{tn,cs}$)
(updated by Robertson, 2009)

It has been recognized for some time that the correlation to estimate $CRR_{7.5}$ for silty sands is different than that for clean sands. Typically a correction is made to determine an *equivalent clean sand penetration resistance* based on grain characteristics, such as fines content, although the corrections are due to more than just fines content and are influenced by the plasticity of the fines.

One reason for the continued use of the SPT has been the need to obtain a soil sample to determine the fines content of the soil. However, this has been offset by the generally poor repeatability of the SPT data. It is now possible to estimate behavior characteristics directly from the CPT. Robertson and Wride (R&W, 1998) suggest estimating an equivalent clean sand cone penetration resistance, $(Q_{tn})_{cs}$ using the following:

$$(Q_{tn})_{cs} = K_c\, Q_{tn}$$

Where K_c is a correction factor that is a function of behavior characteristics (e.g. combined influence of fines content and plasticity) of the soil.

Robertson and Wride (R&W, 1998) suggest estimating behavior characteristics using the normalized soil behavior chart (SBT_n) by Robertson (1990) and the soil behavior type index, I_c, where:

$$I_c = \left[(3.47 - \log Q_{tn})^2 + (\log F + 1.22)^2\right]^{0.5}$$

and

$$Q_{tn} = \left(\frac{q_t - \sigma_{vo}}{P_{a2}}\right)\left(\frac{P_a}{\sigma'_{vo}}\right)^n$$

Q_{tn} is the normalized CPT penetration resistance (dimensionless); n = stress exponent; $F = f_s/[(q_c - \sigma_{vo})] \times 100\%$ is the normalized friction ratio (in percent); f_s is the CPT sleeve friction stress; σ_{vo} and σ'_{vo} are the total effective overburden stresses respectively; P_a is a reference pressure in the same units as σ'_{vo} (i.e. P_a = 100 kPa if σ'_{vo} is in kPa) and P_{a2} is a reference pressure in the same units as q_c and σ_{vo} (i.e. P_{a2} = 0.1 MPa if q_c and σ_{vo} are in MPa). Note, 1 tsf ~ 0.1 MPa.

The soil behavior type chart by Robertson (1990) used a normalized cone penetration resistance (Q_t) based on a simple linear stress exponent of n = 1.0, whereas the recommended chart for estimating $CRR_{7.5}$ is based on a normalized cone penetration resistance (Q_{tn}) based on a variable stress exponent. Robertson

(2009) recently updated the stress normalization to allow for a variation of the stress exponent with both SBTn I_c and effective overburden stress using:

$$n = 0.381\ (I_c) + 0.05\ (\sigma'_{vo}/p_a) - 0.15$$

where $n \leq 1.0$ (see Figure 46 for flow chart).

The recommended relationship between I_c and the correction factor K_c is given by the following:

$$K_c = 1.0 \qquad \text{if } I_c \leq 1.64$$

$$K_c = 5.581\ I_c^3 - 0.403\ I_c^4 - 21.63\ I_c^2 + 33.75\ I_c - 17.88 \qquad \text{if } I_c > 1.64$$

The correction factor, K_c, is approximate since the CPT responds to many factors such as soil plasticity, fines content, mineralogy, soil sensitivity, age, and stress history. However, in general, these same factors influence the $CRR_{7.5}$ in a similar manner. Caution should be used when applying the relationship to sands that plot in the region defined by $1.64 < I_c < 2.36$ and $F < 0.5\%$ so as not to confuse very loose clean sands with sands containing fines. In this zone, it is suggested to set $K_c = 1.0$. Soils that fall into the (dilative) clay-like region of the CPT soil behavior chart (e.g. region FD, Figure 49), in general, are not susceptible to cyclic liquefaction. However, samples should be obtained and liquefaction potential evaluated using other criteria based primarily on plasticity, e.g. soils with plasticity index greater than about 10 are likely not susceptible to liquefaction. Soils that fall in the lower left region of the CPT soil behavior chart defined by region FC (see Figure 49) can be sensitive and hence, possibly susceptible to both cyclic and flow liquefaction. The full methodology to estimate $CRR_{7.5}$ from the CPT is summarized in Figure 46.

For low-risk projects and for preliminary screening in high-risk projects, Robertson and Wride (1998) suggested that soils in region FC and FD (Figure 49) would have clay-like behavior and would likely not be susceptible to cyclic liquefaction. Youd et al (2001) recommends that soils be sampled where $I_c > 2.4$ to verify the behavior type. When $I_c > 2.4$ selected (disturbed) soil samples (for grain size distribution, Atterberg limits and water content) should be obtained and tested to confirm susceptibility to cyclic liquefaction using the criteria in Figure 44. Selective soil sampling based on I_c should be carried out adjacent to some CPT soundings. Disturbed samples can be obtained using

either direct push samplers (e.g. Figure 1) or conventional drilling/sampling techniques close to the CPT sounding.

The factor of safely against cyclic liquefaction is defined as:

$$Factor\ of\ Safety,\ FS = \frac{CRR_{7.5}}{CSR}\ MSF$$

Where MSF is the Magnitude Scaling Factor to convert the $CRR_{7.5}$ for M = 7.5 to the equivalent CRR for the design earthquake.

The NCEER recommended MSF is given by:

$$MSF = \frac{174}{M^{2.56}}$$

The above recommendations are based on the NCEER Workshops in 1996/97 (Youd et al., 2001) and updated by Robertson (2009).

Juang et al., (2006) and Ku et al (2012) related Factor of Safety (FS) to the probability of liquefaction (P_L) for the R&W CPT-based method using:

$$P_L = 1 / (1 + (FS/0.9)^{6.3})$$

$CRR_{7.5}$ can also be estimated using normalized shear wave velocity V_{s1} (Kayen et al, 2013). The combined application of both CPT and shear wave velocity to evaluate the potential for soil liquefaction is very useful and can be accomplished in a cost effective manner using the seismic CPT (SCPT).

The CPT provides near continuous profiles of cone resistance that capture the full detail of soil variability, but large corrections are required based on soil type. The shear wave velocity is typically measured over a larger depth increment (typically every 1m) and hence provides a more averaged measure but requires smaller corrections for soil type. If the two approaches provide similar results, in terms of $CRR_{7.5}$, there is more confidence in the results. If the two approaches provide different results, further investigation can be warranted to identify the cause (such as soil aging, cementation, etc.). Sometimes shear wave velocities may predict a higher $CRR_{7.5}$ due to slight soil bonding. In this case, the degree of bonding should be studied to determine if the earthquake loading is sufficient to break the bonds.

Stratigraphy – transition zones

Robertson and Campanella (1983) showed that the cone tip resistance is influenced by the soil ahead and behind the cone tip. In strong/stiff soils the zone of influence is large (up to 15 cone diameters) whereas in soft soils the zone of influence is rather small (as small as 1 cone diameter). Ahmadi and Robertson (2005) showed that the size of the zone of influence decreased with increasing stress (e.g. dense sands behave more like loose sand at high values of effective stress).

The zone of influence ahead and behind a cone during penetration will influence the cone resistance at any interface (boundary) between two soil types of significantly different strength and stiffness. Hence, it is often important to identify transitions between different soils types to avoid possible misinterpretation. This issue has become increasingly important with software that provides interpretation of every data point from the CPT. When CPT data are collected at close intervals (typically every 20 to 50mm) several data points are '*in transition*' when the cone passes an interface between two different soil types (e.g. from sand to clay and visa-versa). It is possible to identify the transition from one soil type to another using the rate of change of I_c. When the CPT is in transition from sand to clay the SBT I_c will move from low values in the sand to higher values in the clay. Robertson and Wride (1998) suggested that the approximate boundary between sand-like and clay-like behavior is around $I_c = 2.60$. Hence, when the rate of change of I_c is rapid and is crossing the boundary defined by $I_c = 2.60$, the cone is likely in transition from a sand-like to clay-like soil or vise-versa. Profiles of I_c can provide a simple means to identify and remove these transition zones. Software, such as *CLiq* (http://www.geologismiki.gr/Products/CLiq.html) includes a feature to identify and remove transition zones (see example in Figure 47).

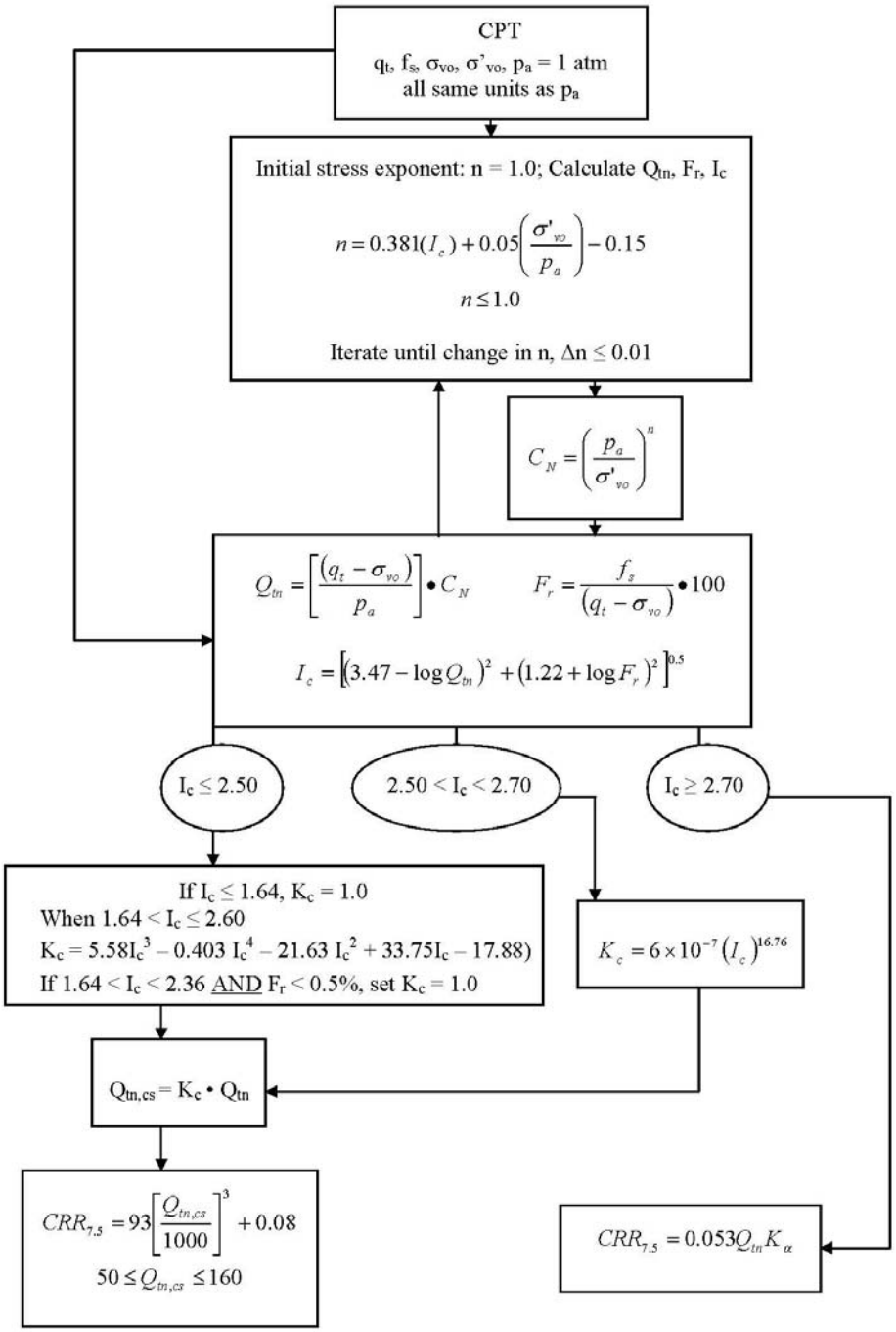

Figure 46 Flow chart to evaluate cyclic resistance ratio ($CRR_{7.5}$) from CPT (after Robertson, 2009)

An example of the CPT method to evaluate cyclic liquefaction is shown on Figure 47 for a Moss Landing site that suffered cyclic liquefaction and lateral spreading during the 1989 Loma Prieta earthquake in California (Boulanger et al., 1995). Note that transitions zones are identified in red.

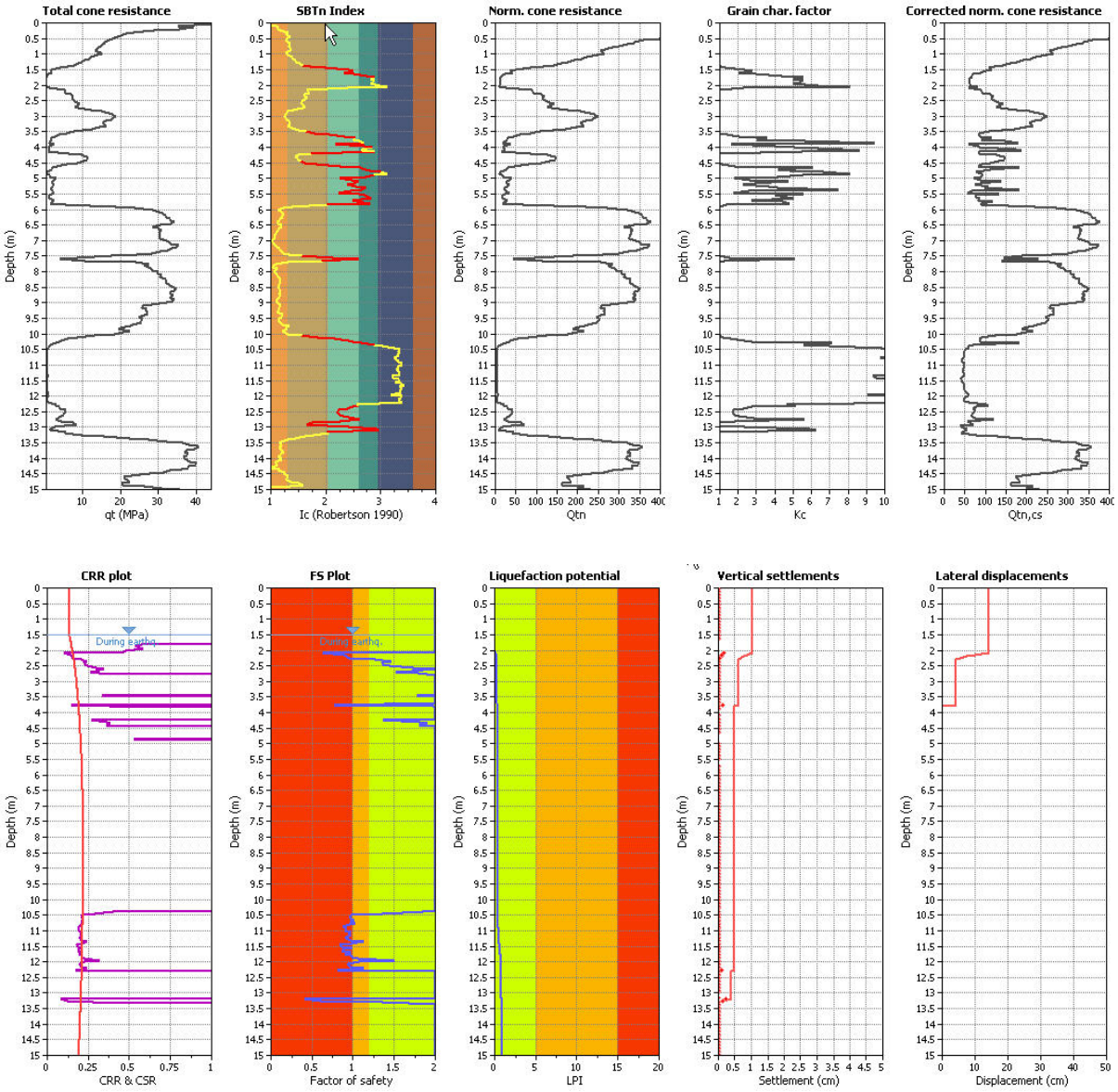

Figure 47 Example of CPT-based approach to evaluate cyclic liquefaction/softening at Moss Landing Site showing (a) intermediate parameters (b) CRR, FS and post-earthquake deformations using '***CLiq***' software (http://www.geologismiki.gr/)

Clay-like Materials

Clay-like materials tend to develop pore pressures more slowly under undrained cyclic loading than sand-like materials and generally do not reach zero effective stress under cyclic loading. Hence, clay-like materials are not susceptible to complete cyclic liquefaction. However, when the cyclic stress ratio (CSR) is large relative to the undrained shear strength ratio of clay-like materials, deformations and softening can develop. Boulanger and Idriss (2007) used the term 'cyclic softening' to define this build-up of deformations under cyclic loading in clay-like soils. Boulanger and Idriss (2007) showed that the CRR for cyclic softening in clay-like materials is controlled by the undrained shear strength ratio, which is controlled by stress history (OCR). Boulanger and Idriss (2007) recommended the following expressions for $CRR_{7.5}$ in natural deposits of clay-like soils:

$$CRR_{7.5} = 0.8\ (s_u/\sigma'_{vc})\ K_\alpha$$

and

$$CRR_{7.5} = 0.18\ (OCR)^{0.8}\ K_\alpha$$

Where:
s_u/σ'_{vc} is the undrained shear strength ratio for the appropriate direction of loading.

K_α is a correction factor to account to static shear stress. For well-designed structures where the factor of safety for static loading is large, K_α is generally close to 0.9. For heavily loaded soils under static conditions, K_α can be significantly less than 1.0. For seismic loading where CSR < 0.6, cyclic softening is possible only in normally to lightly overconsolidated (OCR < 4) clay-like soils.

Boulanger and Idriss (2007) recommended three approaches to determine CRR for clay-like materials, which are essentially:

1. Estimate using empirical methods based on stress history.
2. Measure s_u using in-situ tests (e.g. CPT).
3. Measure CRR on high quality samples using appropriate cyclic laboratory testing.

The third approach provides the highest level of insight and confidence, whereas the first and second approaches use empirical approximations to gain economy. For low-risk projects, the first and second approaches are often adequate. Based on the work of Wijewickreme and Sanin (2007), the $CRR_{7.5}$ for soft low plastic silts can also be estimated using the same approach (even though PI < 10).

The CPT can be used to estimate both undrained shear strength ratio (s_u/σ'_{vc}) and stress history (OCR). The CPT has the advantage that the results are repeatable and provide a detailed continuous profile of OCR and hence $CRR_{7.5}$.

Robertson (2009) recommended the following CPT-based approach that can be applied to all soils (i.e. no I_c cut-off):

When $I_c \leq 2.50$, assume soils are sand-like:

Use Robertson and Wride (1998) recommendation based on $Q_{tn,cs} = K_c\, Q_{tn}$,

where K_c is a function of I_c (see Figure 46)

When $I_c > 2.70$, assume soils are clay-like, where:

$$CRR_{7.5} = 0.053\, Q_{tn}\, K_\alpha$$

When $2.50 < I_c < 2.70$, transition region:

Use Robertson and Wride (1998) recommendations based on $Q_{tn,cs} = K_c\, Q_{tn}$,

where: $K_c = 6x10^{-7}\, (I_c)^{16.76}$

The recommendations where $2.50 < I_c < 2.70$ represent a transition from essentially drained cone penetration to essentially undrained cone penetration where the soils transition from predominately sand-like to predominately clay-like.

Based on the above approach, the contour of $CRR_{7.5} = 0.50$ (for $K_\alpha = 1.0$) on the CPT SBT_n chart is shown in Figure 48, compared to case history field

observations. For low-risk projects, the $CRR_{7.5}$ for cyclic softening in clay-like soils can be estimated using generally conservative correlations from the CPT (see Figure 48). For medium-risk projects, field vane tests (FVT) can also be used to provide site specific correlations with the CPT. For high-risk projects high quality undisturbed samples should be obtained and appropriate cyclic laboratory testing performed. Since sampling and laboratory testing can be slow and expensive, sample locations should be based on preliminary screening using the CPT.

The approach described above (Robertson, 2009 for all soils) tends to work well in soil profiles that have well defined deposits of either sand-like or clay-like soils. However, the approach can be somewhat conservative in profiles where a significant volume of soil plots in the transition region where $2.5 < I_c < 2.7$. In these cases, samples should be obtained to clarify soil behavior. It can be helpful to run analysis using both the NCEER/RW98 method for sand-like soils and Robertson (2009) method for all soils, to evaluate the sensitivity to soil type.

Evaluation of Post-earthquake Deformations

Vertical deformations (free-field)

For low to medium-risk projects and for preliminary estimates for high-risk projects, post-earthquake settlements can be estimated using various empirical methods to estimate post-earthquake volumetric strains (Zhang et al., 2002). The method by Zhang et al (2002) has the advantage that it is based on CPT results and can provide a detailed vertical profile of volumetric strains at each CPT location. The CPT-based approach is generally conservative since it is applied to all CPT data often using either commercially available software (e.g. ***CLiq***) or in-house spreadsheet software. The CPT-based approach captures low (minimum) cone values in soil layers and in transition zones at soil boundaries. These low cone values in transition zones often result in accumulated volumetric strains that tend to increase the estimated settlement. Engineering judgment should be used to remove excessive conservatism in highly inter-bedded deposits where there are frequent transition zones at soil boundaries. Software is capable of removing values in transition zones at soil boundaries (e.g. ***CLiq*** from http://www.geologismiki.gr/). Robertson and Shao (2010) also suggested a CPT-based method to estimate the seismic compression in unsaturated soils.

In clay-like soils the post-earthquake volumetric strains due to cyclic softening will be less than those experienced by sand-like soils due to cyclic liquefaction. A typical value of 0.5% or less is appropriate for most clay-like soils. Robertson

(2009) suggested a simplified approach to estimate the post-earthquake volumetric strains in clay-like soils based on CPT results. For high-risk projects, selected high quality sampling and appropriate laboratory testing may be necessary in critical zones identified by the simplified approach.

Engineering judgment is required to evaluate the consequences of the calculated vertical settlements taking into account soil variability, depth of the liquefied layers, thickness of non-liquefied soils above liquefied soils and project details (see Zhang et al., 2002). Displacement of buildings located above soils that experience liquefaction will depend on foundation details and depth, thickness and lateral distribution of liquefied soils. In general, building movements result from a combination of deviatoric and volumetric strains plus possible loss of ground due to ejected soil (sand boils, etc.).

Lateral Deformations

For low to medium-risk projects and for preliminary evaluation for high-risk projects, post-earthquake lateral deformation (lateral spreading) can be estimated using various empirical methods (Youd et al, 2002 and Zhang et al, 2004). The method by Zhang et al (2004) has the advantage that it is based on CPT results and can provide a detailed vertical profile of strains at each CPT location. The CPT-based approach is generally conservative since it should be applied to all CPT data and captures low (minimum) cone values in soil layers and in transition zones at soil boundaries. These low cone values in transition zones often result in accumulated shear strains that tend to increase the estimated lateral deformations. Engineering judgment should be used to remove excessive conservatism in highly inter-bedded deposits where there are frequent transition zones at soil boundaries. Software is capable of removing values in transition zones at soil boundaries (e.g. ***CLiq*** from http://www.geologismiki.gr/).

Engineering judgment is required to evaluate the consequences of the calculated lateral displacements taking into account, soil variability, site geometry, depth of the liquefied layers and project details. In general, assume that any liquefied layer located at a depth more than twice the depth of the free-face will have little influence on the lateral deformations. However, engineering judgment is required based on specific site details.

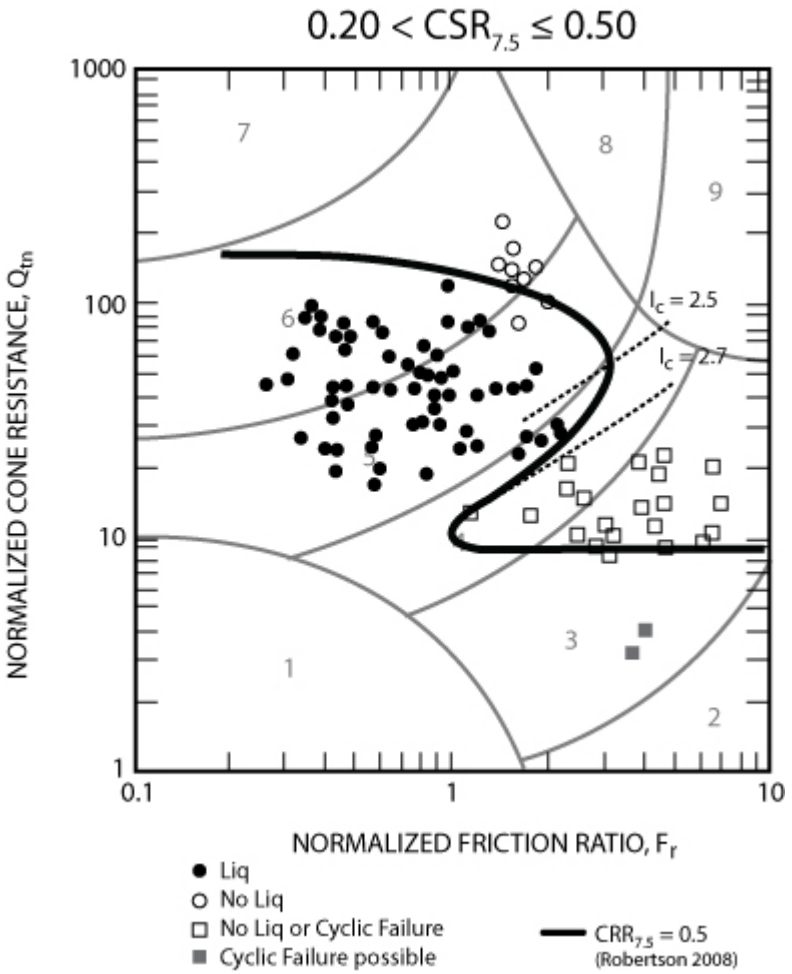

Figure 48 Cyclic Resistance Ratio $(CRR)_{M=7.5}$ using CPT
(After Robertson, 2009**)**

When the calculated lateral deformations using the above empirical methods are very large (i.e. shear strains of more than 30%) the soil should also be evaluated for susceptibility for strength loss (see next section on sloping ground) and overall stability against a flow slide evaluated.

Robertson and Wride (1998) suggested zones in which soils are susceptible to liquefaction based on the normalized soil behavior chart. An update of the chart is shown in Figure 49. The normalized cone resistance in Figures 45 and 49 is Q_{tn}, where the stress exponent varies with soil type.

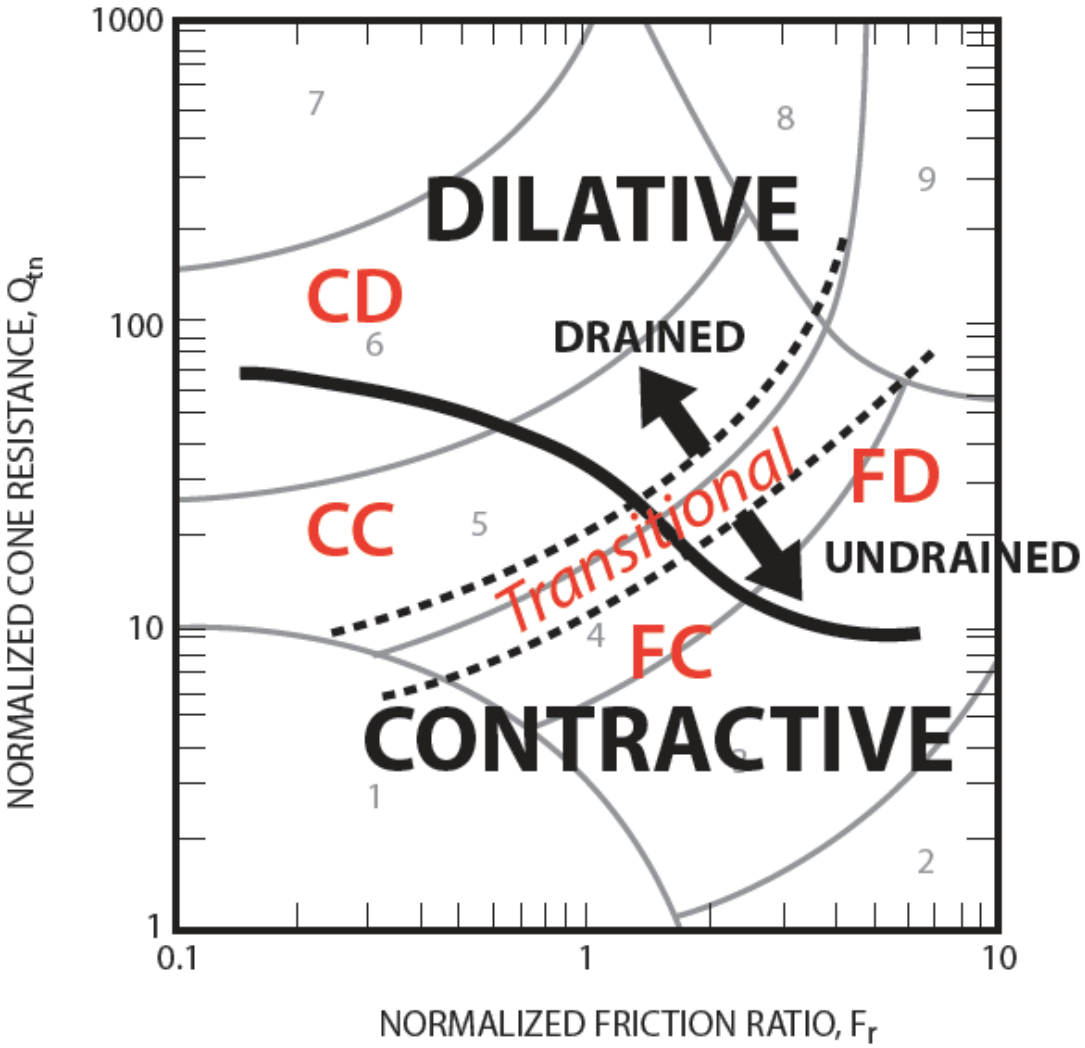

Figure 49 Zones of potential liquefaction/softening based on the CPT (see Figure 26 for details)

Coarse-grained soils (CD & CC ~ I_c < 2.5)- Evaluate potential behavior using CPT-based case-history liquefaction correlations.

CD Cyclic liquefaction possible depending on level and duration of cyclic loading.

CC Cyclic liquefaction and (flow-liquefaction) strength loss possible depending on loading and ground geometry.

Fine-grained soils (FD & FC ~ I_c > 2.7***)*** – Evaluate potential behavior based on in-situ and/or laboratory test measurements.

FD Cyclic softening possible depending on level and duration of cyclic loading.

FC Cyclic softening and (flow-liquefaction) strength loss possible depending on soil sensitivity, loading and ground geometry.

CPT for Flow (static) Liquefaction – Steeply Sloping Sites

Steeply sloping ground is defined as:

1. Steeply sloping ground (slope angle > 5 degrees)
2. Earth embankments (e.g. dams, tailings structures)

Sequence to evaluate flow liquefaction (i.e. strength loss)

1. Evaluate susceptibility for strength loss
2. Evaluate stability using post-earthquake shear strengths
3. Evaluate if strength loss will be triggered
4. Evaluate deformations.

1. Evaluate Susceptibility For Strength Loss

Use the CPT, plus disturbed samples (for grain size distribution, Atterberg limit and water content) to identify materials that are susceptible to strength loss due to earthquake shaking, (i.e. loose sand-like and sensitive clay-like materials). Use conservative evaluation techniques, since experience has shown that when strength loss occurs, instability can be rapid with little warning and deformations can be very large.

a. Loose, sand-like materials (i.e. susceptible to strength loss)
   i. Either fines content < 20% or fines content > 35% and Plasticity Index (PI) < 10 and water content (w_c) > 0.85 Liquid Limit (LL)
   ii. CPT $Q_{tn,cs}$ < 70 and SPT $(N_1)_{60cs}$ < 15. This represents the approximate boundary between CD and CC in Figure 49.

b. Sensitive clay-like materials (test for susceptibility, function of sensitivity and strain to failure)
   i. Fines content > 35%, and water content (w_c) > 0.85 LL
   ii. CPT Zone FC (see CPT chart, Figure 49) and/or FVT (Field Vane Test), where sensitivity, S_t > 5
   iii. Strain to failure less than 1%

c. Insensitive clay-like materials (i.e. not susceptible to strength loss)
   i. Fines content > 20% and PI > 10, and water content (w_c) < 0.80 Liquid Limit (LL)
   ii. CPT Zone FD (see CPT chart, Figure 49)

If layers/zones of low permeability materials exist that could inhibit pore water redistribution after seismic loading and promote void redistribution, increase conservatism when evaluating susceptibility for strength loss.

2. *Evaluate Stability Using Post-earthquake Shear Strengths*

a. Initial stability analysis assuming strength loss is triggered and using conservative estimates of minimum (liquefied/residual/steady state) undrained shear strength, $s_{u(liq)}$, based on either empirical correlations with in-situ tests or field measured values:
   i. $s_{u(liq)}/\sigma'_{vc}$ or $s_{u(liq)}$ from CPT for loose sand-like materials (either Olson and Stark, 2002, Idriss and Boulanger, 2008 or Robertson, 2010 – e.g. Figure 50). Assume a lower bound $s_{u(liq)}/\sigma'_{vc} = 0.05$.
   ii. Use remolded undrained shear strength, $s_{u(rem)}$, for sensitive clay-like materials measured from either CPT or FVT. If the liquidity index (LI) > 1.0, use a lower bound value of s_{ur} = 1 kPa (20 psf).
   iii. 80% of peak undrained shear strength, s_{up}, measured using either CPT or FVT for insensitive clay-like materials
   iv. In zones where strength loss does not occur, use peak undrained shear strength, s_{up} (or drained strength, whichever is lower)

   If Factor of Safety (FS) > 1.2, assume stability is acceptable and check deformations

   If FS < 1.2, evaluate material behavior and triggering in more detail
   - For low-risk structures, redesign or modify
   - For moderate and high-risk structures, perform more detailed investigation

b. If project risk is moderate to high-risk and FS < 1.2, evaluate post-earthquake shear strength in more detail:
   i. Additional in-situ testing, e.g. SCPT, FVT, geophysical logging, and,
   ii. High quality undisturbed samples and appropriate laboratory testing.
   - If FS > 1.2, assume stability is acceptable and check deformations
   - If FS < 1.2, check triggering

If layers/zones of low permeability exist that could inhibit pore water redistribution after seismic loading and promote void redistribution, increase conservatism when evaluating post earthquake shear strengths. For high-risk projects, the potential for void redistribution can be evaluated using more complex effective stress numerical models.

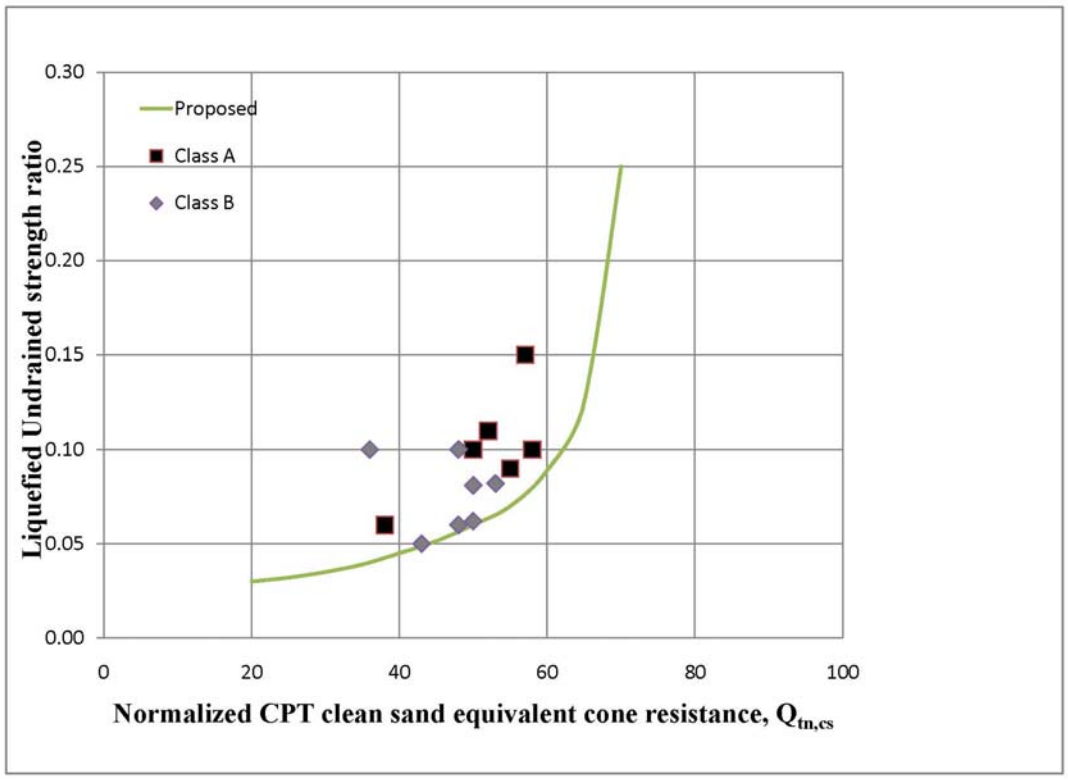

Figure 50 Liquefied shear strength ratio and normalized CPT clean sand equivalent penetration resistance from flow liquefaction failure case histories (after, Robertson, 2010)

$$s_{u(liq)}/\sigma'_{vo} = [0.02199 - 0.0003124\ Q_{tn,cs}]/\ [1 - 0.02676\ Q_{tn,cs} + 0.0001783\ (Q_{tn,cs})^2\ ]$$

3. Evaluate if strength loss will be triggered

When FS < 1.0 using best estimates of post-trigger shear strength parameters, assume that strength loss will be triggered.

When 1.0 < FS < 1.2 using best estimates of post-earthquake shear strength parameters, check if the earthquake (or other mechanisms) will trigger strength loss by applying either of the following approaches:

a. Pore-pressure approach, using CRR (Youd et al. 2001; Robertson, 2009)
b. Strain-based approach (Castro, 1999)
c. Yield-strength approach (Sladen , 1985, Olsen and Stark, 2003)

All approaches should be based on improved knowledge of materials based on combined results from in-situ tests and appropriate laboratory testing on high quality samples. When soils are susceptible to strength loss and slopes are steep, a trigger mechanism should always be assumed to be present (Silvis and de Groot, 1995). Hence, for high-risk structures caution and conservatism should be exercised.

If one or more zones are not expected to trigger strength loss, re-evaluate stability using higher shear strength in these zones.

- If FS > 1.2, assume stability is acceptable and check deformations.
- If FS < 1.2 assume unsafe and redesign or modify.

4. Evaluate Seismic Deformations

If embankment is considered stable, evaluate seismic deformations based on size and duration of earthquake shaking.

a. Preliminary screening
    i. If no liquefaction is identified and the earthquake is small (a_{max} < 0.10g), assume deformations are small.
b. Pseudo-static analysis
    i. If earthquake is small, M < 8, and,
    ii. If no significant zones indicate a potential for strength loss, and,

iii. Small deformations (less than 1m (3 feet)) are not significant to the performance of the embankment

Use limit equilibrium stability analyses using pseudo-static seismic coefficient of 0.5 PGA and 80% of peak undrained strength for clay-like and sand-like materials (but not to exceed 80% of drained strength).

- If $1.0 < FS < 1.2$, deformations are likely to be less than 1m (3 feet).

c. Newmark-type analyses (no cyclic liquefaction)

Perform a Newmark-type analysis if no zones of material indicate cyclic liquefaction.

d. Numerical modeling (cyclic liquefaction)

Perform appropriate nonlinear dynamic numerical analyses (finite element/finite difference) that incorporate special provisions for pore pressure build-up. These types of analyses require a high level of expertise with computational methods and considerable effort to perform, but they are often valuable for addressing complex problems and are increasingly used on large high-risk projects. The accuracy of any nonlinear dynamic analysis depends directly on the site characterization, its simplified representation for analysis, the correlations used to derive soil parameters from in-situ test data, the details of the constitutive models and their numerical implementation, and the selection of input ground motions.

Ground Improvement Compaction Control

Ground improvement can occur in many forms depending on soil type and project requirements. For coarse-grained soils such as sands and silty sands, deep compaction is a common ground improvement technique. Deep compaction can comprise: vibrocompaction, vibroreplacement (stone columns), dynamic compaction, compaction piles, and deep blasting.

The CPT has been found to be one of the best methods to monitor and document the effect of deep compaction due to the continuous, reliable and repeatable nature of the data. Most deep compaction techniques involve cyclic shear stresses in the form of vibration to induce an increase in soil density. Vibratory compaction is generally more effective in soil deposits with a friction ratio less than 1%. When the friction ratio exceeds about 1.5% vibratory compaction is usually not effective. These recommendations apply to average values in a soil deposit. Local seams or thin layers with higher friction ratio values are often of little practical importance for the overall performance of a project and their effect should be carefully evaluated when compaction specifications are prepared. Soils with an initial cone resistance below about 3 MPa (30 tsf) can be compressible or contain organic matter, silt or clay and will generally not respond well to vibratory compaction. Soils with a high initial cone resistance are normally dense and will not show significant compaction and generally do not need compaction. It is also important to establish the level and variation of the groundwater table before compaction since some compaction methods are less effective in dry or partially saturated soils. The CPTu provides the required information on groundwater conditions.

Often the aim of deep compaction is for one or more of the following:

- increase bearing capacity (i.e. increase shear strength)
- reduce settlements (i.e. increase stiffness)
- increase resistance to liquefaction (i.e. increase density).

The need for deep compaction and geotechnical conditions will be project specific and it is important that design specifications take account of these site-specific requirements. Cone resistance in coarse-grained soils is governed by many factors including soil density, in-situ stresses, stress history, and soil compressibility. Changes in shear strength, stiffness and density can be documented with changes in measured cone resistance.

A common problem in many deep compaction projects is to specify a minimum value of q_c for compaction over a large depth range. This results in a variation of relative density with depth, with the required degree of compaction near the surface being much higher than at depth. For certain projects, a high degree of compaction close to the ground surface may be justified, but can be achieved using surface compaction methods. However, this can be very difficult to obtain with certain deep compaction techniques and this decision should be based on engineering judgment related to the geotechnical project requirements. It is generally preferred to specify a minimum normalized value of cone resistance corrected for overburden stress, Q_{tn}. Since, grain characteristics can vary rapidly in many sandy deposits, it is also preferred to specify an acceptance criteria based on *normalized clean sand equivalent* values of cone resistance $(Q_{tn})_{cs}$, using the methodology shown in Figure 46, especially when compaction is performed to reduce the potential for liquefaction. Specification using $(Q_{tn})_{cs}$ can reduce problems in silty zones, where traditional approaches have often resulted in excessive ground improvement in an effort to reach unrealistic criteria.

It is relatively common to have the CPT soil behavior type index (I_c) decrease after compaction (e.g. vibrocompaction). The cause for the decrease is likely due to changes in horizontal effective stresses due to ground improvement. When this has occurred it has been common to use the pre-improvement values of I_c that are less influenced by complex changes in horizontal effective stresses and better represent the correct soil type. Any small change in I_c typically has little influence in the analysis for clean sands (where the initial $I_c < 2.0$).

An important aspect of deep compaction that is not yet fully understood is the increase in cone resistance with time after compaction. This time effect has been observed in different ground conditions and with different compaction methods. Often no measurable change in pore pressure has been observed and the increase takes place without visible ground settlements. Charlie et al. (1992) studied a number of cases where cone resistance was measured with time after compaction. A range of compaction techniques were used and the results are shown in Figure 51. The cases were representative of a wide range of climates and geologic conditions with average temperatures varying from -10°C (Beaufort Sea) to +27°C (Nigeria). Charlie et al. (1992) suggested that the time effect could be linked to the average air temperature. The possibility of time effects should be evaluated for each project. For very large projects, it may be necessary to perform field trials.

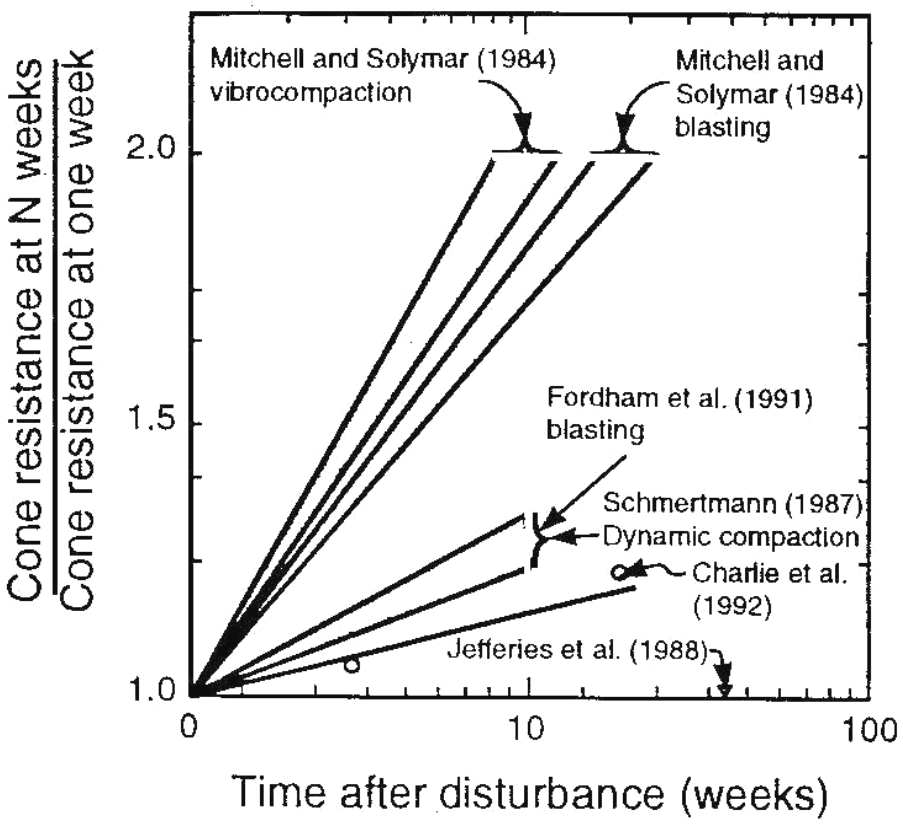

Figure 51 Influence of time after disturbance on CPT results
(after Charlie et al., 1992)

For projects where deep compaction is recommended to either increase resistance to liquefaction or decrease future settlements for shallow foundations, the seismic CPT should be considered, since it provides both penetration resistance and shear wave velocity. The combined values can improve interpretation, especially in silty sands and soils that have some microstructure before improvement.

Ground improvement can also include many other techniques, such as grouting, soil mixing and stone columns as well as pre-loading. The CPT can also be used to evaluate the effectiveness of these other techniques although this will depend on soil conditions and the ground improvement method. The CPT has also found some limited use in monitoring surface compaction. Since surface compaction is often carried out in thin layers with frequent quality control, the CPT has not found extensive application in this area.

Another form of ground improvement is soil mixing, where compounds are mixed with soil to improve their behavior. Sometimes quality control is defined in terms of a target unconfined compressive strength (q_u). The unconfined compressive strength (q_u) is twice the undrained shear strength (s_u) that can be estimate directly from the CPT.

Design of Wick or Sand Drains

Pre-loading is a common form of ground improvement in fine-grained soils where the rate of consolidation is important. Installation of sand drains or wick drains can significantly decrease the time for consolidation settlements. Prior to 1975, vertical sand drains were common to aid consolidation with temporary pre-load. Since 1975, geosynthetics in the form of wick drains have dominated the market. Wick drains are usually fluted or corrugated plastic or cardboard cores within geotextile sheaths that completely encircle those cores. They are usually 100mm wide by 2 to 6mm thick. The wick drain is usually pushed or driven into the ground to the desired depth using a lance or mandrel. The drain then remains in place when the lance or mandrel is removed. Installation can be in the range of 1 to 5 minutes depending on ground conditions, pushing equipment and depth of installation. The design of wick drains is not standardized but most equate the diameter of the particular type of drain to an equivalent sand drain diameter.

The method developed by Barron (1948) and Kjellman (1948), as mentioned by Hansbo (1970), is commonly used, and the relevant design equations are as follows:

$$t = \frac{D^2}{8c_h}\left[\ln(D/d) - 0.75\right]\ln\frac{1}{1-U}$$

Where:

- t = consolidation
- c_h = coefficient of consolidation for horizontal flow
- d = equivalent diameter of the wick drain ($\simeq$ circumference/π)
- D = sphere of influence of the wick drain (for a triangular pattern use 1.05 times the spacing, for a square pattern use 1.13 times the spacing).
- U = average degree of consolidation

The key input parameter for the soil is the coefficient of consolidation for horizontal flow, c_h. This parameter can be estimated from dissipation tests using the CPTu. The value derived from the CPTu is particularly useful since, the cone represents a very similar model to the installation and drainage process around the wick drain. Although there is some possible smearing and disturbance to the soil around the CPT, similar smearing and disturbance often exists around the wick, and hence, the calculated value of c_h from the CPTU is usually representative of the soil for wick drain design.

Details on estimation of c_h from dissipation tests were given in the section on (geotechnical parameters) consolidation characteristics. To provide a reasonable estimate of c_h a sufficient number of dissipation tests should be carried out through the zone of interest. The dissipation tests should be carried out to at least 50% dissipation. Several dissipation tests should be carried out to full dissipation to provide an estimate of the equilibrium groundwater conditions prior to pre-loading.

Software

In recent years, commercial software has become available to aid in CPT interpretation and geotechnical design using CPT results. This author has been involved in the development of two programs; ***CPeT-IT*** (pron. *C-petit*) and ***CLiq*** *(*pron. *slick)*. Both programs are inexpensive and very user friendly and can be downloaded from http://www.geologismiki.gr/Products.html.

CPeT-IT is an easy to use yet detailed software package for the interpretation of CPT and CPTu data. ***CPeT-IT*** takes CPT data and performs basic interpretation based on the methods contained in this Guide and supports output in both SI and Imperial units. Overlay plots can be generated and all results are presented in tabular and graphical format. The program also contains simple design tools for estimating bearing capacity for shallow foundations, 1-D settlement calculations and pile capacity versus depth. It also contains a tool for interpretation of dissipation tests. Example output is shown in Figures 52 to 54.

CLiq provides users an easy to use graphical environment specifically tailored for liquefaction analysis using CPT and CPTu data. The software addresses advanced issues such as cyclic softening in clay-like soils and transition zone detection. ***CLiq*** provides results and plots for each calculation step, starting with the basic CPT data interpretation through to final plots of factor of safety, liquefaction potential index and post-earthquake displacements, both vertical and lateral displacements. ***CLiq*** provides consistent output results by applying the NCEER method (Youd et al, 2001; Robertson & Wride, 1998) along with the calibrated procedures for post-earthquake displacements by Zhang et al (2002 & 2004). It also includes the latest assessment procedure developed by Robertson (2010) that is applicable to all soil type combining a check for cyclic liquefaction (sands) and cyclic softening (clays). It also includes the CPT-based liquefaction methods suggested by Moss et al (2006) and Boulanger and Idriss (2008/2014).

A unique 2D feature provides a means of creating colorful contour maps of the overall liquefaction potential index (LPI) and post-earthquake settlements in plan view thus allowing the user to visualize the spatial variation of liquefaction potential and settlements across a site. The variations of calculated post-earthquake settlements across a site allow estimates of differential settlements for a given site and design earthquake.

A parametric analysis feature allows the user to vary both the earthquake magnitude and surface acceleration to evaluate the sensitivity of both the overall liquefaction potential index and post-earthquake settlements as a function of earthquake loading and results are presented in a 3D graphical form. Example output is shown in Figure 47.

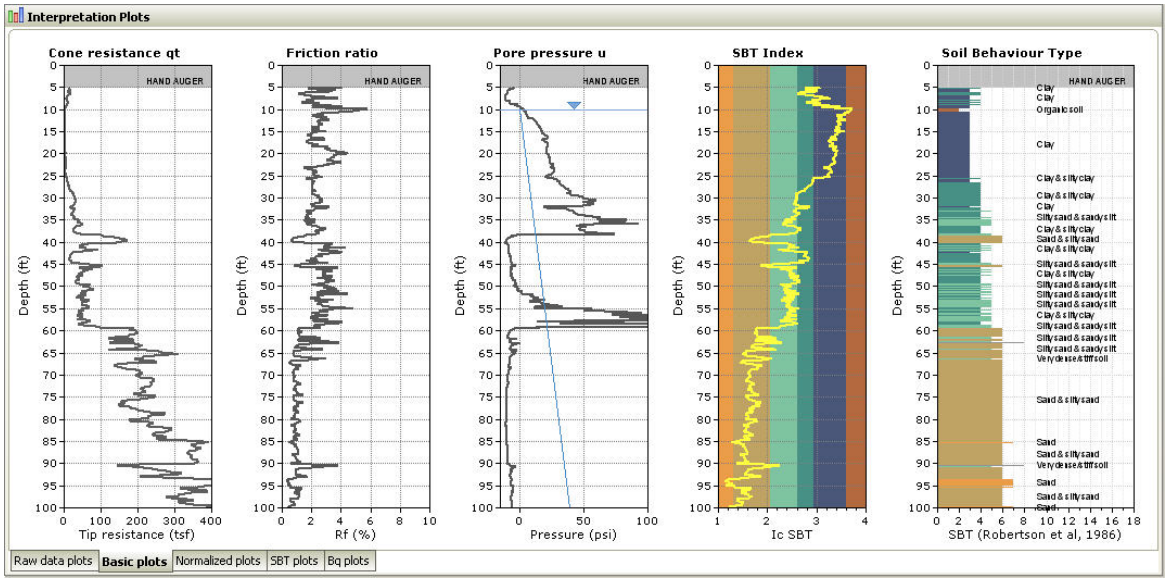

Figure 52 Example CPTu plot from ***CPeT-IT***

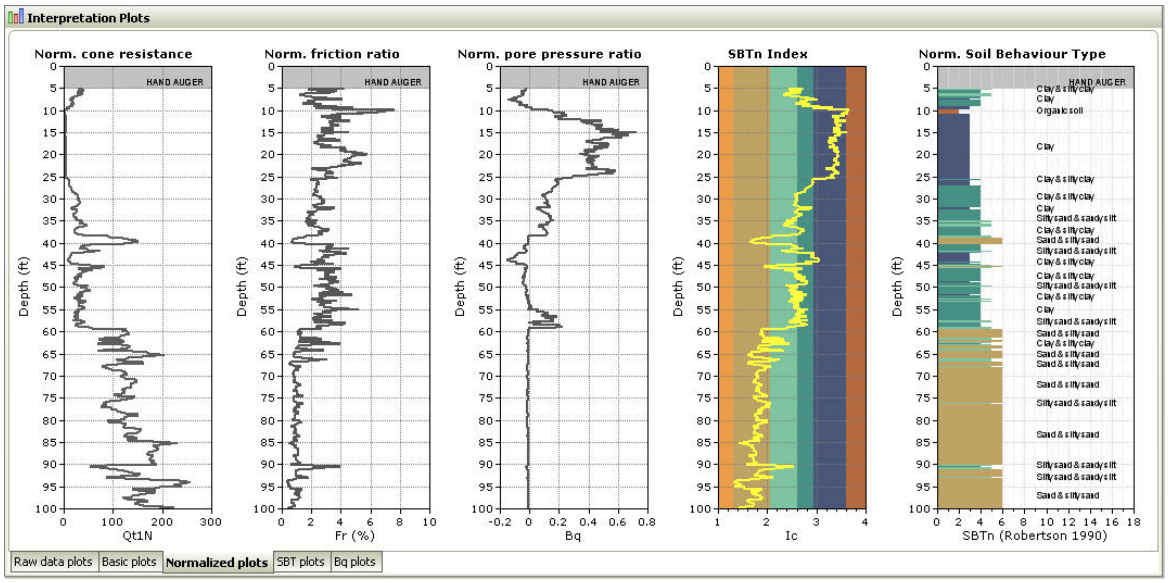

Figure 53 Example CPTu plot based on normalized parameters from ***CPeT-IT***

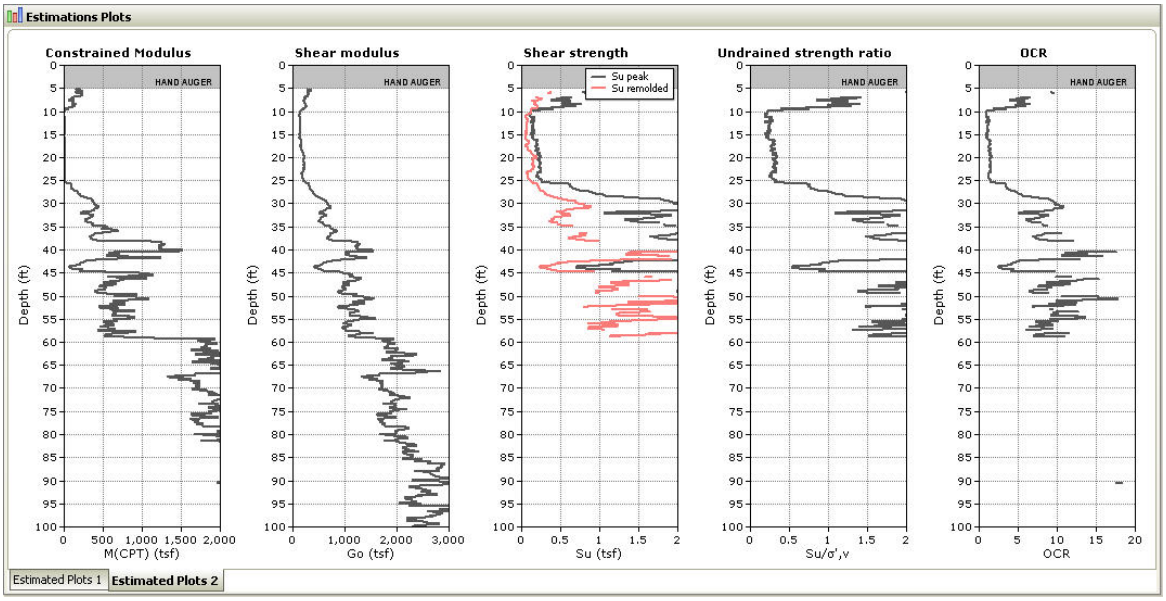

Figure 54 Example of estimated geotechnical parameters from ***CPeT-IT***

Main References

ASTM-D5778-07. 2007. Standard test method for performing electronic friction cone and piezocone penetration testing of soils. ASTM International, West Conshohocken, PA, www.astm.org.

Ahmadi, M.M., and Robertson, P.K., 2005. Thin layer effects on the CPT qc measurement. *Canadian Geotechnical Journal*, **42**(9): 1302-1317.

ASTM D5778-12 (2012). Standard Test Method for Performing Electronic Friction Cone and Piezocone Penetration Testing of Soils, *ASTM International*. www.astm.org.

Baldi, G., Bellotti, R., Ghionna, V.N., Jamiolkowski, M., and Lo Presti, D.F.C., 1989. Modulus of sands from CPTs and DMTs. *In Proceedings of the 12th International Conference on Soil Mechanics and Foundation Engineering*. Rio de Janeiro. Balkema Pub., Rotterdam, Vol.1, pp. 165-170.

Boggess, R. and Robertson, P.K., 2010. CPT for soft sediments and deepwater investigations. *2nd International Symposium on Cone Penetration Testing*, CPT'10. Huntington Beach, CA, USA. www.cpt10.com

Bolton, M.D., 1986. The strength and dilatancy of sands. *Geotechnique*, **36**(1): 65-78.

Canadian Geotechnical Society 2006. *Canadian Foundation Engineering Manual*, 4th Edition, BiTech Publishers, Vancouver, BC.

Campanella, R.G., and Robertson, P.K., 1982. State of the art in In-situ testing of soils: developments since 1978. *In Proceedings of Engineering Foundation Conference on Updating Subsurface Sampling of Soils and Rocks and Their In-situ Testing*. Santa Barbara, California. January 1982, pp. 245-267.

Campanella, R.G., Gillespie, D., and Robertson, P.K., 1982. Pore pressures during cone penetration testing. *In Proceedings of the 2nd European Symposium on Penetration Testing*, ESPOT II. Amsterdam. A.A. Balkema, pp. 507-512.

Eslaamizaad, S., and Robertson, P.K., 1996a. Seismic cone penetration test to identify cemented sands. *In Proceedings of the 49th Canadian Geotechnical Conference*. St. John's, Newfoundland. September, pp. 352 – 360.

Eslaamizaad, S., and Robertson, P.K. 1996b. Cone penetration test to evaluate bearing capacity of foundation in sands. *In Proceedings of the*

49th Canadian Geotechnical Conference. St. John's, Newfoundland. September, pp. 429-438.

Eslaamizaad, S. and Robertson, P.K., 1997. Evaluation of settlement of footings on sand from seismic in-sity tests. *In Proceedings of the 50th Canadian Geotechnical Conference*, Ottawa, Ontario, October 1997, Vol.2, pp. 755-764.

Fahey, M. and Carter, J.P., 1993. A finite element study of the pressuremeter in sand using a nonlinear elastic plastic model. *Canadian Geotechnical Journal*, **30**(2): 348-362.

Hight, D., and Leroueil, S., 2003. Characterization of soils for engineering purposes. *Characterization and Engineering Properties of Natural Soils*, Vol.1, Swets and Zeitlinger, Lisse, pp. 255-360.

Idriss, I.M. and Boulanger, R.W., 2004. Semi-empirical procedures for evaluating liquefaction potential during earthquakes. *Proceedings 11th International Conference on Soil Dynamics and Earthquake Engineering*. Berkeley, 32-56.

IRTP, 1999. International Reference Test Procedure for Cone Penetration Test (CPT). Report of the ISSMFE Technical Committee on Penetration Testing of Soils, TC 16, Swedish Geotechnical Institute, Linkoping, Information, 7, 6-16.

Janbu, N., 1963, Soil Compressibility as determined by oedometer and triaxial tests. *Proceedings of the European Conference on Soil Mechanicxs and Foundation Engineering*, Wiesbaden, pp 19-25.

Jamiolkowski, M., Ladd, C.C., Germaine, J.T., and Lancellotta, R., 1985. New developments in field and laboratory testing of soils. *In Proceedings of the 11th International Conference on Soil Mechanics and Foundation Engineering*. San Francisco, California, August 1985, Vol.1 pp. 57-153.

Jefferies, M.G., and Davies, M.O, 1991. Soil Classification by the cone penetration test: discussion. *Canadian Geotechnical Journal*, **28**(1): 173-176.

Jefferies, M.G., and Davies, M.P., 1993. Use of CPTU to estimate equivalent SPT N_{60}. *Geotechnical Testing Journal*, ASTM, **16**(4): 458-468.

Jefferies, M.G. and Been, K., 2006. *Soil Liquefaction – A critical state approach*. Taylor & Francis, ISBN 0-419-16170-8 478 pages.

Kayen, R., Moss, R.E.S., Thompson, E.M., Seed, R.B., Cetin, K.O., Der Kiureghian, A., Tanaka, Y., and Tokimatsu, K., 2013. Shear-wave velocity-based probabilistic and deterministic assessment of seismic soil liquefaction potential, J. of Geotech. and Geoenvironmental Engineering, ASCE, 2013.139: 407-419.

Karlsrud, K., Lunne, T., Kort, D.A. & Strandvik, S. 2005. CPTU correlations for Clays. Proc. 16th *ICSMGE*, Osaka, September 2005

Kulhawy, F.H., and Mayne, P.H., 1990. *Manual on estimating soil properties for foundation design*, Report EL-6800 Electric Power Research Institute, EPRI, August 1990.

Ladd, C.C., and Foott, R. (1974). "New design procedure for stability of soft clays." *J. of the Geotech. Eng. Div.*, 100(GT7), 763-786.

Ladd, C.C. & DeGroot, D.J. 2003. Recommended practice for soft ground site characterization. *Soil and Rock America,* Vol. 1 (Proc.12th PanAmerican Conf., MIT), Verlag Glückauf, Essen: 3-57.

Lunne, T., Eidsmoen, T., Gillespie, D., and Howland, J.D., 1986. Laboratory and field evaluation on cone penetrometers. *Proceedings of ASCE Specialty Conference In Situ'86: Use of In Situ Tests in Geotechnical Engineering*. Blacksburg, ASCE, GSP 6 714-729

Lunne, T., Robertson, P.K., and Powell, J.J.M., 1997. *Cone penetration testing in geotechnical practice*. Blackie Academic, EF Spon/Routledge Publ., New York, 1997, 312 pp.

Lunne, T., and Andersen, K.H., 2007. Soft clay shear strength parameters for deepwater geotechnical design. *Proceedings 6th International Conference, Society for Underwater Technology*, Offshore Site Investigation and Geomechanics, London, 151-176.

Mayne, P.W., 2000. Enhanced Geotechnical Site Characterization by Seismic Piezocone Penetration Test. Invited lecture, *Fourth International Geotechnical Conference*, Cairo University. pp 95-120.

Mayne, P.W., 2005. Integrated Ground Behavior: In-Situ and Lab Tests, *Deformation Characteristics of Geomaterials*, Vol. 2 (Proc. Lyon), Taylor & Francis, London, pp. 155-177.

Mayne, P.W., 2007. NCHRP Synthesis 'Cone Penetration Testing State-of-Practice'. Transportation Research Board Report Project 20-05. 118 pages. www.trb.org

Mayne, P.W., 2008. Piezocone profiling of clays for maritime site investigations. *11th Baltic Sea Geotechnical Conference*. Gdansk, Poland., 151- 178.

Mayne, P.W., Coop, M.R., Springman, S.M., Huang, A.B, and Zornberg, J.G., 2009. Geomaterail behaviour and testing. State of the Art (SOA) paper, 17th ICSMGE Alexandria.

Mitchell, J.K., Guzikowski, F. and Villet, W.C.B., 1978. The Measurement of Soil Properties In-Situ, Report prepared for US Department of Energy Contract W-7405-ENG-48, Lawrence Berkeley Laboratory, University of California, Berkeley, CA, 94720.

Molle, J., 2005. *The accuracy of the interpretation of CPT-based soil classification methods in soft soils.* MSc Thesis, Section for Engineering Geology, Department of Applied Earth Sciences, Delf University of Technology, Report No. 242, Report AES/IG/05-25, December

Parez, L. and Faureil, R., 1988. Le piézocône. Améliorations apportées à la reconnaissance de sols. *Revue Française de Géotech*, Vol. 44, 13-27.

Robertson, P.K., 1990. Soil classification using the cone penetration test. *Canadian Geotechnical Journal,* **27**(1): 151-158.

Robertson, P.K., 1998. Risk-based site investigation. *Geotechnical News*: 45-47, September 1998.

Robertson, P.K., 2009a. Interpretation of cone penetration tests – a unified approach. *Canadian Geotechnical Journal,* 46:1337-1355.

Robertson, P.K., 2010a. Soil behaviour type from the CPT: an update. *2nd International Symposium on Cone Penetration Testing*, CPT'10, Huntington Beach, CA, USA. www.cpt10.com

Robertson, P.K., 2010b. Estimating in-situ state parameter and friction angle in sandy soils from the CPT. *2nd International Symposium on Cone Penetration Testing*, CPT'10, Huntington Beach, CA, USA. www.cpt10.com

Robertson, P.K., 2010c. Evaluation of Flow Liquefaction and Liquefied strength Using the Cone Penetration Test. *Journal of Geotechnical and Geoenvironmental Engineering*, ASCE, **136**(6): 842-853

Robertson. P.K., Campanella, R.G., Gillespie, D., and Greig, J., 1986. Use of Piezometer Cone data. *In-Situ'86 Use of Ins-itu testing in Geotechnical Engineering*, GSP 6 , ASCE, Reston, VA, Specialty Publication, SM 92, pp 1263-1280.

Robertson, P.K., Sully, J.P., Woeller, D.J., Lunne, T., Powell, J.J.M. and Gillespie, D., 1992. Estimating coefficient of consolidation from piezocone tests. *Canadian Geotechnical Journal*, Ottawa, **29**(4): 539-550.

Robertson, P.K., and Campanella, R.G., 1983a. Interpretation of cone penetration tests – Part I (sand). *Canadian Geotechnical Journal*, 20(4): 718-733.

Robertson, P.K., and Campanella, R.G. 1983b. Interpretation of cone penetration tests – Part II (clay). *Canadian Geotechnical Journal*, 20(4): 734-745.

Robertson, P.K. and Wride, C.E., 1998. Evaluating cyclic liquefaction potential using the cone penetration test. *Canadian Geotechnical Journal*, Ottawa, 35(3): 442-459.

Robertson, P.K., Campanella, R.G., Gillespie, D., and Rice, A., 1986. Seismic CPT to measure in-situ shear wave velocity. *Journal of Geotechnical Engineering Division*, ASCE, 112(8): 791-803.

Sanglerat, G., 1972. *The Penetrometer and Soil Exploration*. Elsevier Pub., Amsterdam, 488pp.

Schnaid, F., 2005. Geocharacterization and Engineering properties of natural soils by in-situ tests. *In Proceedings of the 16th International Conference on Soil Mechanics and Geotechnical Engineering*, Vol.1, Osaka, September, 2005, Millpress, Rotterdam, pp. 3-45.

Schneider, J.A., Randolph, M.F., Mayne, P.W. & Ramsey, N.R. 2008. Analysis of factors influencing soil classification using normalized piezocone tip resistance and pore pressure parameters. *Journal Geotechnical and Geoenvironmental Engrg*. 134 (11): 1569-1586.

Schmertmann, J.H. 1978. *Guidelines for cone penetration tests performance and design*. Federal Highways Administration, Washington, D.C., Report FHWA-TS-78-209.

Teh, C.I., and Houlsby, G.T. 1991. An analytical study of the cone penetration test in clay. *Geotechnique*, 41 (1): 17-34.

Wride, C.E., Robertson, P.K., Biggar, K.W., Campanella, R.G., Hofmann, B.A., Hughes, J.M.O., Küpper, A., and Woeller, D.J. In-Situ testing program at the CANLEX test sites. *Canadian Geotechnical Journal*, 2000, Vol. 37, No. 3, June, pp. 505-529

Wroth, C.P., 1984. The interpretation of in-situ soil tests. Rankine Lecture, *Geotechnique*(4).

Youd, T.L., Idriss, I.M., Andrus, R.D., Arango, I., Castro, G., Christian, J.T., Dobry, R., Finn, W.D.L., Harder, L.F., Hynes, M.E., Ishihara, K., Koester, J., Liao, S., Marcuson III, W.F., Martin, G.R., Mitchell, J.K., Moriwaki, Y., Power, M.S., Robertson, P.K., Seed, R., and Stokoe, K.H., Liquefaction Resistance of Soils: Summary Report from the 1996 NCEER and 1998 NCEER/NSF Workshop on Evaluation of Liquefaction Resistance of Soils, ASCE, Journal of Geotechnical & Geoenvironmental Engineering, Vol. 127, October, pp 817-833

Zhang, Z., and Tumay, M.T., 1999. Statistical to fuzzy approach toward CPT soil classification. *Journal of Geotechnical and Geoenvironmental Engineering*, **125**(3): 179-186.

Zhang, G., Robertson, P.K. and Brachman, R.W.I., 2002, Estimating Liquefaction induced Ground Settlements From CPT for Level Ground, *Canadian Geotechnical Journal*, 39(5): 1168-1180

WORKMEN / EQUIPMENTS CLEARANCE

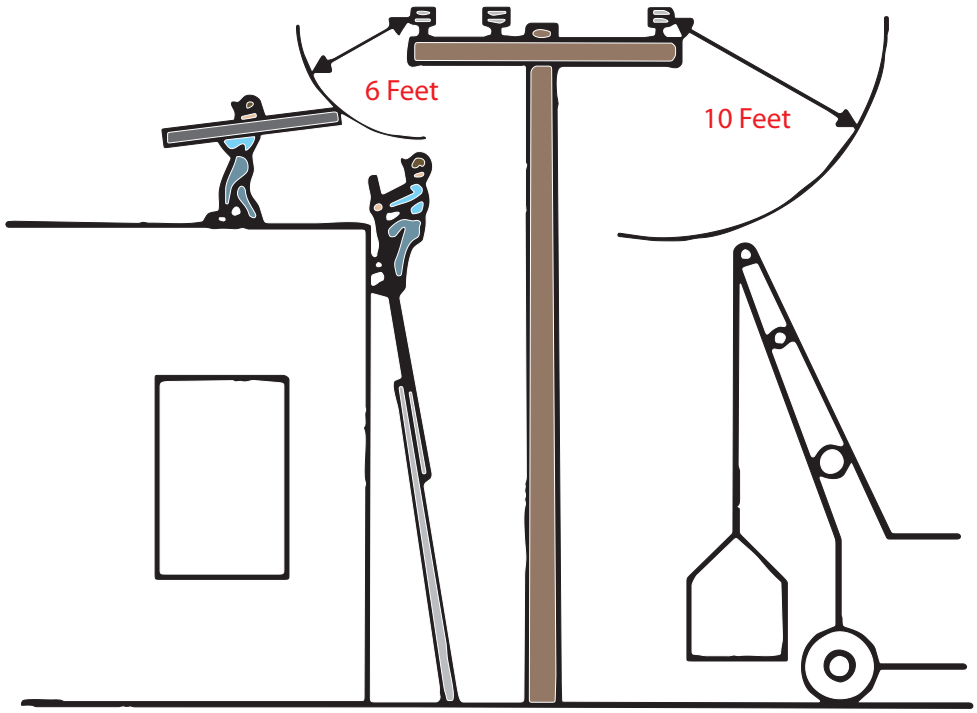

NOTE: Private sector employees are currently under federal OSHA jurisdiction.

Public employees must follow CAL-OSHA regulations.

	Required Clearance of Workmen/ Equipments	*Required Clearance for Cranes, Derricks, etc.*	*Voltage Range in Volts*
California Penal Code	6'	6'	750 and Above
CAL-OSHA	6'	10'	600–50,000
Federal OSHA	No Standard	10'	0–50,000

NOTE: Required clearances are greater for voltages in excess of 50,000 volts.

DIGALERT

COLOR CODE

FOR MARKING UNDERGROUND FACILITIES

PROPOSED EXCAVATION	COMMUNICATION CATV
TEMP. SURVEY MARKINGS	WATER
ELECTRIC	RECLAIMED WATER
GAS-OIL-STEAM	SEWER

Call Toll Free

1-800-227-2600

2 Working Days Before You Dig

Underground Service Alert
of Southern California

Dig Safely.

GREGG DRILLING LOCATIONS

Corporate Headquarters

2726 Walnut Avenue
Signal Hill, California 90755
Tel: 562-427-6899
Fax: 562-427-3314

Northern California

950 Howe Road
Martinez, California 94553
tel: 925-313-5800
fax: 925-313-0302

www.greggdrilling.com

Gregg Drilling & Testing Canada Ltd.

144-4th Ave., SW, Suite 1600
Calgary, Alberta T2P 3N4
tel: 403-303-3372

Fort McMurray field office

tel: 587-646-5316

www.greggdrilling.ca

GREGG DRILLING & TESTING

Site Investigation Services

GREGG